Summer 2019

In Hot Water: Thermal Acclimation is Insufficient to Save Corals in the Anthropocene

Harmony Alise Martell
Old Dominion University, harmonyamartell@gmail.com

IN HOT WATER: THERMAL ACCLIMATION IS INSUFFICIENT TO SAVE CORALS IN THE ANTHROPOCENE

by

Harmony Alise Martell
B. S. May 1999, College of Saint Elizabeth
M. S. July 2012, Nova Southeastern University

A Dissertation Submitted to the Faculty of
Old Dominion University in Partial Fulfillment of the
Requirements for the Degree of

DOCTOR OF PHILOSOPHY

ECOLOGICAL SCIENCES

OLD DOMINION UNIVERSITY
August 2019

Approved by:

Holly D. Gaff (Co-Director)

Richard C. Zimmerman (Co-Director)

David Gauthier (Member)

Mark E. Warner (Member)

ABSTRACT

IN HOT WATER: THERMAL ACCLIMATION IS INSUFFICIENT
TO SAVE CORALS IN THE ANTHROPOCENE

Harmony Alise Martell
Old Dominion University, 2019
Co-Directors: Dr. Holly D. Gaff
Dr. Richard C. Zimmerman

Scleractinian corals are animal partners in exquisite symbioses with a suite of algal, microbial, fungal and viral associates comprising miniature ecosystems collectively referred to as a holobiont. In recent decades, ocean warming has jeopardized the delicate balance of the very symbioses that have enabled coral survival. Thermal stress causes a reduction of algal symbionts, a phenomenon referred to as 'coral bleaching' that represents dysbiosis in the holobiont and often leads to mortality. Current thermal acclimation theory states variation and gradual increases in temperature can ameliorate thermal stress. Indeed, there is evidence some coral species have some capacity to acclimatize to thermally variable environments, increased temperature, or both, leading to enhanced thermal tolerance. However, disadvantages to thermal plasticity have been identified for several coral species, suggesting acclimation may not always be beneficial. In order to better understand coral thermal acclimation, this dissertation investigated the short-term acclimatization potential of two foundational reef species to natural thermal variability, compared thermal performance with acute and cumulative exposures in the absence of acclimation, and explored the potential of corals to acquire thermal tolerance. The studies presented here put the thermal stress response in a dose context to enable cross-experiment comparisons. Corals under gradual stress showed physiological plasticity on the part of the animal, but any benefits appeared to be limited by the algal partner. Acquired thermal tolerance may reduce bleaching in the short term, but whether acquired tolerance can increase

recovery from bleaching requires investigation. Further, no signs of acclimatization to thermal microhabitat variability were detected in a seven-month period, and any small benefits of repeated thermal stress appeared to be short-lived. Hence, despite the adherence of coral respiration to the standing theory, there is overwhelming evidence that thermal acclimation, acclimatization and acquired thermal tolerance are insufficient to enable coral survival in the coming century. The majority of Scleractinian corals will not survive the pace of climate change, dictating the dire need for the restoration of the global carbon balance and other substantial human interventions.

This dissertation is dedicated to my mother, Mary Ellen Lynch, CNM, MS, for exposing me to the natural world, inspiring me to see its incredible beauty, indulging my curiosity and passion for marine ecosystems from my beginning and being the first woman in science in my world. She has worked tirelessly to provide me with unconditional love and encouragement. I would not be the scientist I am today, nor would I have had the grit to succeed in this endeavor, without her example, instilling in me the drive toward to a nearly unachievable level of excellency.

ACKNOWLEDGMENTS

This dissertation would not have been possible without the support of my village. I am incredibly grateful to my mentors, Dr. Holly Gaff and Dr. Richard Zimmerman, with whom I did not begin my doctoral journey, but who undoubtedly saved me from ending it too soon, by way of tremendous support, encouragement and advice. Holly's moral compass steered me through challenging seas. Dick, my Science Dad, drew intellect from me I didn't recognize and pushed me to excellence every time. I'd like to thank Dr. Dave Gauthier for his assistance with molecular work and Dr. Mark Warner who was an ear and expert for all things coral. I have learned so much and am appreciative.

I am thankful to the love of my life, Ryan, whom I met years into my journey, and has supported me in spite of myself, financially, emotionally and occasionally with code. The love and support of our parents and siblings have been a welcome harbor in PhD storms, and I am eternally grateful for their patience and feigned interest as I explained the intricacies of symbiosis. My beautiful nieces and nephews have given me so much joy and welcome distractions, particularly on research days that didn't go as planned. I have endless gratitude for my badass lady scientist friends Ashley Molinaro, Amanda Laverty, and Dr. Marla Valentine, who have cheered me on tirelessly, ate and drank with me, laughed with me, cried with me.

I would also like to thank the members of Old Dominion University's Tick Team and Bio Optics Research Group Lab, who welcomed me with open arms. This work would not have been possible without assistance from Thurman Gardner, John Sua, Samuel Meleisea, Dr. Jing Yu, amazing Nova Southeastern University volunteers and without the in-kind support from Drs. Dave Kerstetter, Bernard Riegl, Dave Gilliam and Abby Renegar at NSU, who opened their labs, tanks and boats to me in Florida.

This research was funded by Old Dominion University via start-up funds to D. J. Barshis, and more than 100 anonymous donations made to H. A. Martell through a Generosity Crowdfunding Campaign entitled “Training Corals to Resist Bleaching,” as well as a research award to H. A. Martell from ODU’s Biology Graduate Study Organization.

TABLE OF CONTENTS

Page

LIST OF TABLES

Table Page

Table Page

LIST OF FIGURES

Figure Page

Figure Page

Figure Page

Figure Page

INTRODUCTION

Coral reefs are among the most important ecosystems in the world (Costanza et al. 1997). Their high biodiversity (Knowlton et al. 2010) and productivity (Odum and Odum 1955) support more than one quarter of all commercially-important fish species and more than one third of all marine species (Knowlton et al. 2010, Fisher et al. 2015), providing food to billions of people (Cesar et al. 2003). Coral reefs form barriers that effectively dissipate wave energy, prevent coastal erosion and provide shore protection (Ferrario et al. 2014, Hernandez-Delgado 2015). Their ecosystem services generate billions of dollars, sustaining human livelihoods (Moberg and Folke 1999). Scleractinian corals have survived at least three extinction events since their appearance during the late Triassic Period (Stanley and Swart 1995, Lathuilière and Marchal 2009, Stanley et al. 2018), and their hermatypic role as geomorphic agents is estimated to have appeared in the last 25 million years (Falkowski and Knoll 2007). However, despite their long geologic age and great importance to humans, anthropogenic pressures of recent years, most notably climate change, severely threaten the persistence of coral reef ecosystems (Hoegh-Guldberg et al. 2007).

THE CORAL-ALGAL SYMBIOSIS

Hermatypic corals are animals that have evolved to rely upon endosymbiotic dinoflagellates belonging to the family Symbiodiniaceae (LaJeunesse et al. 2018a) for much of their energy requirements (Muscatine and Cernichiari 1969, Pearse and Muscatine 1971, Stanley and van de Schootbrugge 2009). This host-algal partnership, combined with a suite of associated

microbes and fungi (Rohwer et al. 2002), is referred to as a holobiont, wherein the colony behaves as an ecological unit (Knowlton and Rohwer 2003, Bosch and Miller 2016a). Under optimal conditions, corals provide their algae with protection, and the nutrients and substrate for photosynthesis (Muscatine and Cernichiari 1969, Steen and Muscatine 1987). In turn, algae provide the host with high energy reduced carbon (Muscatine and Cernichiari 1969, Crossland et al. 1980, Crossland 1987, Jackson et al. 1989, Jackson and Yellowlees 1990, Harland et al. 1992, Grottoli et al. 2006, Burriesci et al. 2012) that enables high productivity (Goreau 1959) and enhanced calcification (Pearse and Muscatine 1971, Gladfelter 1983).

Coral reefs typically occur in tropical, oligotrophic waters too deficient in plankton to support growth from heterotrophy alone (Muscatine and Porter 1977, Fournier 2013). Thus, the coral animal depends on the photosynthetically-fixed carbon translocated from its symbiotic algae to meet its metabolic demands, enabling reef accretion (Pearse and Muscatine 1971, Muscatine and Porter 1977, Muscatine et al. 1981, Glynn 1996). Healthy corals are necessary for the maintenance of healthy, productive reefs (Hughes 1994a, Hughes and Connell 1999, Hughes et al. 2003), and coral reef resiliency depends upon the health of individual corals (Hughes et al. 2003).

The amount of photosynthetically-derived nutrients provided to the host depends upon the light harvesting capability of the symbiont as well as nutrient availability. Light quality and quantity impact photosynthesis (Brunelle et al. 2007, Sorek and Levy 2012). In order to optimize photosynthesis under fluctuating conditions, algae possess photoacclimatory capabilities, such as alteration of the amount of chlorophyll or number and size of photosynthetic units in response to irradiance (Porter et al. 1984, Iglesias-Prieto and Trench 1994, Hennige et al. 2009). The algae are nutrient limited *in hospite* (Cook and Delia 1987, Hoegh-Guldberg and

Smith 1989, Jackson et al. 1989, Jackson and Yellowlees 1990, Lesser et al. 1994, Davy and Cook 2001, Koop et al. 2001, Davy et al. 2006), and their growth is regulated by the host (Smith and Hughes 1999) via control of mitotic division (Wilkerson et al. 1988, Jones and Yellowlees 1997) and host modulation of the *in hospite* light regime (Brunelle et al. 2007, Wang et al. 2008).

Studies have estimated 40 to 95% of carbon fixed by the algae is translocated to the host (Muscatine et al. 1981, 1984, Porter et al. 1984, Dubinsky et al. 1990). The nutrient contributions from algae to host are dynamic (Leletkin 2000), varying as a function of the environment (Anthony et al. 2007), and between individuals, as well as species, of both partners (Warner et al. 1996, Stat et al. 2006, Abrego et al. 2008, Stat and Gates 2011, Baker et al. 2015). Coral-algal associations exist along a continuum of symbiosis, ranging from mutualistic to parasitic, which makes understanding their relationship all the more complex (Lesser et al. 2013). Regardless, such a large contribution by the algae to the holobiont energy budget makes an intact symbiosis critical for coral fitness and survival.

CORAL BLEACHING

Holobiont symbiosis represents a delicate balance in community composition and function. When the holobiont becomes stressed, community composition can be drastically altered. This phenomenon is referred to as dysbiosis (Douglas 2003, Petersen and Round 2014). Holobiont dysbiosis due to stress in one or multiple partners can lead to the loss of algae (Glynn 1984), their photosynthetic pigments (McDougall et al. 2006), or both (Brown 1997). In severe cases, loss can be so great that the coral appears white, which has given rise to the term ‘coral bleaching’ (Glynn 1984).

Stress in general, and bleaching in particular, have been linked to reduced coral growth rates, inability to repair damaged tissue, and increased disease susceptibility (Brown 1997, Douglas 2003). If the stressful conditions are not promptly alleviated, bleaching leads to mortality (Glynn 1993, 1996), reducing reef biodiversity (Connell 1978, Connell et al. 2004). Coral skeletons are quickly bioeroded (Reaka-Kudla et al. 1996), and without their structure, there is loss of ecosystem function (Glynn 1993).

The 'oxidative theory of coral bleaching' suggested by Lesser (2006) posits bleaching is initiated when algae become photoinhibited under radiative and/or thermal stress (Mydlarz et al. 2010, Hoogenboom et al. 2012, Downs et al. 2013). This renders the Photosystem II (PSII) light harvesting complex unable to efficiently transfer the absorbed energy (Hoogenboom et al. 2012). Reactive oxygen species (ROS) accumulate in the photosynthetic machinery (Downs et al. 2013), creating the potential for cellular damage and eliciting a stress response within the chloroplasts and the citric acid cycle of the algae (Hillyer et al. 2016). In an attempt to mitigate damage from ROS, the host mounts an immune response (Weis 2008). This can lead to a reduction in algal density via several pathways, including autophagy (Brown et al. 2002a), apoptosis (Dunn et al. 2004), degradation (Weis 2008), and necrosis (Dunn et al. 2004). Declines in membrane lipids and reduced turnover of light harvesting complex structural D1 and D2 proteins also occur (Warner et al. 1996, 1999, Tchernov et al. 2004), leading to photodamage, a reduction of chlorophyll, and ultimately a net reduction in photosynthesis. Fluorescence-based photochemical efficiency decreases with increased temperature (Warner et al. 1996), putting more reliance upon non-photochemical quenching to manage excess energy. With reduced photosynthetic capacity, a deficit in holobiont metabolism occurs. As temperatures increase, respiration demands in both the host and algae increase, while ratios of

gross photosynthesis to respiration decrease (Coles and Jokiel 1977). Thermal stress in concert with ultraviolet radiation often leads to even more devastating effects (Lesser and Farrell 2004).

THERMAL STRESS AND MASS CORAL BLEACHING

The effect of temperature on corals has long been studied (Edmondson 1928). Coral thermal stress has been examined in the animal, across life history stages from larvae (Polato et al. 2010, Schnitzler et al. 2011) to adult corals (Coles and Jokiel 1977, Porter et al. 1984, Hoegh-Guldberg et al. 2007), and in the algae, both *in hospite* (Gates et al. 1992, Ainsworth et al. 2008) and *in vitro* (Dove et al. 2006). Thermal stress often leads to coral bleaching (Glynn 1996, Douglas 2003). Increases in the rate, magnitude and duration of warming make bleaching more severe (Hoegh-Guldberg 1999a). Consequently, thermal stress has been implicated as the predominant cause of global-scale coral bleaching events (Hughes 1994a, 1994b), referred to as 'mass bleaching.'

Mass bleaching events have increased in frequency and severity in recent decades (Glynn and D'Croz 1990, Hoegh-Guldberg et al. 2007, Heron et al. 2016, Hughes et al. 2017, Eakin et al. 2018, 2019). Such events are caused by prolonged periods of sea surface temperatures greater than 1°C beyond local maxima (Hoegh-Guldberg 2006), often driven by El Niño-Southern Oscillation (Glynn and D'Croz 1990). The 2014-2017 Global-Scale Coral Bleaching Event was the longest, most severe event in history (Eakin 2019, Heron et al. 2016, Hughes et al. 2017), causing mortality worldwide. For example, more than one third of the live coral cover on the Great Barrier Reef was lost (Hughes et al. 2017). There is no doubt that climate change implications for reefs are severe (Frieler et al. 2012), yet a growing body of evidence suggests corals may possess mechanisms to persist in the face of a changing ocean environment.

THERMAL TOLERANCE MECHANISMS

Coral thermal tolerance is the ability of corals to withstand large deviations from mean monthly sea surface temperature (Hoegh-Guldberg et al. 2007). Coral resiliency to climate change is largely based on coral thermal tolerance. Coral thermal tolerance limits are governed by standing genetic diversity (Barshis et al. 2013, Palumbi et al. 2014) and the mechanisms of acclimatization (Dunn et al. 2004, Castillo and Helmuth 2005, Haslun et al. 2011 Oliver and Palumbi 2011, Bellantuono et al. 2012a, b, Edmunds 2014) and local adaptation (Barshis et al. 2010, Kenkel et al. 2012, Kenkel and Matz 2016). The genotypes of the host and algal partners can influence thermal tolerance (Barshis et al. 2013, Berkelmans and Willis 1999). Recent research has sought to understand the capacity for corals to persist by: (1) acclimatization, whereby an organism adjusts its phenotype in response to the environment, or (2) local adaptation, wherein corals historically subjected to warmer temperatures become inherently more thermally tolerant by natural selection over generations (reviewed in Coles and Brown 2003, Barshis 2014). Current thermal adaptation theory states that variability and gradual increases in temperature can ameliorate thermal stress (Angilletta 2009). However, recent unprecedented mass bleaching events suggest rates of warming may outpace the ability of corals to persist, challenging this theory. Therefore, the scope of coral thermal tolerance limits must be quantified.

Corals may have the ability to acclimatize to non-lethal thermal stress, a concept referred to as acquired thermal tolerance (Brown et al. 2002a, 2014, Coles and Brown 2003, Middlebrook et al. 2008, Brown and Cossins 2011, Haslun et al. 2011, Bellantuono et al. 2012a). There is evidence that a particular type of acquired thermal tolerance, coral stress memory, contributes to overall thermal tolerance of individual corals (e.g., Brown et al. 2002a, 2002b, 2014,

Middlebrook et al. 2008). While stress memory has been well-characterized in a variety of taxa (Feder 1999, Guan et al. 2012, Walter et al. 2013, Arts et al. 2016, Domínguez-Andrés et al. 2019), it has not been explored for corals. The purpose of this dissertation was to investigate the thermal tolerance mechanisms of acclimatization and acquired thermal tolerance in scleractinian corals.

RESEARCH AIMS

The overall aim of this dissertation was to better understand the capacity of corals to acclimatize and persist with thermal stress based on current thermal adaptation theory. There were three main objectives:

(1) To test the acclimatization potential of two dominant massive coral species, *Porites lobata* and *Goniastrea retiformis*, to differing thermal variability and thermal magnitudes. Corals were moved to three sites with known differences in thermal variability and magnitude, where both species naturally occur. To account for possible confounding factors of thermal tolerance, all coral colonies were sourced from a single site of moderate thermal variability to control for local adaptation, and symbiont communities were characterized before and after the incubation period. Bleaching resistance was measured before and after seven-month incubations in the three sites.

(2) To examine thermal performance of *Acropora cervicornis* in acute heat shock and cumulative warming exposures, in the absence of acclimation, to determine whether gradual warming could ameliorate thermal stress. Thermal stress doses on par with a tidal cycle in a highly variable nearshore environment were applied (as identified in Objective 1), and holobiont respiration, gross photosynthesis, and photochemical efficiency were measured.

(3) To investigate the potential for acquired coral stress memory in *Acropora cervicornis*, by characterizing bleaching resistance in a standardized bleaching exposure both with and without pre-exposure to a sublethal dose of stress.

All experiments were intentionally conducted on short term timescales, due to the rapid and labile nature of current warming trends (Belkin 2009; Lima and Wethey 2012), and thermal stress doses were calculated to incorporate the magnitude and duration into a single value (i.e., degrees heating days, ° C days), making exposures comparable and ecologically relevant.

NO FREE LUNCH: BEATING THE HEAT COMES AT A COST FOR SOME CORALS

INTRODUCTION

Coral bleaching, the dysbiosis of coral host and symbiotic dinoflagellate, threatens the health of reefs worldwide (Hoegh-Guldberg et al. 2007, Hernandez-Delgado 2015) and potentiates downstream impacts on ocean health, human culture, and economics (Hughes 1993, 1994a, Brown 1997, Moberg and Folke 1999, Cesar et al. 2003, Ferrario et al. 2014). Mass coral bleaching is the wide-scale bleaching across species, reefs and seas globally (Glynn 1984). In the past few decades, anthropogenic ocean warming has led to an increase in the frequency and severity of mass bleaching events (Hughes et al. 2017). The main culprit of mass bleaching appears to involve several weeks of exposure to water temperatures at least 1° C above local mean monthly maxima (Lesser and Farrell 2004, Hoegh-Guldberg 2006).

The increased magnitude and frequency of global-scale bleaching events (Heron et al. 2016) suggests that hermatypic scleractinians will be unable to keep pace with the changing climate (Barshis 2014). Sea surface temperature (SST) observations and predictions suggest severe coral bleaching will occur annually in multiple locations within the next 20-50 years (van Hooidonk et al. 2016), making coral recovery in those areas impossible without intervention (National Academies of Sciences 2018). Some corals have the ability to withstand large deviations from mean monthly SST (Hoegh-Guldberg et al. 2007), referred to as thermal tolerance (Brown and Cossins 2011, Barshis 2014). Symbiont-host associations, and two important mechanisms, physiological acclimatization and local adaptation via natural selection, contribute to thermal tolerance. Like all organisms, it is possible all coral species possess these

mechanisms, albeit to varying degrees. Yet, there are limitations to even the most thermally tolerant corals (e.g., Coles and Riegl 2013); it is unlikely corals will persist via any single mechanism alone (van Hooidonk et al. 2016, National Academies of Sciences 2018). Therefore, to predict coral survival accurately, each factor that governs coral thermal tolerance must be considered.

Physiological acclimatization, the alteration of individual coral phenotypes in response to the environment, has been examined in the context of thermal tolerance. Corals have exhibited increased bleaching resistance (e.g., enhanced symbiont retention, antioxidant enzyme and heat shock protein abundances, and Photosystem II recovery potential) on portions of coral colonies previously exposed to high irradiance while the unstressed sides bleached (Brown et al. 2002a, 2002b). Some coral species, such as *Pocillopra eydouxi*, have displayed increased growth rates after being transplanted into warmer, more thermally variable environments (Smith et al. 2008), supporting the beneficial acclimation hypothesis (BAH), wherein "hotter is better" (Leroi et al. 1994, Edmunds 2014). Acclimatory responses such as these provide evidence that corals can improve their physiological performance in response to stress (reviewed in Coles and Brown 2003).

Both the host (Parkinson et al. 2015) and algal symbiont (Baker 2003, Baskett et al. 2009, Putnam et al. 2012) partners contribute to coral thermal tolerance; thus, to assess changes in thermal tolerance, identification of symbiont types is required. Certain algal types can bestow bleaching resistance to thermal stress (Baker 2004, Berkelmans and van Oppen 2006, Baker et al. 2008, Jones and Berkelmans 2010). For example, a common Pacific *Cladocopium* species, C15, has been attributed to the enhanced thermal tolerance of poritid corals (LaJeunesse et al. 2003). Symbionts belonging to the genus *Durusdinium* are considered tolerant opportunists (Stat

and Gates 2011, LaJeunesse et al. 2014, Hume et al. 2015), and *Durusdinium* spp. are often abundant on reefs that experience frequent local stressors (Mieog et al. 2007, Jones and Berkelmans 2010, Stat and Gates 2011). Yet, the same symbiont types in different locations can vary in thermal tolerance (Hume et al. 2013), suggesting that species-specific interactions between host and symbiont, and not just the symbionts are responsible for enhanced thermal tolerance (LaJeunesse et al. 2004, Abrego et al. 2008). Symbiont shuffling, a change in relative abundance of phylotypes following a stress event (Baker 2003, Jones et al. 2008, LaJeunesse et al. 2009, Cunning et al. 2015, Reich et al. 2017), and switching, wherein novel phylotypes are taken up from the environment (Baker 2001, Boulotte et al. 2016), can also occur, leading to changes in bleaching resistance.

There is also evidence that differential survival of thermo-tolerant individuals may result in local populations with increased thermal tolerance (i.e., local adaptation; Howells et al. 2012, Kenkel et al. 2012, Matz et al. 2018). Corals have been reported living at extreme temperatures in places around the world (Gardiner 1903, Vaughan 1914, Orr and Moorhouse 1933, Coles et al. 1976, Tomascik 1997, Craig et al. 2001), and those that routinely experience warmer water conditions or higher thermal variability (e.g., nearshore versus offshore and backreef versus forereef) often have increased thermal tolerance (Barshis et al. 2010, Kenkel et al. 2012). Their persistence in extreme thermal environments is a strong indication that the genetic material for survival is present in at least some corals, thus, to quantify thermal tolerance, local adaptation must be considered.

The islands of Ofu and Olosega, American Samoa provide naturally variable microhabitats that have been used to study thermal tolerance and acclimatization in hermatypic corals (Smith et al. 2007, 2008, Barshis et al. 2010, 2013, Palumbi et al. 2014, Bay and Palumbi

2015, Thomas et al. 2018). Corals moved to more thermally variable backreef pools from less variable sites have shown increased growth rates (Smith et al. 2007, 2008), higher protein levels (Barshis et al. 2010, 2018), and retention of pigments and symbionts in heat shock assays (Oliver and Palumbi 2011, Palumbi et al. 2014). Differences in the bleaching resistance of corals on Ofu Island have been related to symbiont species associations (Oliver and Palumbi 2009), differences in gene expression (Barshis et al. 2013), and thermal stress exposures (Bay and Palumbi 2015), revealing potential physiological mechanisms of acclimatization (Palumbi et al. 2014) that can act on short (daily to weekly) and/or long (monthly to yearly) timescales (Bay and Palumbi 2015).

The backreef lagoons of Ofu Island host at least 85 species of scleractinians (Craig et al. 2001). Many studies on Ofu Island have focused on bleaching resistance mechanisms in the fast-growing, branching species *Acropora hyacinthus* (reviewed by Thomas et al. 2018). Relatively less is known about the bleaching resistance of the slow-growing, massive species on Ofu and Olosega Islands. Two such massive species, *Porites lobata* and *Goniastrea retiformis*, are important reef-builders that are abundant on the shallow reefs of Ofu and Olosega Islands (Craig et al. 2001) and across the Pacific (Polato et al. 2010, DeVantier et al. 2014). Building on the existing work done in the region, acclimatization was examined in these long-lived, robust corals after relocation from a native thermal microhabitat characterized by moderate temperature variability to sites of high and low thermal variability. To assess coral thermal tolerance, donor and transplanted coral colonies were screened for changes in symbiont associations and measured four metrics of bleaching resistance before and after a seven-month acclimatization period. In this study, acclimatization was identified when a significant difference in the same direction was observed for at least two bleaching metrics.

MATERIALS AND METHODS

Field Sampling

A common garden transplantation experiment was conducted in the National Park of American Samoa on Ofu and Olosega Islands, Manu'a, American Samoa (14° 11' S, 169° 36' W, Figure 1). To simplify comparisons with previous studies, the site and naming convention defined by Craig et al. (2001) were employed here. The high (HV) and moderate variability (MV) sites lie in the backreef lagoon on the south coast of Ofu Island and form isolated pools during low tide, that routinely see austral summer water temperatures that range from 32° C to 35° C, and daily fluctuations of 6° C (Smith and Birkeland, 2007). In contrast, the low variability site (LV) is 3 km away, on the west side of Olosega Island, adjacent to a narrow channel separating the two islands, which leads to higher flow rates and thus a similar mean, but more stable temperature (Morikawa and Palumbi 2019).

In late June of 2015, approximately 40 nubbins (i.e., coral cores) of *G. retiformis* (n = 5 colonies) and *P. lobata* (n = 5 colonies) were cut from parent coral colonies growing in the moderate variability (MV) site using a 2.5 cm diameter hole-saw attached to a pneumatic drill and SCUBA tank. Nubbins were glued to a 2.5 cm hex-head nylon screw with marine epoxy and labeled with a plastic tag. The buoyant weight (g) of each nubbin was measured by placing it on a platform submerged in seawater and attached to a balance (Davies 1989). Nubbins were

Figure 1. Ofu (left) and Olosega Islands (right), Manu'a, American Samoa (image downloaded from Google Earth, 2016). The highly variable (HV, red) and moderately variable (MV, orange) sites are located in Toaga Lagoon (inset) on the south side of Ofu Island (photograph taken from an airplane by the author). The low variability (LV, blue) site is on the west side of Olosega Island adjacent to a narrow channel separating the islands.

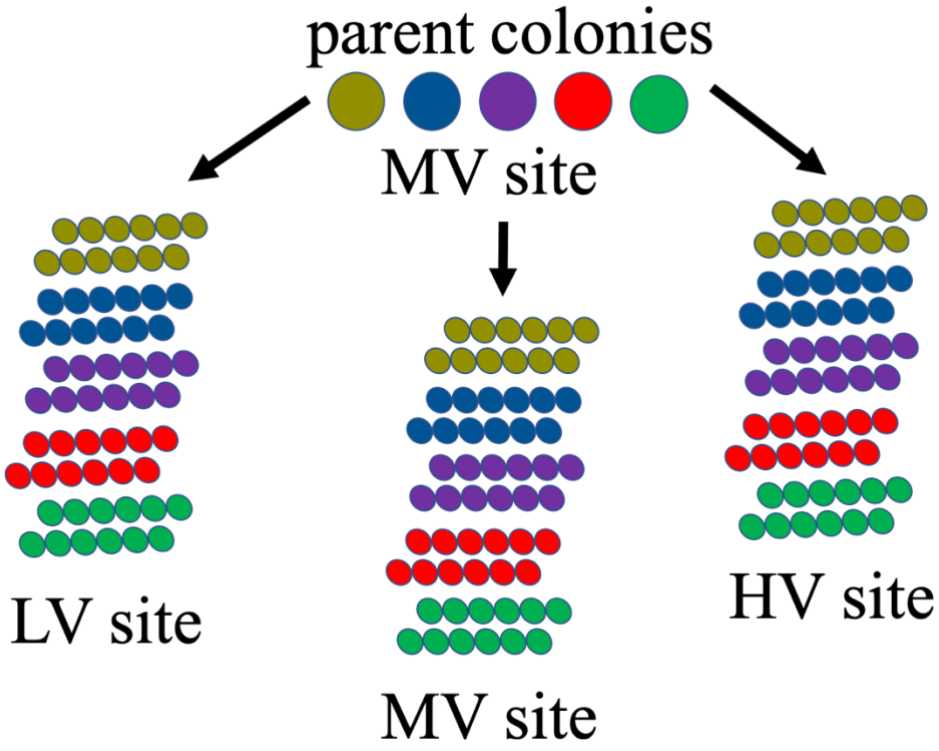

Figure 2. A cartoon of the transplantation experiment. Colors represent parent colonies. Large circles are parent colonies; small circles are coral nubbins. Nubbins native to the MV site were transplanted into the low variability (LV), moderate variability (MV), and high variability (HV) sites. Coral bleaching resistance was tested once before and five times after seven months of acclimatization.

affixed to 50 x 38 cm grids of egg crate material with nylon wingnuts, and all grids were returned to the donor MV site to heal after coring.

One week after nubbins were collected, one set of populated grids each were transplanted from the donor MV site into the LV, MV, and HV sites. Both species naturally occur in all three sites. Approximately 38 nubbins were placed on each set of grids so that a total of 12 nubbins of each parent colony (n = 5 colonies per species) were represented at each site (Figure 2). At the LV site, grids were attached to U-bolts with cable ties to two concrete slabs placed in the sand

(Figure 3a). At the MV and HV sites, grids were secured to re-bar that was hammered into concrete portions of the reef (Figure 3b). The depth of all grids was 1.25 to 1.5 m at mean low tide. Temperature loggers were attached to grids in each site to record *in-situ* temperature every 12 minutes (the greatest sampling rate without battery changes) for the duration of the acclimatization period.

Parrotfish predation had removed live tissues from *P. lobata* nubbins at the LV site ten days after coring, so twelve additional nubbins were cored, weighed and photographed from each of the same *P. lobata* parent colonies. These nubbins were transferred to the LV site and caged for two weeks to prevent further predation during healing. The delayed start of this treatment was accounted for in growth rate measurements.

Symbiont Genotyping

Symbiont ITS2 types were identified, and relative abundances (%) were compared in parent colonies between seasons, between parent colonies and nubbins within the MV site, and between sites after the acclimatization period to compare Symbiodiniaceae community composition. Samples of parent colonies were obtained in July 2015 and January 2016 (n = 20 samples). No nubbin tissue samples were taken for symbiont genotyping in 2015, as it was assumed replicate nubbins taken from the same general area of a parent colony harbored the same symbiont types and proportions as the parent colony. In January 2016, tissue samples were obtained from nubbins in the LV and MV sites (n = 1 nubbin per colony x 10 colonies x 2 sites = 20 samples). In the HV site, nubbins of both species were lost due to Cyclone Victor and mortality, leaving only three *P. lobata* nubbins and one *G. retiformis* nubbin available for tissue sampling (n = 1 nubbin per colony x 4 colonies = 4 samples).

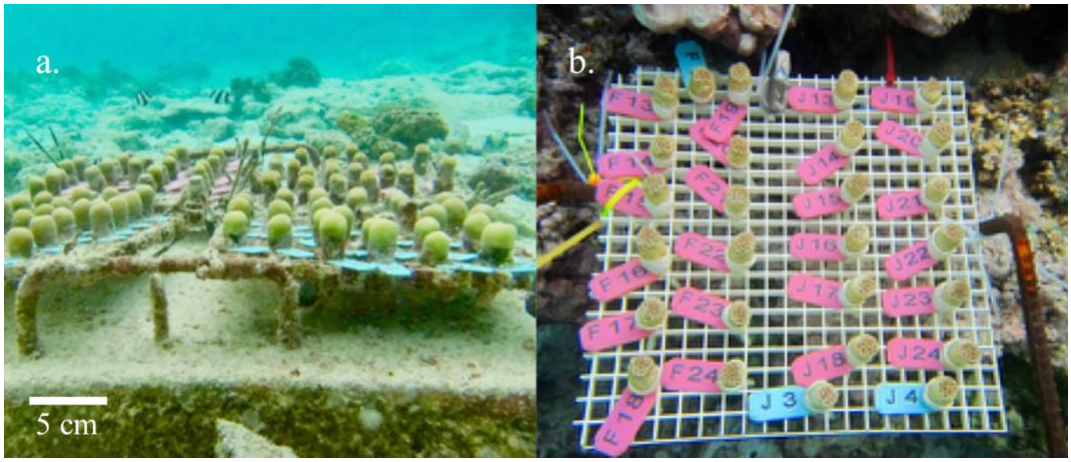

Figure 3. *P. lobata* and *G. retiformis* coral nubbins on grids secured by cable ties to rebar at the transplant sites. (a) A profile view of grids at the LV site on a concrete slab. (b) A plane view of a grid at the HV site attached to rebar hammered into the reef. Grids in the MV site were secured as in b (not shown).

Tissue sampling & DNA extraction

A small chip of coral tissue and skeleton (~1 to 4 g) was cut with a clean razor blade from each parent colony or nubbin and immediately placed in a vial containing 1% sodium dodecyl sulfate (SDS) in a DNA Buffer solution (0.4 M NaCl + 0.05 M EDTA in MilliQ water). Genomic DNA was extracted (Cunning et al. 2015) and agarose gel electrophoresis was used to confirm the presence of high molecular weight genomic DNA from each extraction. The absorbance of each sample was measured on a Nanodrop spectrometer to ensure adequate DNA concentration (> 100 ng uL^{-1}) and quality ($A_{260/280}$ > 1.8).

Target Amplification & Barcoding

The ITS2 region of symbiont DNA was amplified using polymerase chain reaction (PCR) to identify Symbiodiniaceae ITS2 strains in each sample. Briefly, standard PCR reactions were subjected to between 15 and 36 cycles of the following thermal profile: 95° C for 45 min | 95° C for 40 s (melting), 59° C for 2 min (annealing), 72° C for 1 min (extension) | 72° C for 7 min. To avoid overamplification, all samples were amplified until a faint band was detected (checking every 2-5 cycles), then PCR products were cleaned using the ExoSAP-IT PCR Product Cleanup kit following the manufacturer's protocol (Affymetrix™ product no. 78200/01/02/05/50). Hybrid barcoded primers were added to the ITS2 region of each sample using four cycles of the same thermal profile as above to enable multiplexing. The hybrid barcoded primers consisted of Illumina (Nextera) Primers (forward = AATGATACGGCGACCAC; reverse = CAAGCAGAAGACGGCATAC) + unique sequences (n = 8 forward and 6 reverse) plus a barcode sequence (forward = AGTCAA; reverse = GCTCTA) + an adapter sequence (forward = TCGTCGGCAGCGTC; reverse = GTCTCGGTCCGG). After barcoding, samples were run on a single gel to confirm an increase in size consistent with successful barcoding. All barcoded samples were pooled and sequenced in a single lane on an Illumina MiSeq.

Heat Shock Experiments

Nubbins of both species were assessed for bleaching resistance six times via standardized heat shock experiments. The first experiments were performed in July 2015 after nubbins had been transferred into the LV (12 days), MV (22 days), and HV sites (22 days). In January 2016, five additional, independent heat shock experiments were conducted after the seven-month acclimatization period in the LV, MV, or HV sites (183 to 211 days). The morning of each

experiment, two nubbins from each colony were collected from each site and brought to the lab in bins filled with seawater. Fleshy and crustose coralline algae were gently removed from the epoxy base of each nubbin with a wire brush on a rotary tool. All nubbins were weighed and photographed. One nubbin of each colony from each site was assigned to either the control or heat tank, so that paired nubbins were split between treatment tanks.

Each tank system was comprised of an experimental tank and sump tank constructed from 25 L insulated coolers and outfitted with an Arduino-based temperature control box (Figure 4). Circulation between the experimental and sump tanks were driven by a 450 W pump and a gravity return. Each experimental tank had a set of 6 white LED lamps and a diffuser that supplied 450 to 500 μmol photons s^{-1} m^{-2} from 0700 h to 1800 h after local sunrise and sunset. Flow-through seawater was supplied at a rate of 7.2 L h^{-1} to all experimental tanks from a large, common seawater reservoir, and the addition of water to the system was balanced by outflow through the sump overflow. All experimental systems were filled with fresh seawater and allowed to stabilize to a temperature of 28° C (mean local field seawater temperature) before nubbins were introduced.

Each heat shock experiment began at noon each day (0 h) and ended at 1000 (22 h) the following morning. The control temperature remained at 28° C while corals in the heated tanks were subjected to a temperature increase from 28° C to T_{MAX} over 3 h, held at T_{MAX} for 3 h, then returned to 28° C within 6 h and held at 28° C overnight (Figure 5). Preliminary experiments were conducted at a series of temperatures to determine the T_{MAX} that would result in ~50% bleaching of corals at the conclusion of the 22 h experiment for each species (*G. retiformis* T_{MAX} = 36° C; *P. lobata* T_{MAX} = 36.5° C, D. Barshis, *unpubl.*). During the 2016 experiments, in-tank measurements of dark-adapted photochemical efficiency of photosystem II (F_V/F_M) were taken in

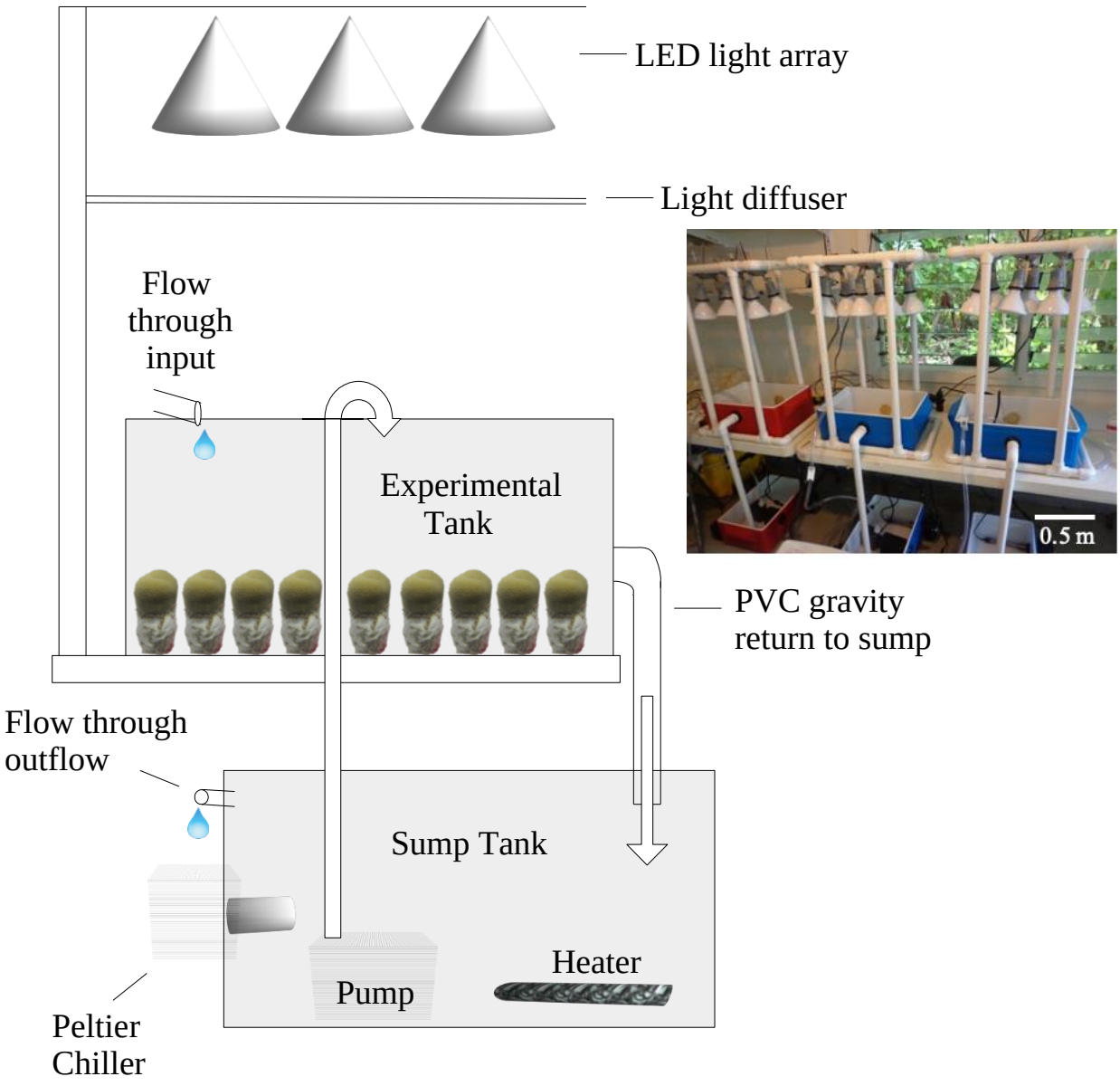

Figure 4. A diagram of a tank system used in heat shock experiments. Each system included an experimental tank and sump tank with flow through seawater, a 6-LED light array, and a temperature controller (not shown) that powered two Peltier chillers and a submersible titanium heater. Three tank systems in the lab on Ofu Island are pictured in the photograph taken by the author (right).

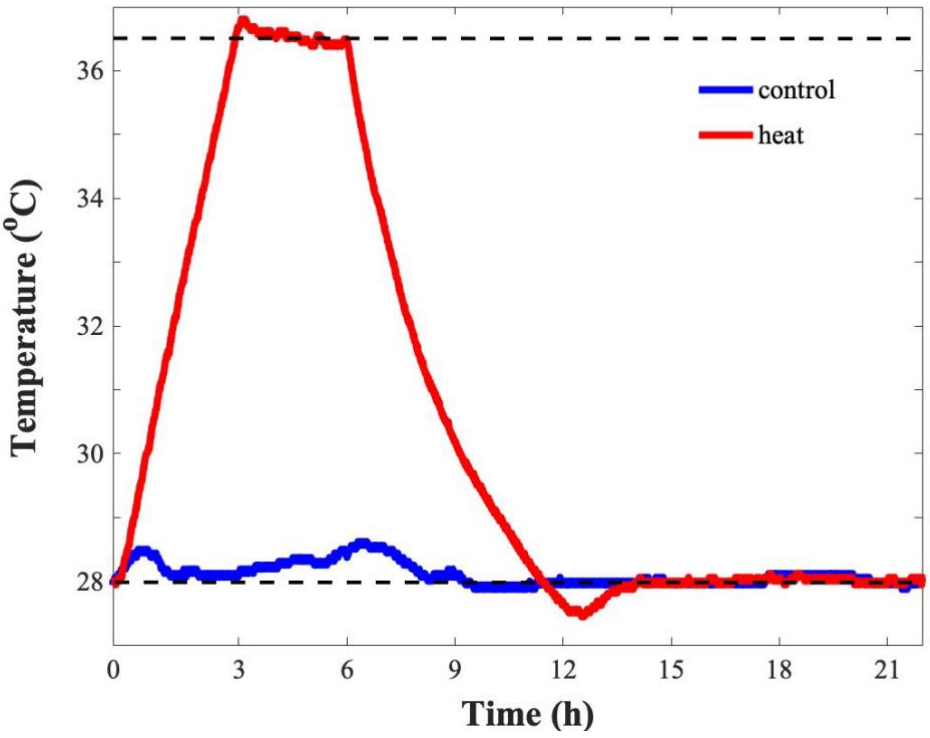

Figure 5. The temperature time-course of a standard heat shock experiment; control tanks were 28° C, while corals in the heat tanks were subjected to an increase in temperature from 28° C to T_{MAX} (3 h), held at T_{MAX} for 3 h, and then cooled to 28° C overnight (~ 6 h). All corals were removed at 22 h. The dotted black lines are the set temperatures of the control (28° C) and heat tank (T_{MAX} = 36.5° C). The blue and red lines are actual tank temperatures measured continuously via loggers in the experimental tanks.

triplicate and averaged for each coral at 0 h (12:00) and 21 h (09:00) the following morning with a pulse amplitude modulation chlorophyll fluorometer (Heinz Walz GmbH). At the conclusion of each experiment (22 h), all nubbins were wrapped in foil and frozen at -20° C until they were processed (3 to 21 days).

Frozen coral processing

Coral nubbins were thawed at room temperature. Tissue was removed from the skeleton using an airbrush gun (~100 psi) and seawater, collected in a tube, and homogenized with an electric homogenizer for at least 30 s on ice in the dark to prevent chlorophyll degradation. In July 2015, the homogenate volumes of all samples were recorded, and an aliquot of homogenate was fixed in zinc-formaldehyde solution (Z-fix) for cell counting via flow cytometry. The remaining homogenate was used to determine chlorophyll concentration as described below. Sample volumes in 2016 were much larger, thus the homogenate was spun down at 5000 x *g* for 2 minutes, and the pellet was resuspended in a standard volume with artificial sterile seawater measured by refractometer (salinity = 35 PSS-78, Lewis 1980) and preserved with formaldehyde (1% final concentration). Processed coral skeletons were dried at 55° C for at least 24 h and weighed. Surface area of each nubbin was determined by the wax method (Stimson 1991). Briefly, nubbins were weighed on a balance before and after being dipped in hot wax (65° C), then the weight of the wax was used to determine surface area based on a standard curve.

Symbiont Density

Preserved aliquots for cell counting were push filtered through a 35 μm mesh to remove large non-algal particles and stored at 4° C until cells were counted on a BD FACS Aria II cell

counter and sorter. Fluorescent green (488/510nm) and red (570/600nm) flow cytometry beads were added to each sample immediately prior to counting (Thermo Scientific™ FC7 Cyto-Cal™ Count Control, Catalog #09-980-698, 7μm microspheres). All nine fluorescence channels were examined in pairwise scatterplots to determine the parameter combination that provided the best differentiation of the symbiont cell population. Cells were gated on size and chlorophyll autofluorescence using the Per CP-A vs. PE-A channels for samples and APC-A vs. PE-Texas Red channels for beads. Two heated and two control samples were randomly selected and sorted with the BD FACS Aria II for examination under the microscope to confirm the counted cells were the target of interest. A single gating was applied to all samples, and symbiont cell counts were adjusted by the fraction of beads counted in each sample to calculate the final cell concentration. Sample concentrations were multiplied by aliquot dilution factor and scaled to total sample volume. Final cell concentrations were normalized to coral surface area.

Total Chlorophyll

The remaining homogenate was centrifuged at 5000 x *g* for 10 minutes, and the pellet was resuspended in a known volume of 90% acetone, sonicated for 20 s on ice in the dark and extracted for 24 h at -20° C. Samples were centrifuged at 5000 x *g* for at least 1 min, and the extract absorbance was measured with an STS VIS spectrometer and BluLoop lamp (Ocean Optics). Resulting spectra were blank corrected for the absorbance of 90% acetone, and the difference in mean absorbance between 715 to 725 nm was subtracted from absorbance at every wavelength from 400 to 725 nm to account for any residual turbidity. Chlorophyll *a* and c_2 concentrations were calculated using the spectrophotometric equations for Cnidarian dinoflagellates (Jeffrey and Haxo 1968), normalized to surface area (cm^2), summed to give total

chlorophyll (Chl), and expressed as μg cm^{-2}. Chl per algal symbiont cell was also calculated for each sample by dividing the Chl by the cell density and expressed as pg Chl $cell^{-1}$.

Analyses

Analyses were performed in Matlab 2017a and R v. 3.5.1. Sea surface temperature data were retrieved from NOAA's Coral Reef Watch program to obtain the mean monthly maximum sea surface temperature of Ofu Island in January 2016 (NOAA Coral Reef Watch 2017a). Temperature data from each site were obtained from HOBO loggers (Onset Corp.), and the thermal stress at each site was quantified as degree heating days (DHD), by taking the sum of the magnitude and duration of temperatures > 30° C from the preceding 84 days (12 weeks) over the seven-month transplant period. The temperature series at each site were analyzed with fast Fourier transform (FFT). Briefly, Fourier transform was used to decompose the time function of the temperature series into frequencies represented by a sum of sine waves of different periods, in order to identify the dominant periods in the series at each site. Periodograms of the variance in the component frequencies as a function of time (i.e., power spectra) were constructed. The peaks were examined to compare patterns and identify the drivers of thermal stress at each site.

Growth rate (% $month^{-1}$) was calculated for each nubbin as the difference in buoyant weight (initial minus final weight, g), normalized by the initial buoyant weight (g) x 100 and the time (months) between weight measurements. Growth rates did not meet assumptions for normality (Shapiro-Wilk test) or equal variances (Bartlett's test), thus a non-parametric Kruskal Wallis (KW) test was performed to compare January 2016 growth rates between sites for each species (*P. lobata*: n = 51, 50, 48; *G. retiformis*: n = 50, 50, 37 in the LV, MV, and HV sites,

respectively). When a significant difference in growth rates was found, a Dunnett's *post hoc* test was performed with the MV site as the control.

Reaction norms (i.e., ratios of heated to control nubbins) were calculated, which gave the symbiont density, Chl cm^{-2}, and Chl $cell^{-1}$ retention of every colony pair from each of the three sites in all heat shock experiments. Retention was calculated to make these results comparable to previous work done on Ofu Island (Palumbi et al. 2014). F_V/F_M retention was calculated for each individual coral, as the ratio of the final F_V/F_M at 21 h (after the heat shock exposure) to the initial F_V/F_M at 0 h (prior to heat shock), which gave $\Delta F_V/F_M$. Bleaching responses were non-normal; thus, non-parametric KW tests were performed for all bleaching resistance ratios to test for differences among sites. If significant differences were noted, a Dunnett's *post hoc* test was performed to compare other sites to the control (MV) site. Initial "pre-incubation" bleaching resistance ratios obtained in July 2015 were tested for differences between each site, to determine whether the nubbins transplanted to each site began with the same bleaching resistance. Seasonal patterns in coral bleaching resistance have been observed (Berkelmans and Willis 1999); thus, to identify a seasonal shift in bleaching resistance, bleaching resistance ratios from July 2015 were compared to the mean ratios from MV nubbins of all five post-acclimatization experiments in January 2016. Finally, post-acclimatization bleaching resistance ratios from January 2016 were compared to identify phenotypic shifts in bleaching resistance as a result of moving corals into the HV or LV site. Chl and F_V/F_M changes can occur on the order of hours to weeks (Fitt et al. 2000; Warner and Berry-Lowe 2006; Winters et al. 2009); thus, acclimatization was identified only when a significant difference in the same direction was observed for at least two bleaching metrics.

Symbiont Community Composition

Algal symbiont species were identified using the sequences of ITS-2 nrDNA. Hybrid primer sequences (including the degenerate adapter and barcode bases) were identified and removed from all sequences using regex at the command line. Resulting ITS2 sequences free of hybrid primers were screened for quality scores using the Illumina threshold (Q>33), and low-quality reads were discarded at the command line. Quality profiles were plotted for all samples, and sequence lengths were trimmed at 240 base pairs (bp) for forward reads and 160 bp for reverse reads using the DADA2 pipeline v. 1.8 in R (Callahan et al. 2016). Error rates were examined, identical sequences were de-replicated, and the core algorithm was applied to infer samples. One sample, a *Goniastrea retiformis* parent colony from 2015, had low read count (samples HAH08, n = 7 reads), and thus was removed from remaining analyses. Paired-end reads were merged, and 1 chimera was detected in a single sample (HAH41) and removed, resulting in 26 unique operational taxonomic units (OTUs). ITS-2 sequence lengths were between 252 and 318 bp, but most OTUs were 300 bp in length.

A maximum likelihood phylogeny was constructed using the MUSCLE algorithm (Qiagen Aarhus A/S) in CLC Genomics Workbench v 9.5.2. The optimal phylogeny model type (HKY) was determined using jModelTest v2.1.1 (Guindon and Gascuel 2003, Darriba et al. 2012), from a Symbiodiniaceae database containing 435 unique sequence variants (Franklin et al. 2012) and the OTUs from this study. OTUs on the same tree nodes were compared to the top BLASTn hits from two separate BLAST results: (1) NCBI's nr database and (2) a custom Symbiodiniaceae database derived from Arif et al. (2014). Any OTUs with the same top BLAST hit that were less than 0.003 apart in node distance and differed by < 5 bp were assumed to be intragenomic variants and collapsed. The tree was reconstructed, and the top BLASTn hits from

both databases were compared to identify symbiont genera and types. Consensus occurred when there was agreement of genus and type from both database top hits. When there was not consensus between top database hits, the custom Symbiodiniaceae database that provided the highest type resolution was always preferred over genus level classification based on the NCBI nr hit.

Relative abundances of sub-clade symbiont types were visualized in R v 3.5.1 using the ampvis2 package (Andersen et al. 2018), following the most recent revision of the family into Symbiodiniaecae genera (LaJeunesse et al. 2018). It was assumed rare Symbiodiniaecae types (< 0.05 %) would not amount to any differences in bleaching resistance in this study; thus, they were removed from remaining analyses. Bray Curtis Indices were calculated, and PERMANOVAs were used to identify significant differences in symbiont community composition.

RESULTS

Temperature

In situ temperature series revealed increasing thermal variability in the MV and HV sites with the progression of the austral summer, and temperature maxima were greatest in the HV site and the least in the MV site (Figure 6), confirming previously characterized differences in site variability. The mean monthly maximum SST of Ofu Island was 29° C in January 2016 (NOAA Coral Reef Watch 2017a). Thus, DHD were calculated based on the local threshold for bleaching (30° C), and there was a significant gradient in thermal stress dose across the three sites (Figure 7). Corals were transplanted to each site in July 2015 of the austral winter, before the onset of

the summer period of thermal stress (Figure 7). Thermal stress values greater than zero were detected in mid-October, 88 to 100 days after transplanting. However, site thermal stress began to diverge as the austral spring progressed, with sites representing a gradient of thermal stress doses by the summer (Figure 7). The LV site had negligible thermal stress and the fewest DHD for the seven-month duration, while the MV and HV sites had moderate and high thermal stress, respectively (Figure 7).

Fast Fourier transform (FFT) periodograms revealed that all three sites shared a predominant peak at 1 d, and smaller common signals at 15 d and 17 d (Figure 8). A closer look revealed that peaks were present at 23.98 h for all three sites, but differed in magnitude, indicating that solar insolation was the primary driver for warming at all sites (Figures 9, 10). A series of smaller peaks were observed at 8 h, 12 h, and between 24.3 h and 25.9 h (Figure 9). The 12 h peak is likely a harmonic of the major peak at 23.98 h (Figure 9). There were also smaller signals with the same period around 24 h that differed in magnitude, such as the 24.68 h feature (Figure 10). These smaller signals around 24 h were likely reflections of tidal oscillations, as the tidal cycle in American Samoa oscillates between 24 h 30 min and 24 h 45 min. Variance in peaks occurred at 9 d, 26 d, 30 d and 42 d, with peak height differences occurring between the LV and the more variable sites.

Growth

The growth rates of both coral species moved to the HV site were significantly lower than growth rates in the MV or LV sites (Figure 11, Table 1a, b). *P. lobata* growth rates were 1.58 % month^{-1} higher in the LV site and 1.22 % month^{-1} lower in the HV site, compared to the native MV site (Table 1b). There was no difference in growth of *G. retiformis* between the LV

and MV sites, but both groups grew 1 % month^{-1} faster than *G. retiformis* nubbins placed at the HV site. There was no significant effect of time or the interaction of site × time on growth rates for either species (Table 1a). In addition to reduced growth, endolithic, encrusting and turf algae growth was observed on several *P. lobata* nubbins in the HV site (Figure 12).

Bleaching Resistance Ratios

There were no significant between site differences in initial bleaching resistance for either coral species in July 2015, < 22 days after transplantation (Figure 13, Table 2). As such, July 2015 retention ratios of all three sites were averaged to represent the baseline bleaching resistance at the start of the acclimation period, and mean 2015 bleaching resistance ratios were used in further analyses. There were no significant changes in bleaching resistance of MV corals from July 2015 to January 2016 in either species (Figure 14, Table 3). In January 2016, significant differences in bleaching resistance ratios were detected in *P. lobata*, but not *G. retiformis*, across sites after the seven-month acclimatization period (Figure 15, 16, Table 4a). However, *post hoc* comparisons of *P. lobata* bleaching resistance ratios revealed only one significant difference (for F_V/F_M) between the native MV site (i.e., control site) and any transplant site (Table 4b); thus, significant differences in bleaching resistance ratios were due to differences between HV and LV corals. *P. lobata* from the LV site experienced greater reductions in F_V/F_M compared to those from the MV in heat shock experiments ($p = 0.008$), indicating the LV corals were more subject to bleaching.

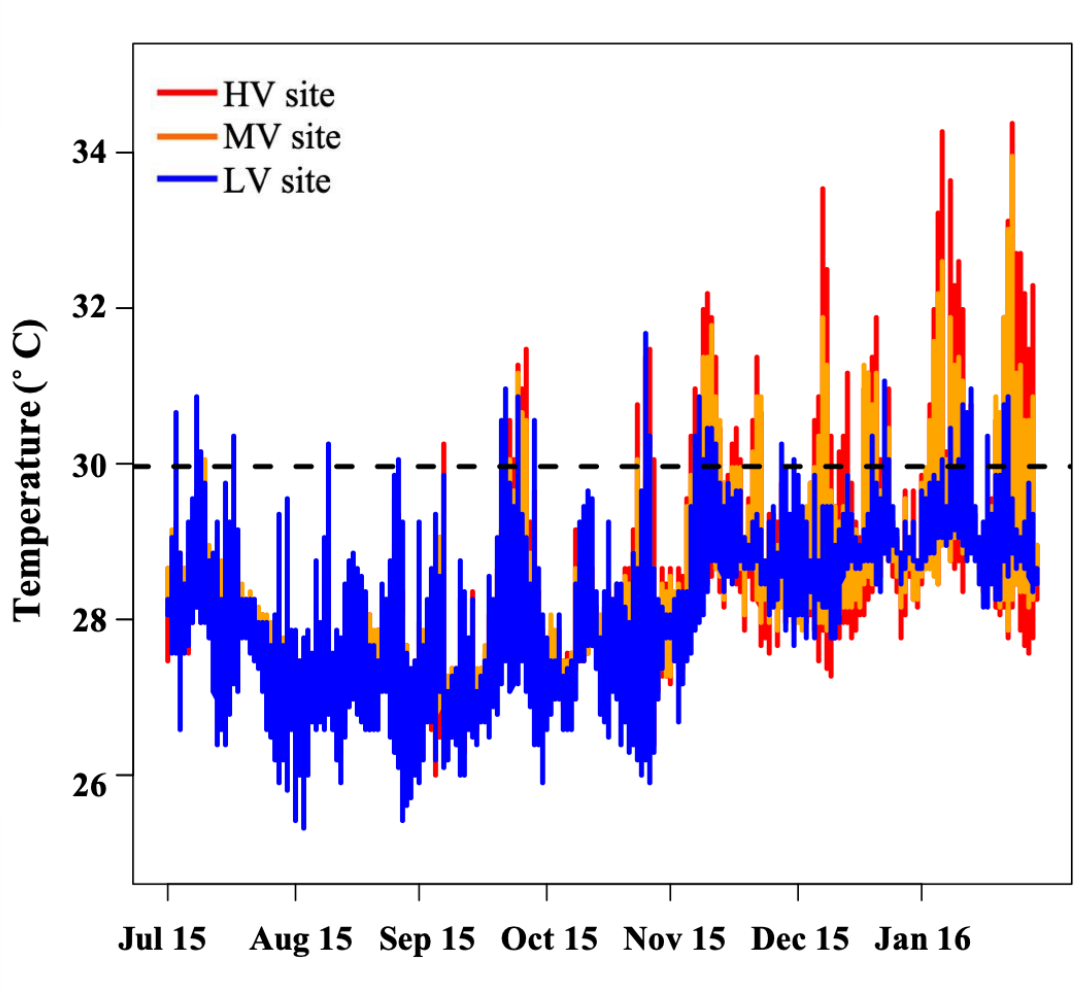

Figure 6. The 7-month temperature series of three sites on Ofu and Olosega Islands, American Samoa. The black dotted line is the local bleaching threshold in January 2016 (NOAA Coral Reef Watch 2017a).

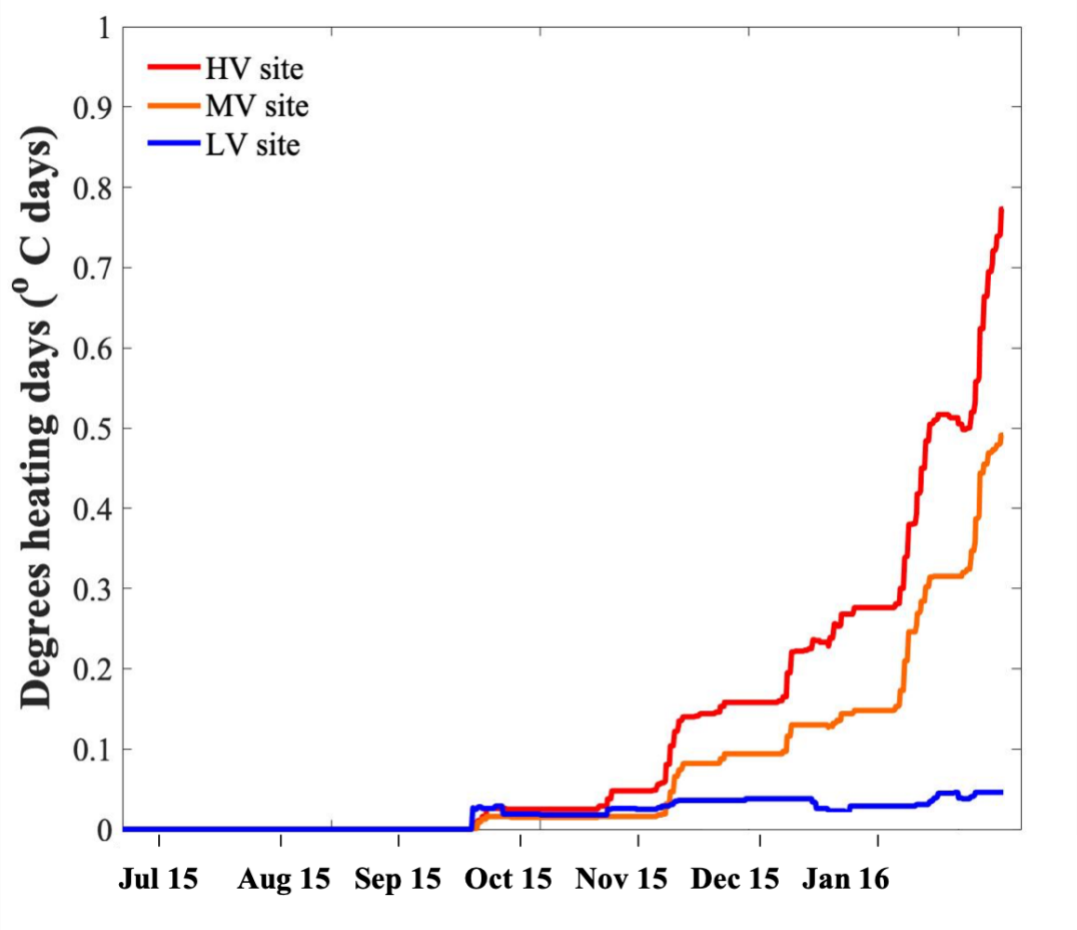

Figure 7. The thermal stress dose for three sites in the Manu'a Islands, American Samoa, expressed as the 84-day (12-week) rolling average of degrees heating days (DHD, ° C days) for over a 7-month incubation period.

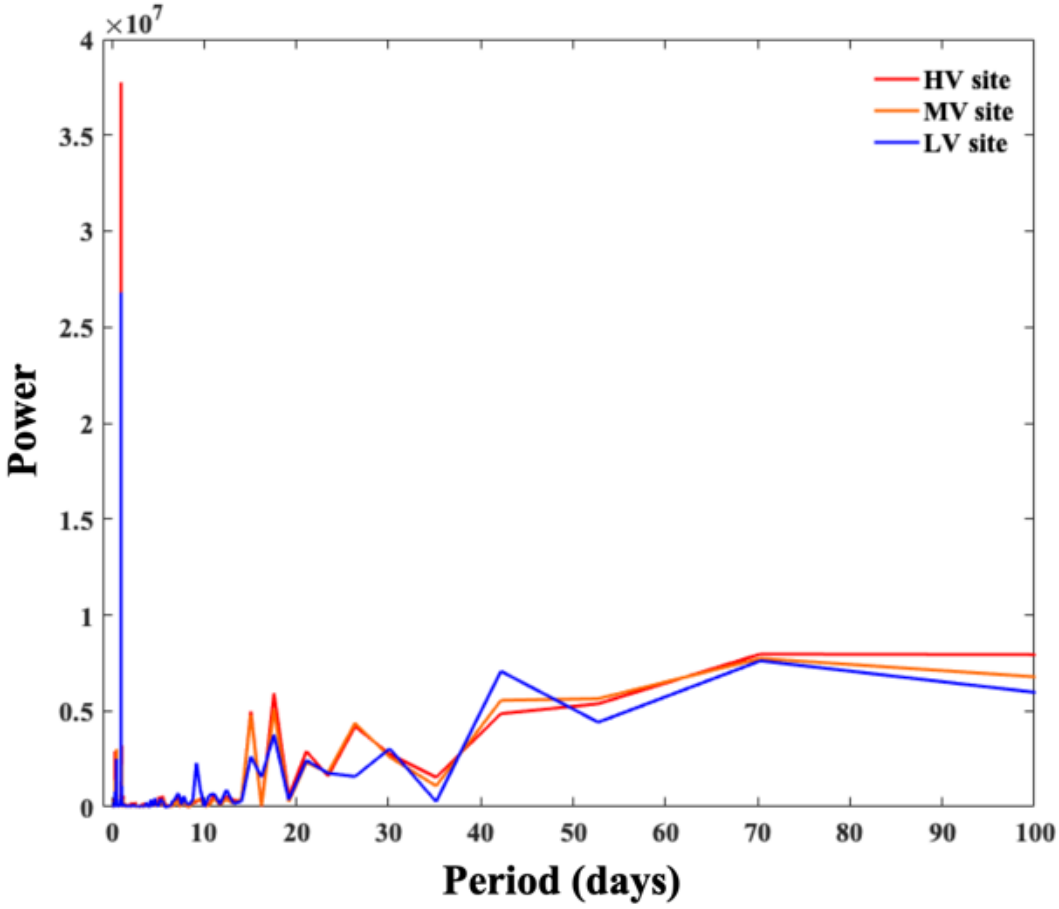

Figure 8. Fast Fourier transform periodograms of the power spectra (i.e., the variance in DHD) at each site over days.

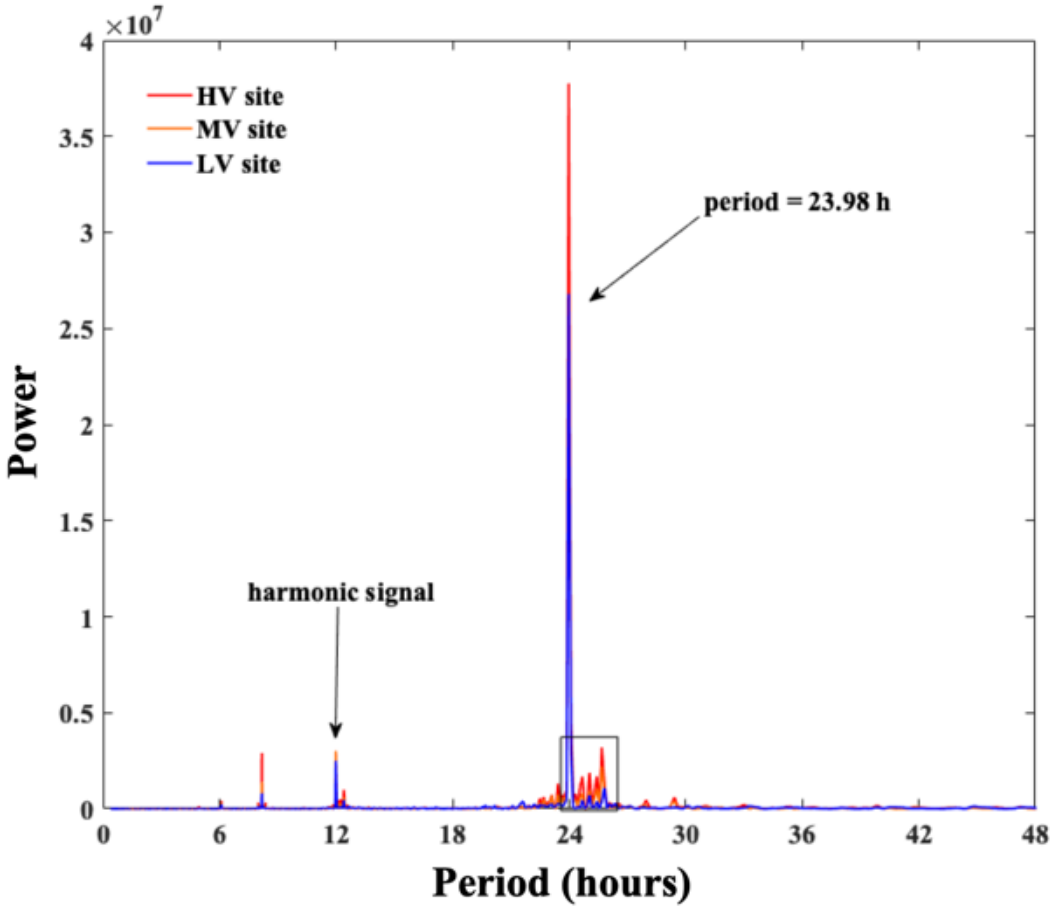

Figure 9. Fast Fourier transform periodograms of the power spectra (i.e., the variance in DHD) at each site from the first 48 hours.

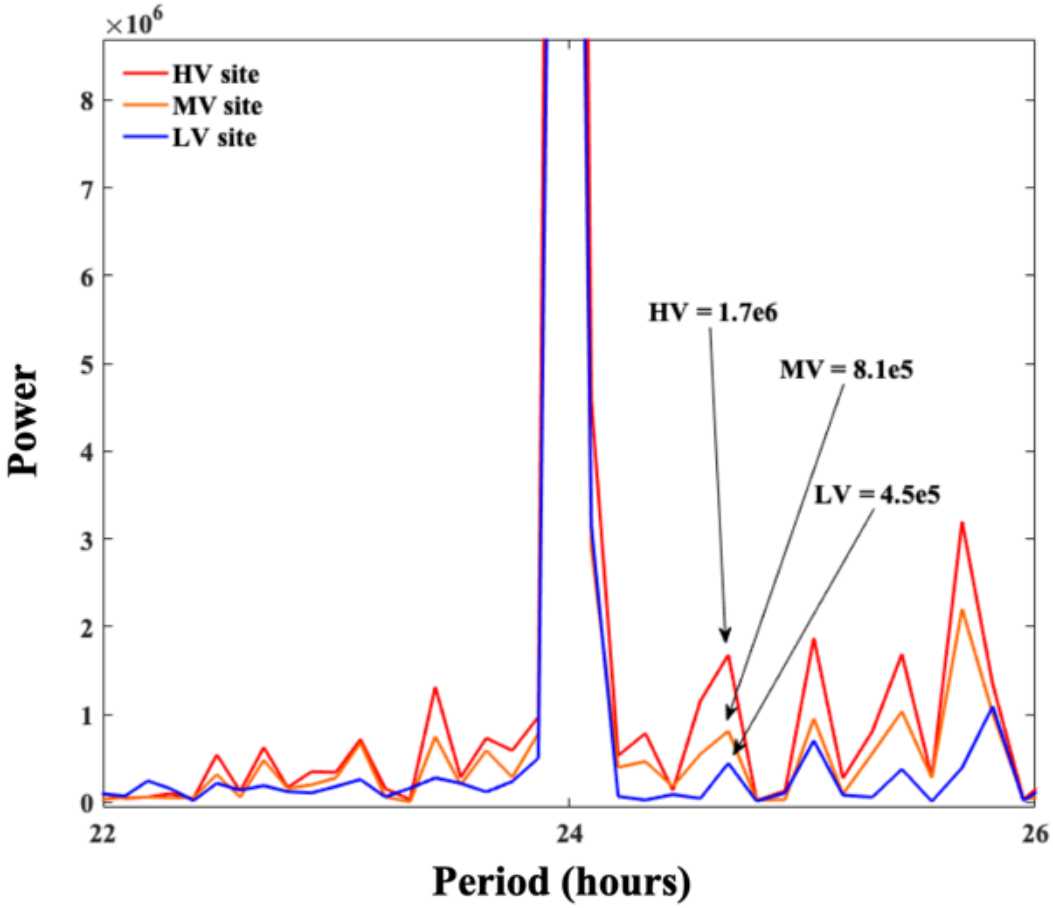

Figure 10. Fast Fourier transform periodograms of the power spectra (i.e., the variance in DHD) at each site from the 22- to 26-hour period.

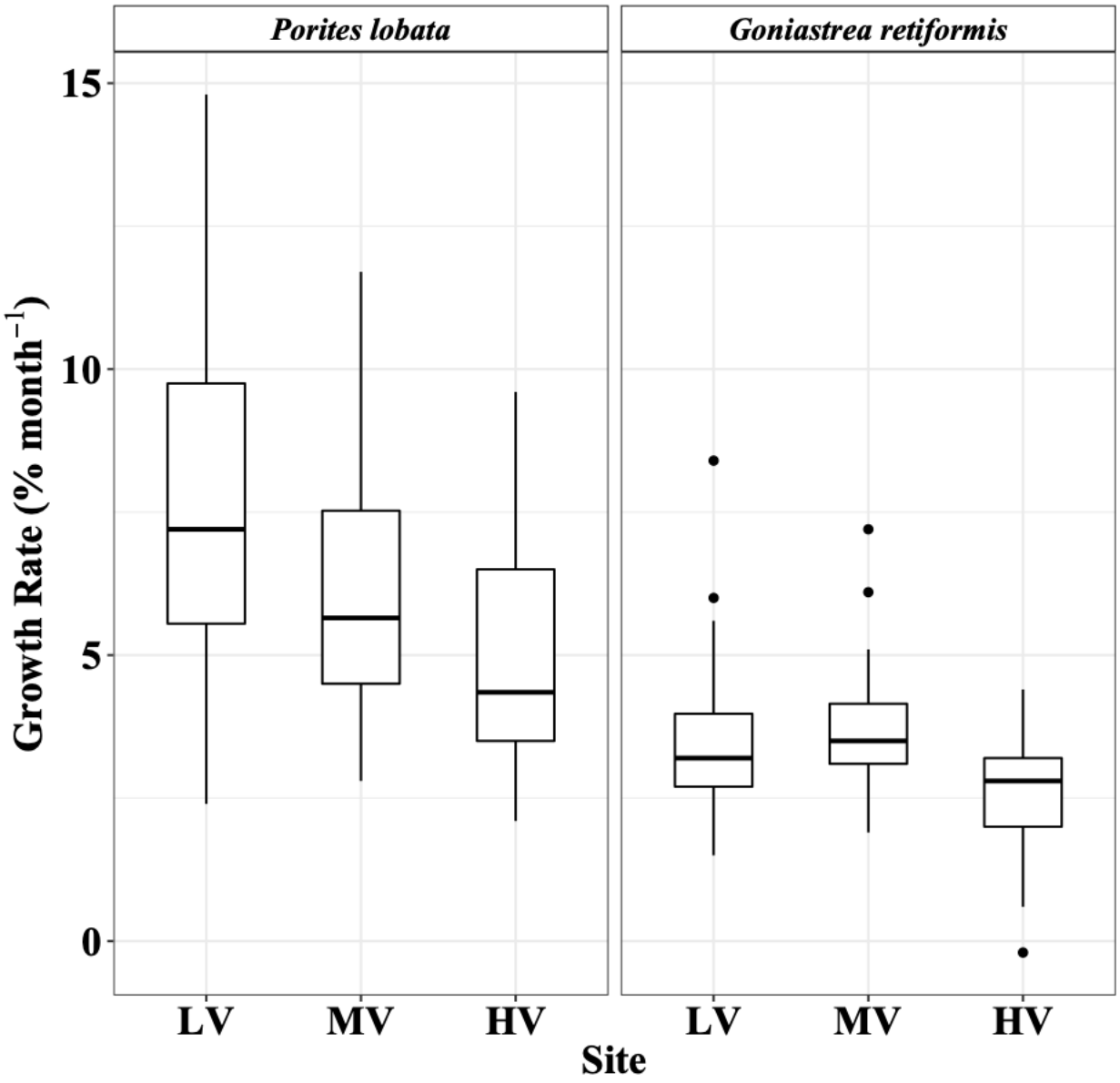

Figure 11. Growth rates (% month^{-1}) of *Porites lobata* and *Goniastrea retiformis* nubbins grown for seven months in sites of low (LV), moderate (MV) and high (HV) thermal variability on Ofu and Olosega Islands, AS. Thick horizontal bars are median growth rates, thin horizontal lines are quartiles, whiskers are 2 standard errors, and points are outliers.

Table 1. (a) Results of the Kruskal Wallis test for differences between sites and timepoints on growth rates (% month^{-1}) of *Porites lobata* and *Goniastrea retiformis* corals moved into three thermal microhabitats. χ^2 is the critical value of chi-squared, *df* is degrees of freedom, *p* is the *p*-value (α <0.05). (b) Dunnett's *post hoc* comparisons to the control (MV) site, with the estimated difference, lower and upper confidence intervals (CI, 2 standard errors) and *p*-values.

a.

Species	Effect	χ^2	*df*	*p*
Porites lobata	Site	23.37	2	**8.43E-6**
	Time	1.99	4	0.74
Goniastrea retiformis	Site	18.59	2	**9.21E-5**
	Time	1.25	4	0.87

b.

Species	Comparison	Difference	Lower CI	Upper CI	*p*
Porites lobata	LV - MV	1.580	0.46	2.70	**0.004**
	HV - MV	-1.215	-2.35	-0.08	**0.034**
Goniastrea retiformis	LV - MV	-0.184	-0.67	0.30	0.605
	HV - MV	-1.033	-1.56	-0.51	**4.00E-5**

Figure 12. Photographs comparing *Porites lobata* coral nubbins in the HV (a), MV (b), and LV (c) sites after a seven-month acclimatization period.

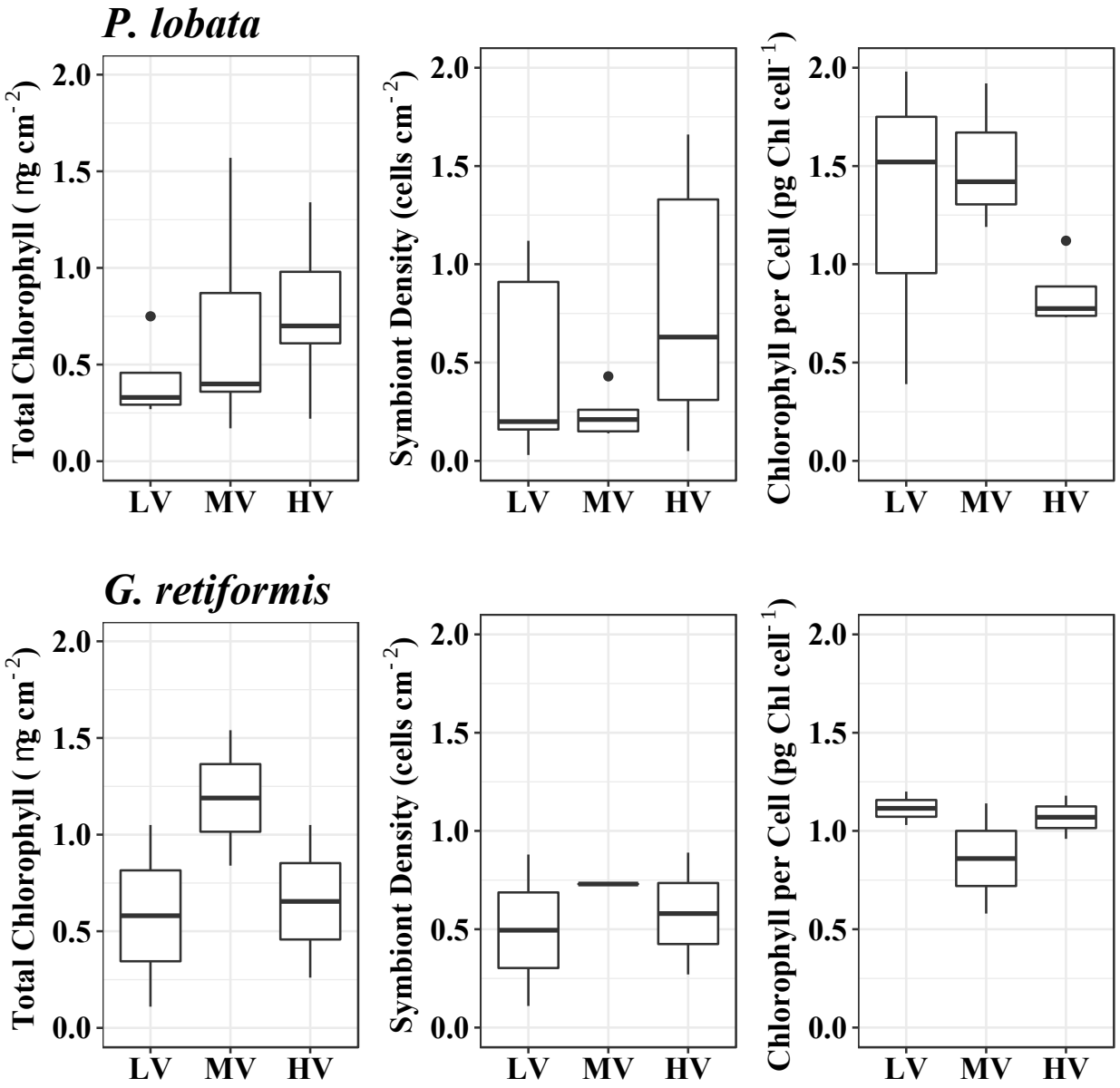

Figure 13. Bleaching resistance ratios, expressed as ratios of heated:control nubbins, to give total Chl cm^{-2}, symbiont density, and Chl $cell^{-1}$ comparing resistance of *Porites lobata* (top panel) and *Goniastrea retiformis* (bottom panel) between sites at the start of the acclimatization period (July 2015). Thick horizontal bars are median growth rates, thin horizontal lines are quartiles, whiskers are 2 standard errors, and points are outliers.

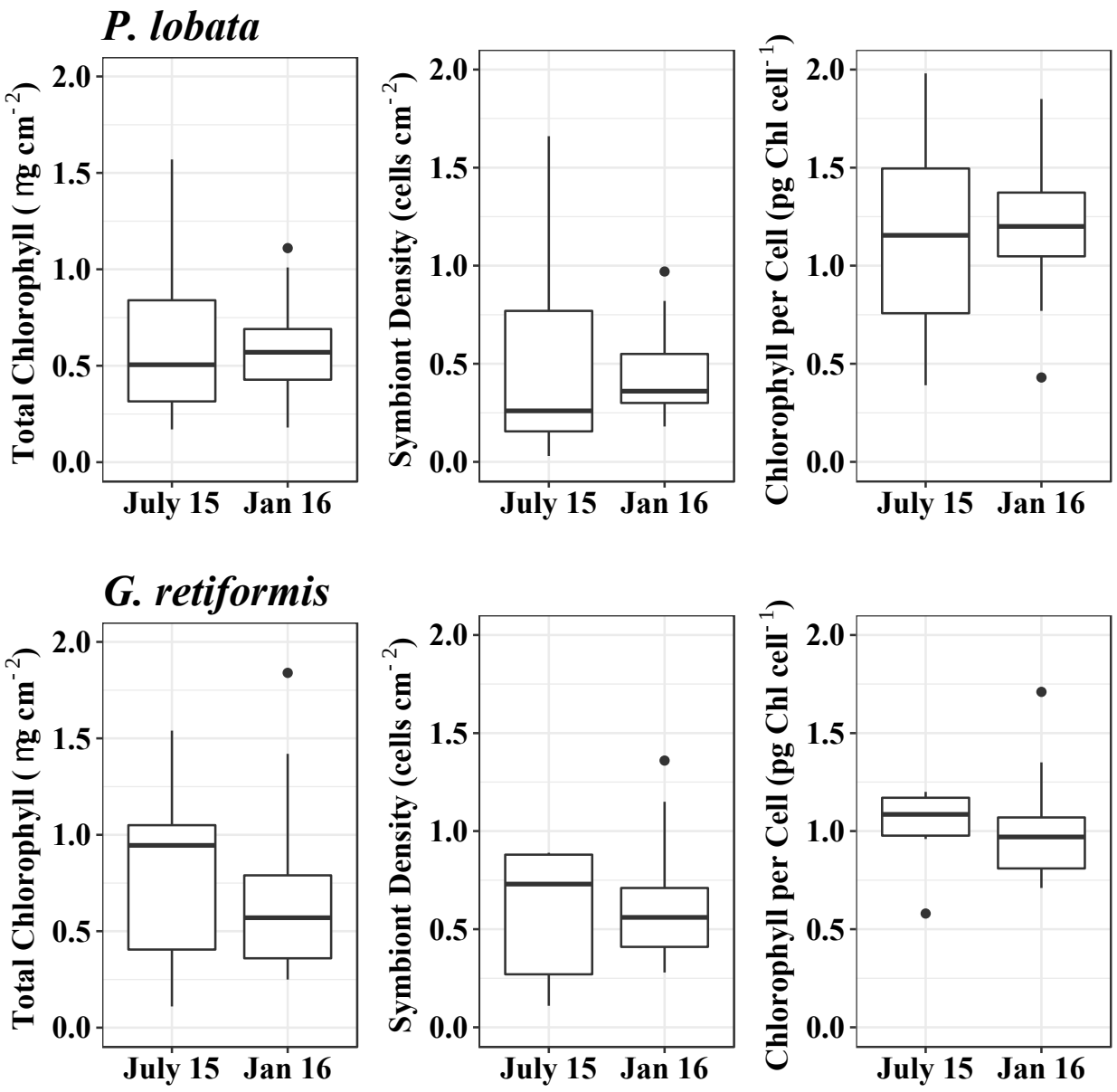

Figure 14. Bleaching resistance ratios expressed as ratios of heated:control nubbins to give total Chl cm^{-2}, symbiont density, and Chl $cell^{-1}$ comparing resistance of *Porites lobata* (top panel) and *Goniastrea retiformis* (bottom panel) between seasons (July 2015 and January 2016) in the donor MV site. Thick horizontal bars are median growth rates, thin horizontal lines are quartiles, whiskers are 2 standard errors, and points are outliers.

Table 2. Kruskal Wallis results of bleaching resistance ratios between sites after < 22 days in each site in July 2015. χ^2 is the critical value of chi-squared, *df* is degrees of freedom, *p* is the *p*-value (α <0.05).

Species	Bleaching Resistance Ratio	χ^2	*df*	*p*
Porites lobata	Chl cm^{-2}	0.245	2	0.885
	Symbiont density	1.940	2	0.379
	Chl $cell^{-1}$	1.860	2	0.395
Goniastrea retiformis	Chl cm^{-2}	0.956	2	0.620
	Symbiont density	1.143	2	0.565
	Chl $cell^{-1}$	1.143	2	0.565

Table 3. Kruskal Wallis results comparing bleaching resistance ratios between MV site corals in July 2015 and January 2016. χ^2 is the critical value of chi-squared, *df* is degrees of freedom, *p* is the *p*-value (α <0.05).

Species	Bleaching Resistance Ratio	χ^2	*df*	*p*
Porites lobata	Chl cm^{-2}	0.002	1	0.967
	Symbiont density	1.581	1	0.209
	Chl $cell^{-1}$	1.799	1	0.180
Goniastrea retiformis	Chl cm^{-2}	0.724	1	0.395
	Symbiont density	0.141	1	0.708
	Chl $cell^{-1}$	0.391	1	0.532

Symbiont Community Composition

There were 26 unique sequences that passed QA/QC in all samples. Initial sequence alignment revealed that OTU #26 was identical to OTU #2 from 1 to 298 bp but had 20 additional bp on the end. OTU #26 accounted for a single read present in only one sample where OTU #2 was abundant. OTU #2 was also abundant in several other samples. It appeared OTU #26 was the result of PCR or sequencing error, thus the single read was consolidated with the read counts in OTU #2, and the errant sequence was discarded.

The initial phylogenetic tree of 25 OTUs was collapsed to 14 unique OTUs (Figures 17, 18) on four nodes excluding the outgroups. All top hits were greater than 98% matches to both the NCBI nr and Symbiodiniaceae databases (Table 5). Hits from both databases agreed at the genus level but did not always have type consensus (Table 6). Of the 14 OTUs, 11 were *Cladocopium* species (formerly Clade C), and there was one type from the *Symbiodinium* (formerly Clade A), *Durusdinium* (formerly Clade D), and *Fugacium* (formerly Clade F) genera. Four hits had genus and type consensus from both databases (*Cladocopium* species C15, C3 and C91). NCBI nr BLAST results either did not specify types or were less specific than the custom Symbiodiniaceae database; thus the remaining 21 OTUs were identified using the Symbiodiniaceae database.

No significant changes in symbiont composition were detected in parent colonies between seasons (Figure 19), among parent colonies and coral nubbins in the MV site (Figure 20), or between corals in all sites in 2016 (Figure 21) for either coral species (Table 7). All samples of *P. lobata* were consistently dominated by *Cladocopium* C15. *Cladocopium* types C40, C3, and C115 made up the majority of the read abundance from *G. retiformis*. The remaining 10 types identified were < 1 % in relative read abundance.

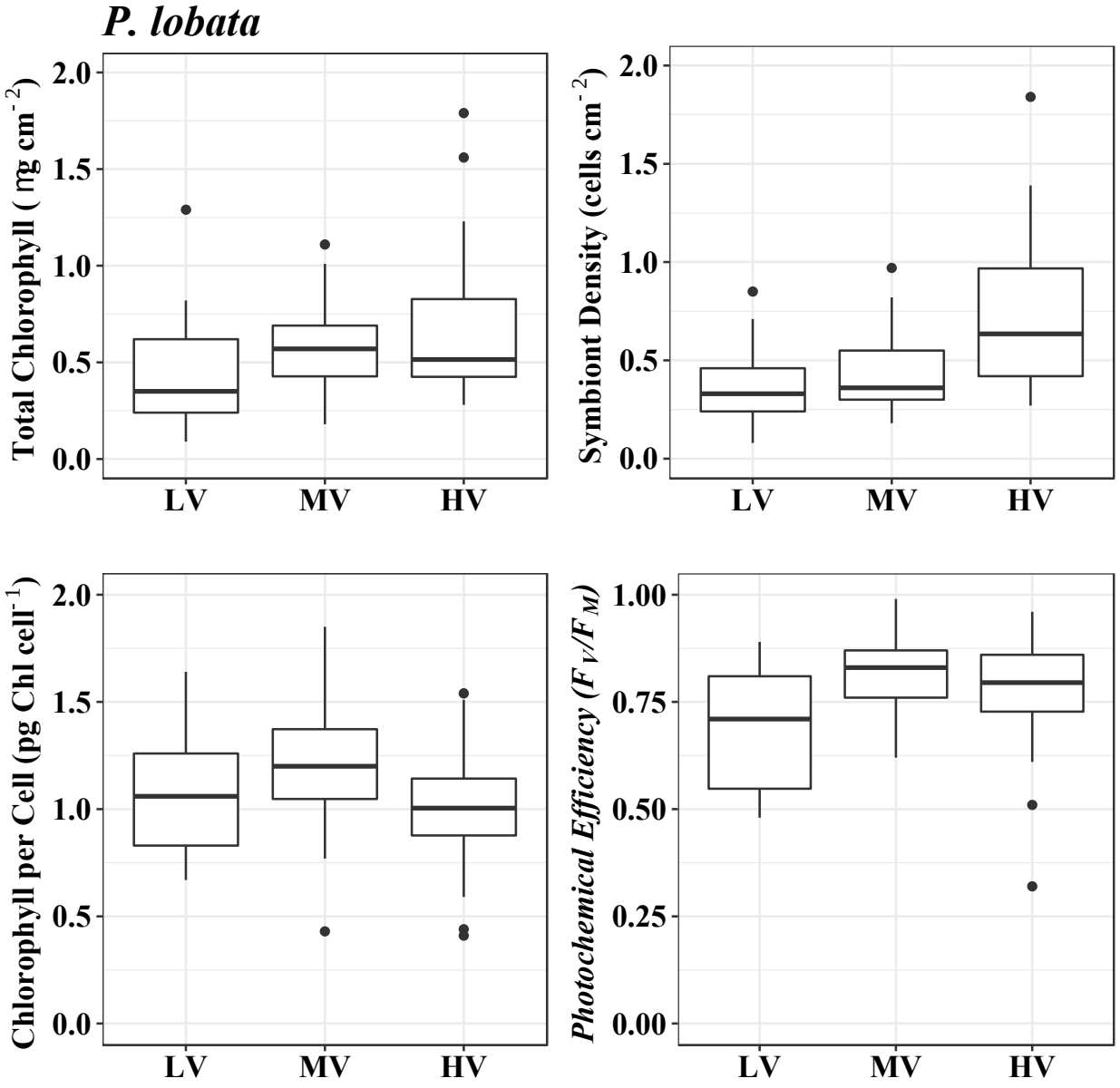

Figure 15. Bleaching resistance ratios expressed as ratios of heated:control nubbins to give total Chl cm^{-2}, symbiont density, and Chl $cell^{-1}$ comparing resistance of *Porites lobata* between sites after a 7-month acclimatization period (January 2016). Thick horizontal bars are median growth rates, thin horizontal lines are quartiles, whiskers are 2 standard errors, and points are outliers.

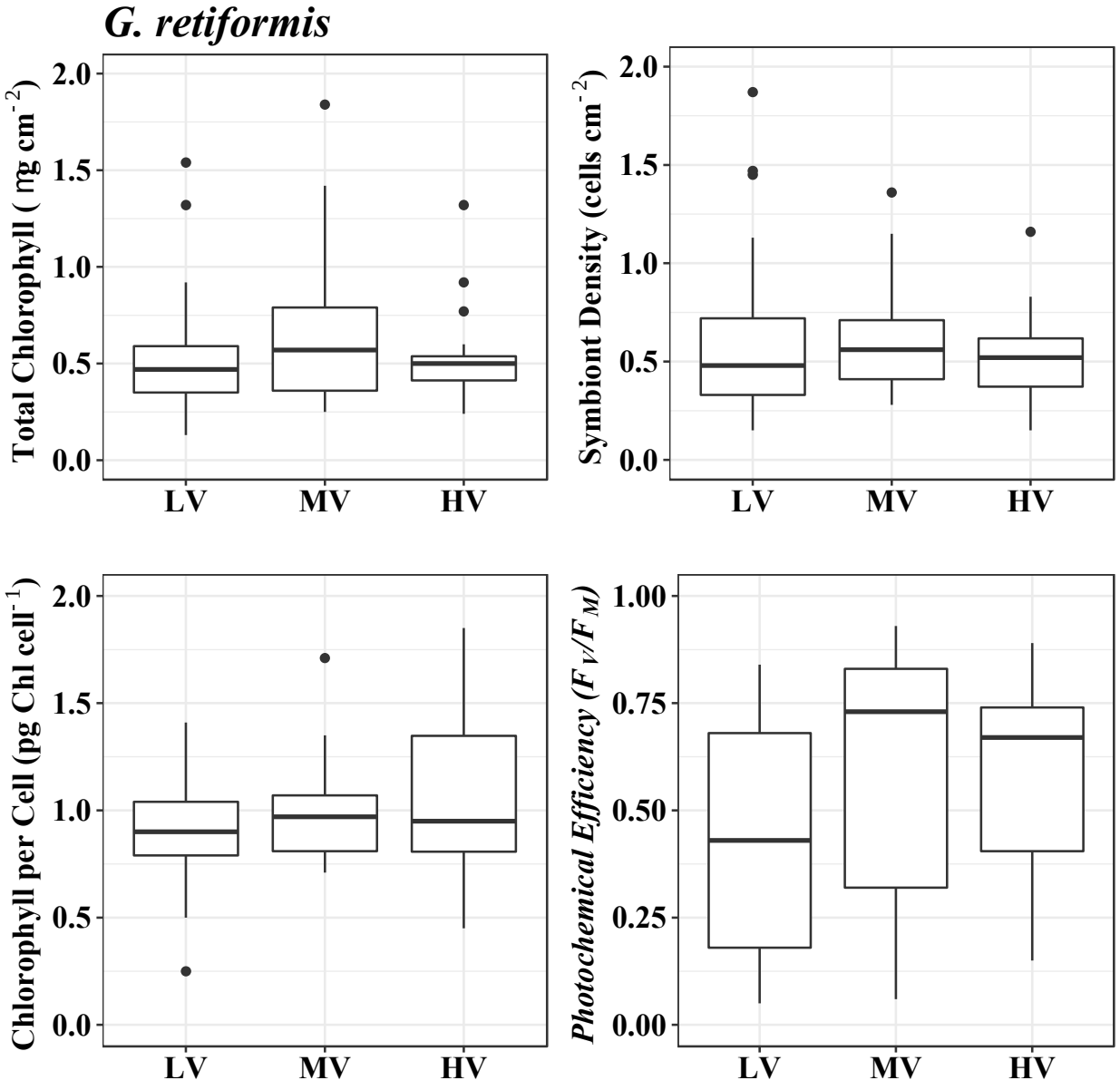

Figure 16. Bleaching resistance ratios expressed as ratios of heated:control nubbins to give total Chl cm^{-2}, symbiont density, and Chl $cell^{-1}$ comparing resistance of *Goniastrea retiformis* between sites after a 7-month acclimatization period (January 2016). Thick horizontal bars are median growth rates, thin horizontal lines are quartiles, whiskers are 2 standard errors, and points are outliers.

Table 4. (a) Kruskal Wallis results of bleaching resistance in January 2016 for *Porites lobata*, *Goniastrea retiformis*. χ^2 is the critical value of chi-squared, *df* is degrees of freedom, *p* is the *p*-value (α <0.05). (b) A Dunnett's *post hoc* comparison between the native MV site and transplant sites, with the estimated difference, lower and upper confidence intervals (CI, 2 standard errors) and *p*-values.

a.

Species	Bleaching Resistance Ratio	χ^2	*df*	*p*
Porites lobata	Chl cm^{-2}	7.149	2	**0.028**
	Symbiont density	13.390	2	**0.001**
	Chl $cell^{-1}$	6.030	2	**0.049**
	$\Delta F_V/F_M$	7.384	2	**0.025**
Goniastrea retiformis	Chl cm^{-2}	1.726	2	0.422
	Symbiont density	0.712	2	0.701
	Chl $cell^{-1}$	1.800	2	0.407
	$\Delta F_V/F_M$	5.733	2	0.057

b.

Bleaching Ratio	Comparison	Difference	Lower CI	Upper CI	*p*
Chl cm^{-2}	LV - MV	-0.224	-0.485	0.036	0.101
	HV - MV	0.010	-0.253	0.273	0.995
Symbiont density	LV - MV	-0.243	-0.529	0.043	0.106
	HV - MV	0.116	-0.173	0.405	0.567
Chl $cell^{-1}$	LV - MV	-0.089	-0.563	0.385	0.878
	HV - MV	-0.383	-0.861	0.096	0.134
$\Delta F_V/F_M$	LV - MV	-0.112	-0.196	-0.027	**0.008**
	HV - MV	-0.036	-0.122	0.049	0.532

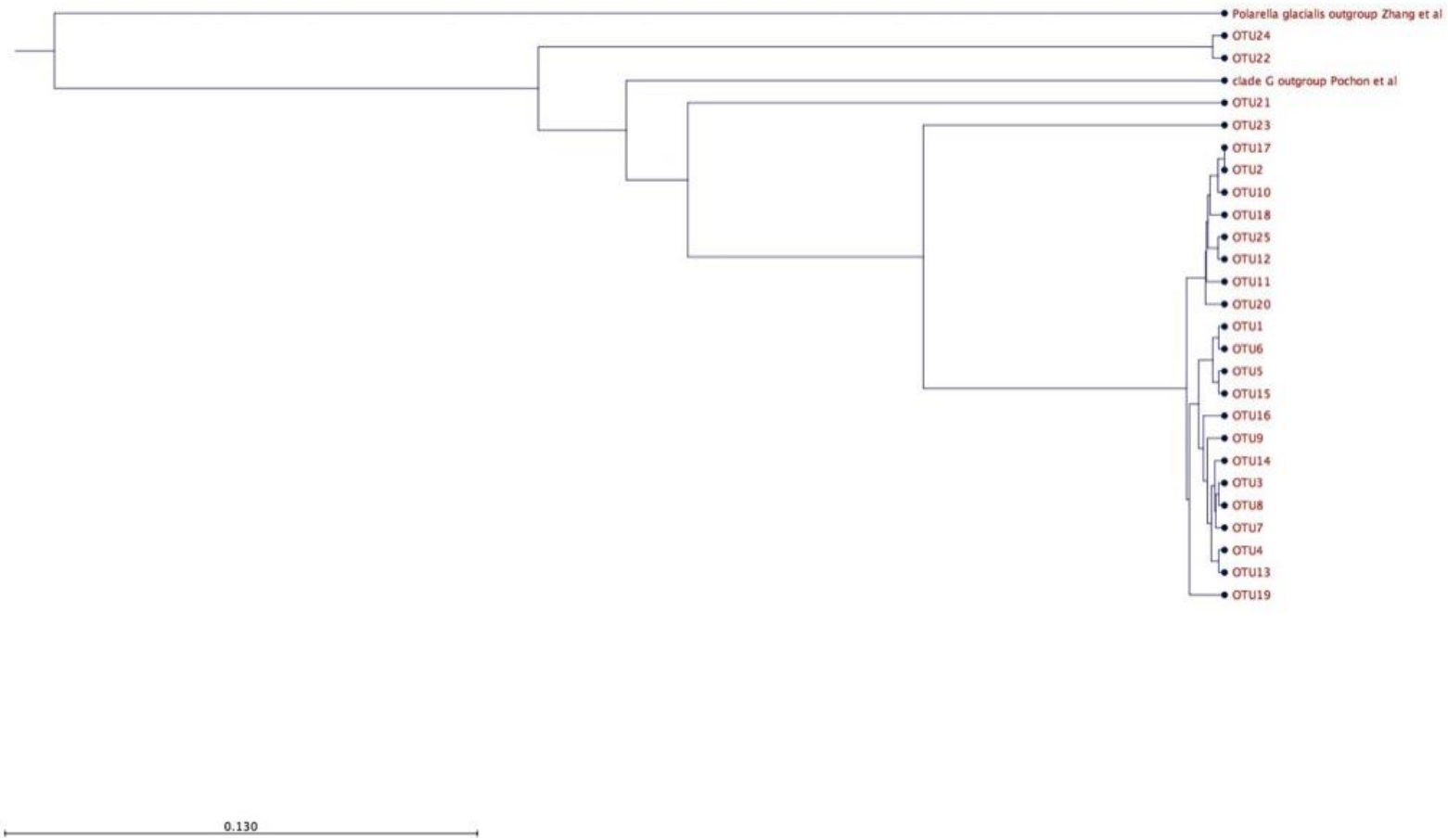

Figure 17. The maximum likelihood phylogenetic tree of 25 unique OTUs from all samples constructed using the HKY model and MUSCLE algorithm with *Polarella glacialis* (Zhang et al. 2013) and a Clade G Symbiodiniaceae (Pochon et al. 2012) as outgroups.

Table 5. Multiple BLASTn results from the NCBI nr database and a custom Symbiodiniaceae database (Arif et al. 2014), showing the accession number or Symbiodiniaceae Database ID (*Sym*. ID), percent match (%), greatest number of high-scoring segment pairs (Length), bit-score and e-value.

	NCBI nr Database Hits					**Symbiodiniaecae Database Hits**				
Query	**Accession #**	**Match**	**Length**	**Bit Score**	**E-Value**	***Sym*.ID**	**Match**	**Length**	**Bit Score**	**E-Value**
OTU1	MH236777	99.67	300	537.79	1.26E-148	GS_C40	100.00	293	511.64	3.05E-147
OTU2	JN558044	100.00	301	542.30	2.97E-150	GS_C15	100.00	293	511.64	3.05E-147
OTU3	AB778606	100.00	300	542.30	2.97E-150	GS_C3	100.00	293	511.64	3.05E-147
OTU4	AB778606	99.67	300	537.79	1.26E-148	GS_C115	100.00	293	511.64	3.05E-147
OTU9	MH243723	99.32	300	520.66	9.70E-144	GS_C21	99.28	293	490.00	9.73E-141
OTU11	JN558044	99.33	301	533.28	1.54E-147	GS_C15.2	99.65	293	506.23	1.30E-145
OTU12	JN558050	100.00	301	542.30	2.97E-150	GS_C91	100.00	293	511.64	3.05E-147
OTU16	AB778606	99.00	300	528.77	6.54E-146	GS_C115	99.29	293	502.62	1.58E-144
OTU18	JN558044	99.33	301	533.28	1.54E-147	GS_C15.6	99.65	293	506.23	1.30E-145
OTU19	AB778606	98.67	300	524.26	7.96E-145	GS_C3	98.59	293	493.61	8.19E-142
OTU20	JN558044	99.33	301	533.28	1.54E-147	GS_C15.2-1	99.29	293	502.62	1.58E-144
OTU21	MK007303	99.27	274	486.39	2.00E-133	GS_A5	100.00	259	246.54	1.75E-67
OTU22	KU535564	100.00	298	538.69	3.62E-149	LJ_D17	100.00	279	499.02	1.91E-143
OTU23	EU786061	98.39	310	537.79	1.26E-148	GS_F3.1	98.32	298	515.25	2.58E-148

Table 6. Top hits from the NCBI nr and custom Symbiodiniaceae databases (DB) for each OUT (Query). Hits were compared for consensus (Consensus). Hits designated "na" in the Consensus column were cases where type resolution did not agree, or a particular type was not identified. The most specific type was used whenever available (e.g., OTU#1, C40 is more specific than Clade C). In cases of no consensus, the type with the highest % match and bit-score was selected, with preference given to the Symbiodiniaceae database hit, if values were similar (e.g., OTU#23).

	Symbiodiniaecae Hit Information			***Consensus***	**Symbiont Identity**	
Query	**NCBI nr DB**	**Associated Study**	**Symbiodiniaecae DB**	**(Y/N/na)**	**Genus**	**Type**
OTU1	Clade C	(Brian et al. 2019)	C40	na	*Cladocopium*	C40
OTU2	C15	Pochon et al. 2012	C15	Y	*Cladocopium*	C15
OTU3	C3	(Yorifuji et al. 2015)	C3	Y	*Cladocopium*	C3
OTU4	C3	Yorifuji et al. 2015	C115	N	*Cladocopium*	C115
OTU9	Clade C	(Kunihiro and Reimer 2018)	C21	na	*Cladocopium*	C21
OTU11	C15	Pochon et al. 2012	C15.2	na	*Cladocopium*	C15.2
OTU12	C91	Pochon et al. 2012	C91	Y	*Cladocopium*	C91
OTU16	C3	Yorifuji et al. 2015	C115	N	*Cladocopium*	C115
OTU18	C15	Pochon et al. 2012	C15.6	na	*Cladocopium*	C15.6
OTU19	C3	Yorifuji et al. 2015	C3	Y	*Cladocopium*	C3
OTU20	C15	Pochon et al. 2012	C15.2-1	na	*Cladocopium*	C15.2-1
OTU21	SCF026.01	*unpubl.*	A5	na	*Symbiodinium*	A5
OTU22	SGC1	*unpubl.*	D17	na	*Durusdiniun*	D17
OTU23	F3.5	(Fay et al. 2009)	F3.1	N	*Fugacium*	F3.1

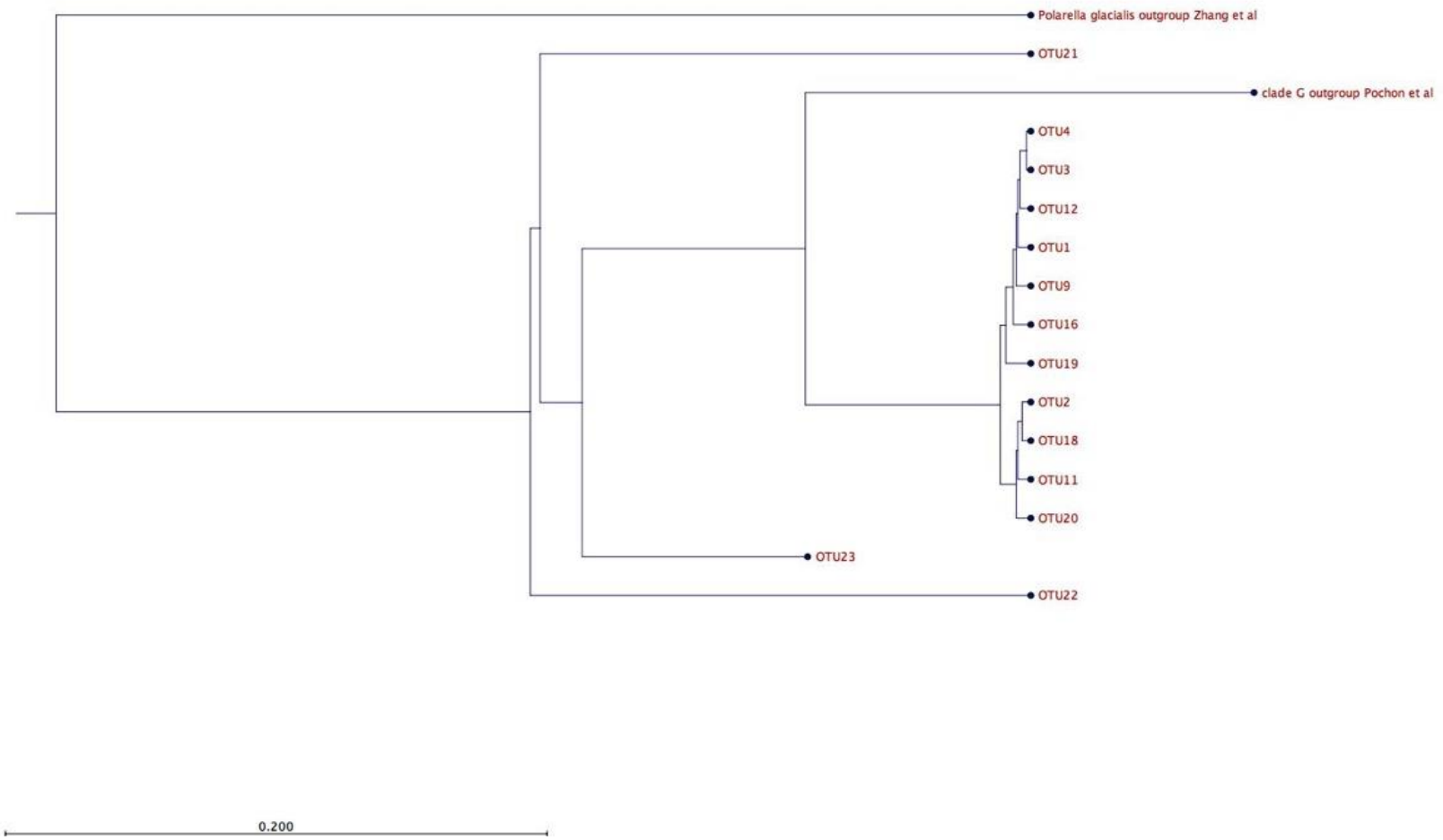

Figure 18. The finalized maximum likelihood phylogenetic tree containing collapsed OTUs. OTUs with the same top BLASTn hit that differed by fewer than 5 bp and were less than 0.003 node distance away from a neighboring OTU were collapsed, resulting in 14 OTUs that were used in downstream analyses.

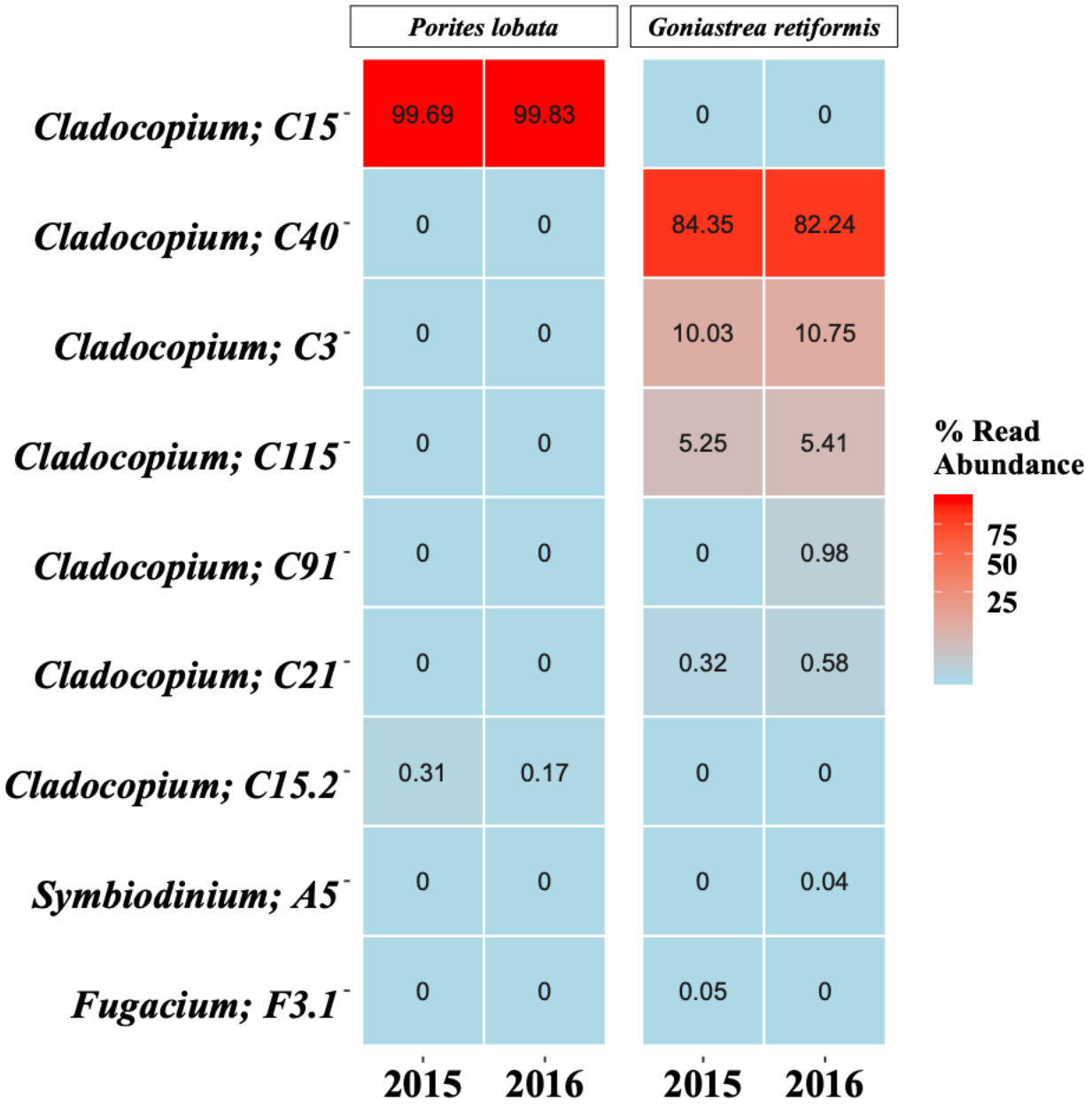

Figure 19. A heat map comparing relative abundances (%) of symbiont genera in parent colonies sampled across season in July 2015 and January 2016 from the MV site. Percent composition is given in each box, colors correspond to read abundace. Presented genera are based on the most recent taxonomic conventions (LaJeunesse et al. 2018b).

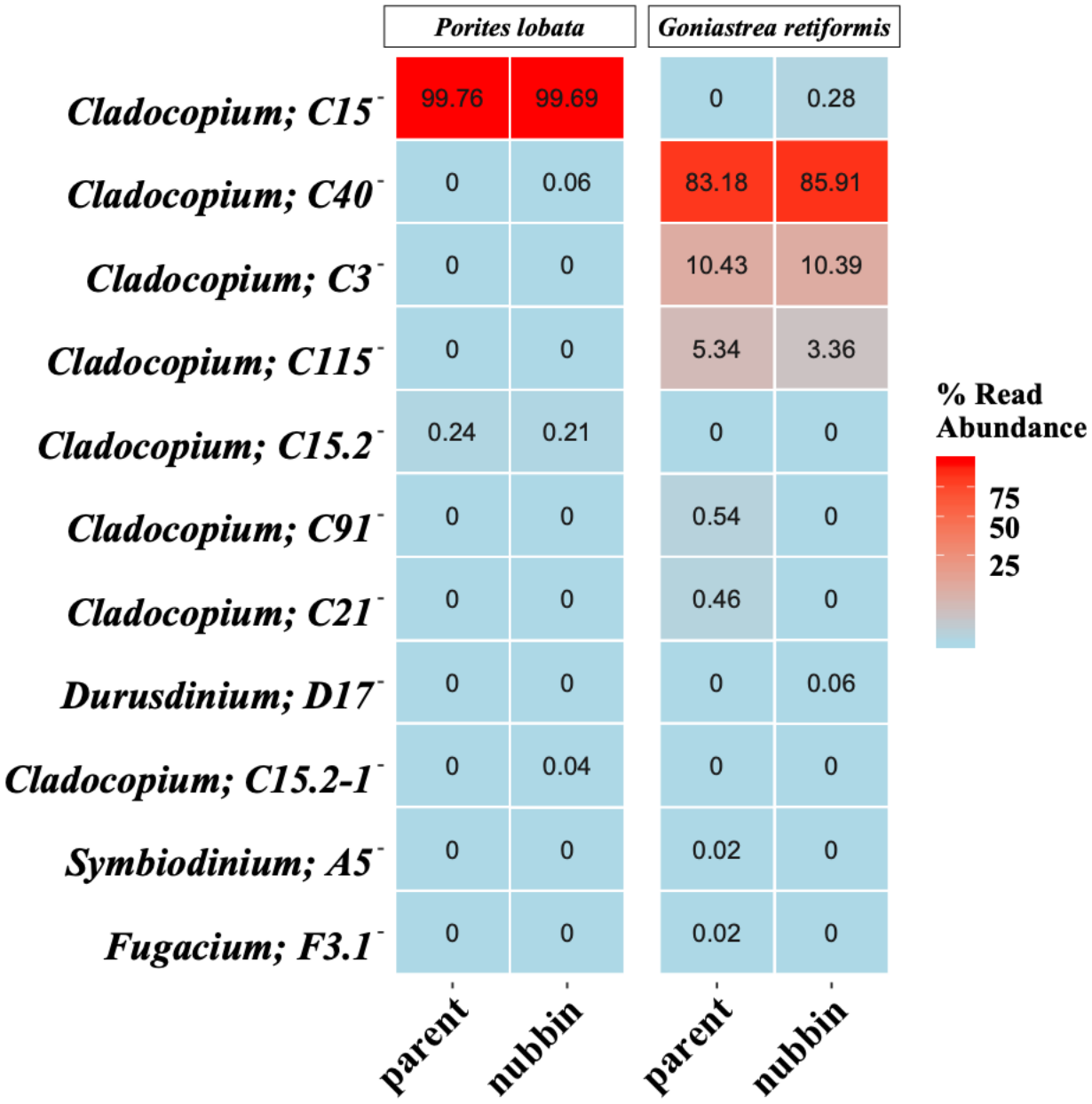

Figure 20. A heat map comparing relative abundances (%) of symbiont genera between parent colonites and nubbins in the MV site. Of note, background levels of D17 were detected in 2 nubbins in the MV site in 2016, but were not detected in parents in 2015 or 2016.

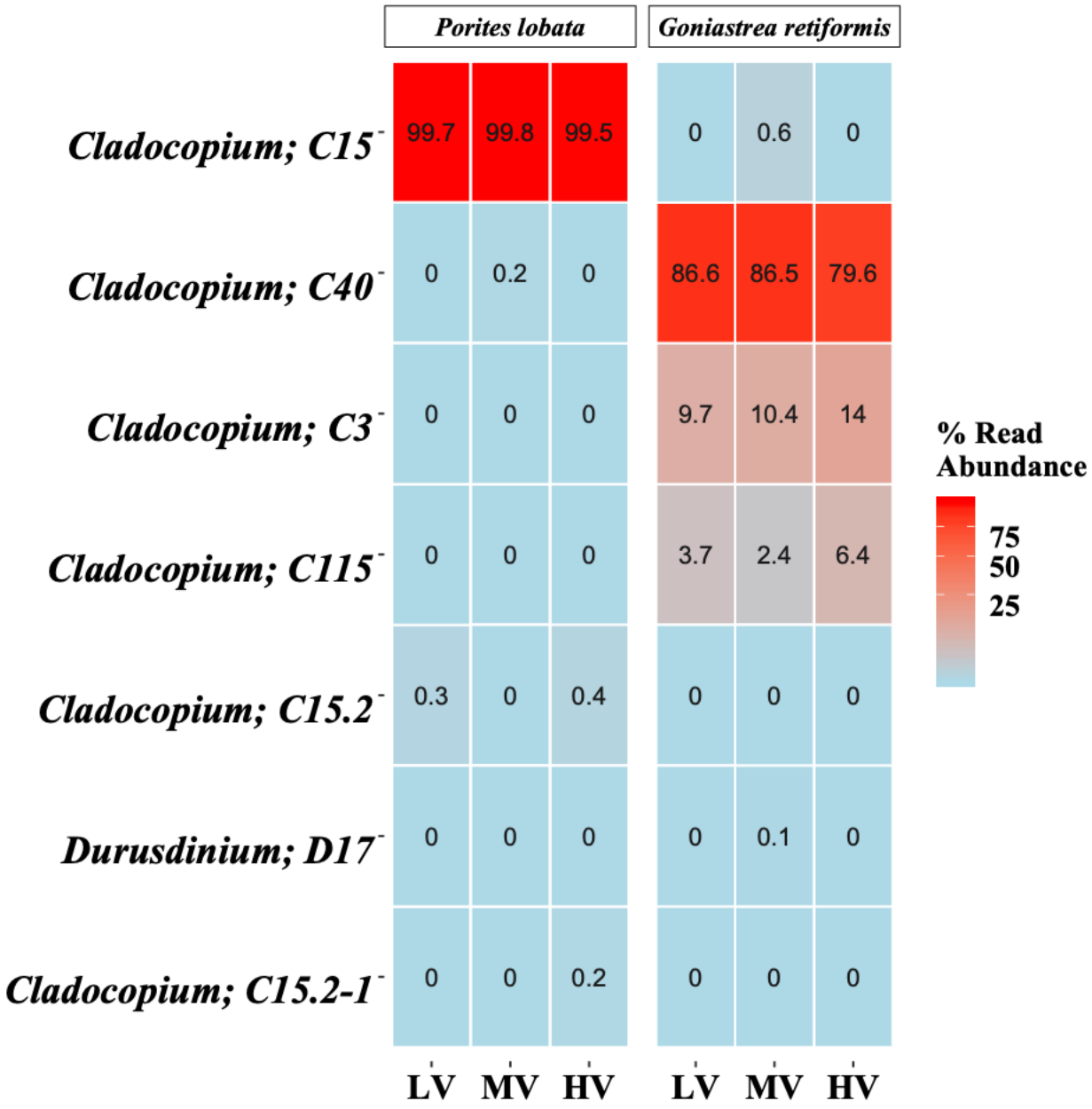

Figure 21. A heat map comparing relative abundances (%) of symbiont genera across sites in January 2016. Samples here include both parent and nubbins sampled in 2016.

Table 7. PERMANOVAs were conducted to determine differences in symbiont community composition between 2015 and 2016 parent colony samples, between parent colonies and nubbins in the MV site, and between sites after a seven-month acclimatization period. Degrees of freedom (*df*), sum of squares (SS), mean sum of squares (MS), F statistic (*F*), coefficient of variation (R^2), and *p*-value (*p*) are given.

Source	*df*	SS	MS	*F*	R^2	*p*
Porites lobata						
Parent Colonies × Season	1	0.026	0.026	0.272	0.033	0.699
Residuals	8	0.770	0.096	0.967		
Total	9	0.797	1			
MV Parents – Nubbins	1	0.111	0.111	2.266	0.221	0.174
Residuals	8	0.391	0.049	0.78		
Total	9	0.501	1			
Nubbins × Site	2	0.125	0.063	1.139	0.186	0.330
Residuals	10	0.549	0.054	0.8145		
Total	12	0.674	1			
Goniastrea retiformis						
Parent Colonies × Season	1	0.034	0.034	0.327	0.045	0.693
Residuals	7	0.737	0.105	0.955		
Total	8	0.772	1			
MV Parents – Nubbins	1	0.030	0.030	0.287	0.035	0.716
Residuals	8	0.840	0.105	0.965		
Total	9	0.870	1			
Nubbins × Site	2	0.074	0.037	0.305	0.071	0.906
Residuals	8	0.971	0.121	0.929		
Total	10	1.045	1			

DISCUSSION

The temperature series from the LV, MV, and HV sites represented a gradient of thermal variability, as in previous studies on Ofu Island (Craig et al. 2001, Smith et al. 2007, Thomas et al. 2018). However, this is the first study to describe each site in a thermal stress dose context (i.e., DHD) and to determine that solar insolation was driving the warming in all three sites, despite differences in site volume and isolation from the ocean. The differences in peak magnitudes across sites can be related to physical differences among the sites. The LV site is situated in an exposed area on the west side of Olosega Island, adjacent to a channel between Ofu and Olosega Islands, with large volumes of water moving past the site; thus the temperature was relatively stable from July 2015 to January 2016. In contrast, the MV and HV sites are backreef tidepools on the south side of Ofu Island that become isolated from the ocean at low tide, making them vulnerable to daytime heating. The HV site is most strongly affected by tidal isolation and concomitant reduced water flow (Smith and Birkeland 2007), as it has roughly 1.8 times less volume than the MV pool (*pers. obs*). Thus, peak magnitude differences at 23.98 h were likely related to the volume of water being heated. Because the LV site is not isolated at low tide, the reduced or absent signals in the LV site were likely related to mixing and currents. FFT peak magnitudes consistently decreased from HV to LV sites. Peaks at 15 and 17 days may be related to variations in local weather patterns characteristic of the tropics, such as variable cloud cover and rain, as well as tidal strength driven by the lunar phase.

This is the first study to report *G. retiformis* growth rates on Ofu and Olosega Islands, however several studies have examined *P. lobata* in the region. HV *P. lobata* corals have been found to have higher calcification rates but lower skeletal densities compared to LV corals, and no differences in growth rates were found between the MV and HV sites in an 18-month

reciprocal transplant experiment (Smith et al. 2007, 2008). Contra to these findings, in this study *P. lobata* growth rates increased with decreasing thermal stress in each site. This disparity may be due to differences in transplant duration or thermal stress; perhaps DHD between the MV and HV sites in 2004-2006 were less pronounced than that of this study. In the HV site, both species of massive corals had significantly reduced growth rates, and nubbins appeared to be less able to compete with turf, crustose coralline, and endolithic algae, suggesting they were less healthy. Parrotfish predation on *P. lobata*, though not on *G. retiformis*, was observed at the LV site. It is possible other stressors that were not measured, such as predation, contributed to the reduced growth and health at the HV site during the acclimatization period. However, given that both species had reduced growth, predation may not explain lower growth rates for *G. retiformis*.

Based on the criteria established *a priori* for acclimatization in this study, neither species acclimatized to novel thermal microhabitats. Heat shock experiments revealed that *P. lobata* $\Delta F_V/F_M$ retention was highest in the MV site and lowest in the LV site, indicating the algae in LV nubbins may have de-acclimatized and become more sensitive to bleaching. LV site symbiont and chlorophyll retention was reduced by > 20% compared to corals in the native MV site. While not significantly different, this reduction could indicate LV site *P. lobata* corals had begun to reallocate energy to growth rather than bleaching resistance after seven months in more stable temperatures. There was no significant difference in seasonal bleaching resistance in either species. Few studies have examined seasonal changes in thermal tolerance (Fitt et al. 2001, Scheufen et al. 2017); thus, future work should be aimed at understanding seasonal modulation of thermal tolerance. It is also possible that seven months was insufficient time for detectable acclimatization to occur in these slow-growing species. This is unlikely, however, as

turnover rates in both algal and coral cells are on the order of weeks to months (Davy et al. 2012), and well within the acclimatization period used in this study.

The lack of acclimatization to warmer temperatures in both species found here contrasts with experiments performed on *Acropora hyacinthus* in the exact same sites on Ofu Island using the same style of standardized heat shock experiments (Barshis et al. 2013, Palumbi et al. 2014). *A. hyacinthus* experiments found increased bleaching resistance (determined solely by chlorophyll retention ratios) when corals were moved into the HV site (Palumbi et al. 2014). In addition, baseline expression of thermal stress genes was more pronounced in *A. hyacinthus* corals from the HV site compared to the MV population, leading the authors to conclude expression level differences in response to the higher thermal stress dose at the HV site gave HV corals higher bleaching resistance than their MV counterparts (Barshis et al. 2013). No phenotypic evidence was found in this study to support enhanced bleaching resistance for these two massive species, underscoring that predicting the future of many coral species requires consideration of different survival strategies.

The aforementioned studies estimated bleaching resistance by a single bleaching proxy, Chl retention (reviewed in Thomas et al. 2018). Using multiple bleaching proxies, specifically symbiont density and Chl $cell^{-1}$, provided more insight into the bleaching response in the current study. In addition, Chl was extracted without sonication or disruption of the algal theca in previous studies (Palumbi et al. 2014). Dinoflagellates have a tough theca that can withstand repeated freezing and thawing (*pers. obs.*); mechanical disruption is necessary to get accurate measurements of chlorophyll. Such sample processing/handling protocols should be standardized to enable comparisons between studies.

Several studies of different thermal stress exposures have found that heat shock and acclimation to gradual stress elicit markedly different responses in the transcriptome, proteome, metabolome, and cellular biology of corals and the Cnidarian model *Exaiptasia pallida* (Oakley et al. 2017, Hawkins and Warner 2017, Hillyer et al. 2016, Bay and Palumbi 2015, Gibbin et al. 2018). Given the different physiological responses of Cnidarians in response to thermal exposure, perhaps more fine-scale metrics such as a metabolic thermal performance curves (e.g., Padfield et al. 2017) may be more appropriate to reveal shifts in bleaching resistance. While application of acute heat shock provides a method for rapid, repeatable assessment, heat shock experiments may reduce any ecologically-relevant signal of interest. The bleaching experiments in this study used a thermal stress dose that was on par with a daily dose of thermal stress from the HV site; however, the warming rate (2.5° C h^{-1}) and maximum temperatures (36 to 36.5° C) were greater than those seen in the 2016 austral summer on Ofu Island (1° C h^{-1} and 35° C, respectively). Thus, when designing thermal bleaching experiments, dose and rate should be considered.

There were no changes detected in core symbiont genera among parent colonies in 2015 and any parent colonies or replicate nubbins from any site in 2016. Further, there were no differences in core symbiont taxa between corals moved to different sites. A previous study found no differences in symbiont species composition with reciprocal transplants of *P. lobata* between the LV and HV sites (Smith et al. 2007); similiarly, the symbiont communities in this study were stable in both species. *Durusdinium* spp. (formerly Clade D *Symbiodinium*) symbionts have been linked to thermal resistance (Baker 2004, Berkelmans and van Oppen 2006), and thermally resistant symbionts from this genus have been detected in the HV and MV sites, previously (Oliver and Palumbi 2009, 2011, Barshis et al. 2013). A *Durusdinium* sp.

(formerly *Symbiodinium* type D17, LaJeunesse et al. 2018) was only detected in two *G. retiformis* nubbins in the MV pool in January 2016 (Figures 20, 21). The thermal tolerance of *Porites* species has been attributed to its association with C15 (LaJeunesse et al. 2003). Indeed, the thermally tolerant *Cladocopium* spp. C15 was the most abundant type, and the association remained stable across all *P. lobata* corals in this study.

Evidence for acclimatization was not found in this study. Further, the reduced growth rates of both species indicate that moving corals into the more thermally variable environment has a fitness cost. While other species on Ofu Island have shown enhanced growth and bleaching resistance in the more thermally variable HV site, this study reveals that thermally variable conditions can reduce fitness in *P. lobata* and *G. retiformis* without an apparent acclimatory benefit. No evidence of acclimatization was found in either species between the donor MV site and other sites. *P. lobata*, but not *G. retiformis*, growth rates were highest with the least amount of thermal stress, suggesting lower stress enabled higher growth rates. These differences between the species remind us that multiple survival strategies may exist among corals, even among those similar morphologies. These strategies must be described to better predict acclimatization in the context of the changing climate.

THE EFFECTS OF ACUTE AND CUMULATIVE THERMAL STRESS ON *ACROPORA CERVICORNIS*

INTRODUCTION

Coral reefs protect coastal communities from hazards (Ferrario et al. 2014), offer critical habitat to more than a quarter of all marine species (Fisher et al. 2015), and provide food and livelihoods to billions of people, particularly in impoverished nations (Kent 1997, Hughes et al. 2012, Cinner 2014, McClanahan et al. 2015). Coral reef health and function are intrinsically linked to the health of individual coral colonies (Hughes 1993, 1994a, Hughes and Connell 1999, Hughes et al. 2003); thus the decline of live coral cover is widely accepted as an indicator of reef degradation (Glynn 1993, 1996). Coral bleaching, the dissociation of the coral animal host from its obligate symbiotic algae (Brown 1997), has caused the greatest decline in coral numbers (Hoegh-Guldberg 1999b) and represents the biggest threat to the persistence of coral reef ecosystems worldwide (Hughes et al. 2003, Hoegh-Guldberg et al. 2007, Wilkinson 2008).

Corals participate in a delicate symbiosis with endosymbiotic dinoflagellates in the family Symbiodiniaceae (LaJeunesse et al. 2018b), which they rely upon for most of their metabolic energy (Muscatine and Hand 1958, Muscatine and Cernichiari 1969, Pearse and Muscatine 1971, Muscatine and Porter 1977, Muscatine et al. 1981). The partnership is analogous to a tenant-lease agreement. Under optimal light and temperature conditions, corals provide their algal partners with the substrates required for photosynthesis, and the nutrients required for growth in otherwise oligotrophic waters (Muscatine and Cernichiari 1969, Steen and Muscatine 1987). In exchange, the algae provide the host with photosynthetically-reduced carbon in the forms of glucose (Burriesci et al. 2012), glycerol (Grottoli et al. 2006), lipids

(Crossland et al. 1980, Crossland 1987, Harland et al. 1992), and carbon skeletons for the synthesis of amino acids (Swanson and Hoegh-Guldberg 1998) and organo-phosphates (Jackson and Yellowlees 1990). This exchange leads to high productivity (Goreau 1959) and enhanced calcification (Gladfelter 1983) that enables reef formation in an otherwise oligotrophic ocean.

Scleractinian corals are especially sensitive to > 1º C deviations above local temperature maxima and sustained, high levels of irradiance (Fitt and Warner 1995, Lesser and Farrell 2004, Hoegh-Guldberg 2006). Consequently, exposure to high temperature and/or irradiance stress results in the loss of the algae via subsequent expulsion, digestion and/or degradation of the algae *in hospite* (Lesser 2006, Weis 2008), a process broadly known as dysbiosis (Brown 1997). Dysbiosis is generally defined as the maladaptive perturbation of the normal coral-associated microbiome, which includes both a bacterial consortium and algal symbionts in the family Symbiodiniaceae (Bosch and Miller 2016b). The oxidative theory of coral bleaching suggests bleaching and subsequent dysbiosis are caused by the production of reactive oxygen species (ROS) in the host mitochondria, the algal photosystem II, or both (Downs et al. 2002). ROS can damage DNA, chloroplast and mitochondrial membranes, and overload the endoplasmic reticulum associated degradation pathway (Lesser 2006, Weis 2008, Oakley et al. 2017). Therefore, when ROS exceed what cellular removal mechanisms can manage, corals may expel their algal symbionts in an effort to prevent cellular damage.

Although the obscurity of cellular bleaching mechanisms has made it difficult to understand the physiological winnowing of symbioses, accurate measures of photochemical efficiency, gross photosynthesis and respiration may provide an integrated physiological perspective for interpreting the effects of temperature on symbiotic corals. Thermal acclimation theory suggests gradual changes in temperature ameliorate loss of performance (Angilletta

2009). Yet, most studies comparing the effects of thermal exposures on Cnidarians have largely focused on physiological differences between heat shocked and acclimated organisms (Middlebrook et al. 2008, Putnam and Gates 2015, Hawkins and Warner 2017, Oakley et al. 2017). For example, increased photosynthetic activity, respiration rates, and photoprotection have been observed in response to brief periods of thermal preconditioning from the sea anemone *Exaiptasia pallida* (Hawkins and Warner 2017) and the coral *Acropora aspera* (Middlebrook et al. 2008), respectively. More drastic proteomic changes have been found in heat shocked vs. acclimated *E. pallida* in the absence of significant reductions in photosynthetic efficiency or symbiont densities (Oakley et al. 2017). In addition, many studies have utilized heat shock exposures to elicit a bleaching response in the lab in order to estimate resilience in the environment (e.g., Palumbi et al. 2014). However, natural coral bleaching is not often the result of acute heat shock exposure; therefore examining coral thermal performance under different exposure regimes can improve our understanding of coral resilience.

To date, no studies have explored how fine-scale changes in thermal stress exposures affect metabolism in the absence of acclimation. Thus, this study exposed corals to acute and cumulative thermal stress to determine how differences in exposure affected metabolic thermal performance. Physiological sensitivity to acute heat shock and cumulative warming was measured in seven genets (i.e., coral host genotypes) of the threatened staghorn coral, *Acropora cervicornis*. This study was conducted on *A. cervicornis* as it is one of two ecologically important Acroporid corals that dominates the Caribbean reefscape, and it is a target species in a large number of restoration efforts. Due to the challenges of performing fine-scale metabolic measurements in remote field locations such as Ofu Island (Chapter 2) and the availability of many corals from a coral nursery, this study was conducted in Broward County, Florida, USA.

Unlike other studies, acute thermal stress was examined in the context of thermal dose response, Degrees Heating Minutes (DHM, ° C min). Each exposure experiment was conducted within a single day to make the exposures comparable but avoid acclimation.

MATERIALS AND METHODS

Coral sampling

Nubbins of the staghorn coral *Acropora cervicornis* Lamarck were obtained from a nearshore coral nursery in Broward County, FL (26° 06 N, 80° 05 W) maintained by Nova Southeastern University's (NSU) Halmos College of Natural Sciences and Oceanography. A total of seven genets of local origin were collected from the nursery. The genets used in this study were previously identified by microsatellite loci (Baums et al. 2010), and designated B through J for this study. Genets were selected by the nursery manager *a priori* that represented a wide range of coral resiliency based on outplant survival (Goergen and Gilliam 2018). In late February 2017, six 4 - cm nubbins from six genets (B, C, E, F, H J), plus a single nubbin from an additional genet (D), were cut from nursery colonies with bone cutters. The additional genet D nubbin was included to increase sample size. Each nubbin was glued to a hex-head bolt *in situ* with marine epoxy, tagged, and attached to a grid on a polyvinyl chloride (PVC) array 0.5 m above the sandy seafloor (Figure 22). The resulting nubbins were left to heal (n = 6 genets x 6 nubbins = 36 + 1 = 37 nubbins). A HOBO logger (Onset Corp.) was attached to the array to record *in situ* temperature every 30 s.

After one month, only one nubbin had died (genet F), and the 36 surviving nubbins had healed completely and grown. Nubbins were collected from the field nursery and transported to

the lab in an insulated cooler filled with seawater. Nubbins were placed in a common outdoor 1.5 m^3 tank with multidirectional, circulating seawater, and temperature control in the land-based nursery at the Halmos College of Natural Sciences and Oceanography, NSU. Encrusting organisms were gently removed with a handheld rotary tool from areas without live tissue. All nubbins were rinsed and returned to the outdoor tank for five days, during which temperature was recorded every 30 s by a HOBO logger.

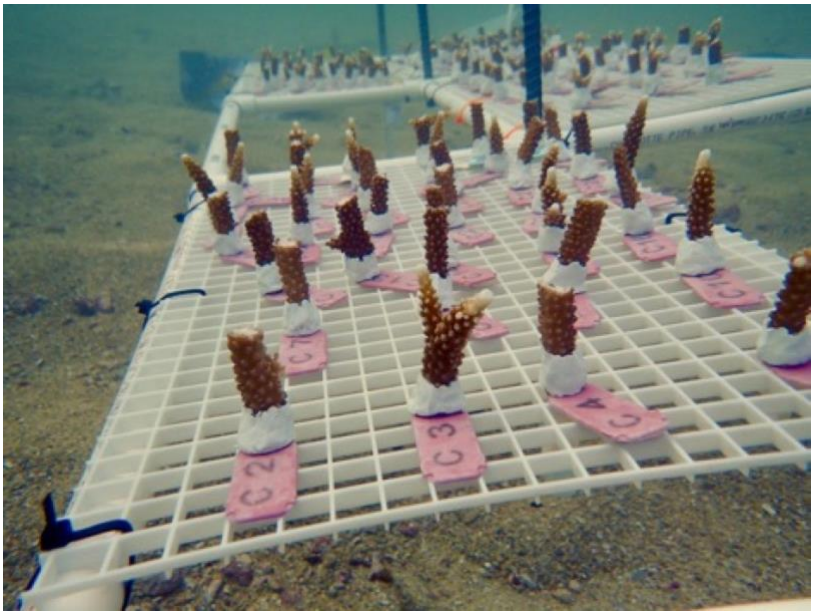

Figure 22. Photograph of the tagged coral nubbins anchored to a PVC array 0.5 m above the sandy bottom at the coral nursery site off Ft. Lauderdale, FL. Tagged coral nubbins were epoxied to bolts and attached to grids using wingnuts (not visible).

Experimental System

Laboratory aquaria consisted of two tank systems: a staging system and a heat treatment system as in Chapter 2 (Figure 4), with one difference. Rather than Peltier chilling apparatus plumbed into the sump tank, the sump was outfitted with a 450 W pump that circulated tank water through a stainless-steel coil in an ice bath. Temperature was controlled by the heater or chiller pump in the sump, driven by an Arduino microprocessor and custom software. Tank water temperature was recorded at 1 kHz by a HOBO logger that was calibrated to 0.1° C against a NIST-traceable spirit-filled thermometer. The staging tank system was held at 25.5° C, the daily mean temperature of the outdoor tank during all experiments. The heat treatment system contained a custom respirometry apparatus submerged in the experimental tank (Figure 23). Coral respiration chambers were mounted on an acrylic base in the experimental tank. Each chamber was fitted with a glass-enclosed magnetic stir bar and a fiber optic O_2 sensor connected to a Pre-Sens OXY-10 mini instrument. O_2 concentrations were recorded at 0.17 Hz simultaneously in all chambers.

Thermal Exposures

Experiments were carried out over two days between 09:00 and 17:30 local time. Measurements were made between 25.4° C and 35.7° C at 2.5° C to 3° C intervals in each experiment. Metabolic rates of dark respiration and gross photosynthesis were quantified by measuring oxygen evolution with the coral respirometry apparatus. Approximately 30 minutes before measurements began, corals were moved from the outdoor tank to the staging tank in the lab. A single nubbin was randomly assigned to one of eight respirometry chambers; the chamber was sealed, and oxygen concentration was measured in the dark for at least 10 min. After at least

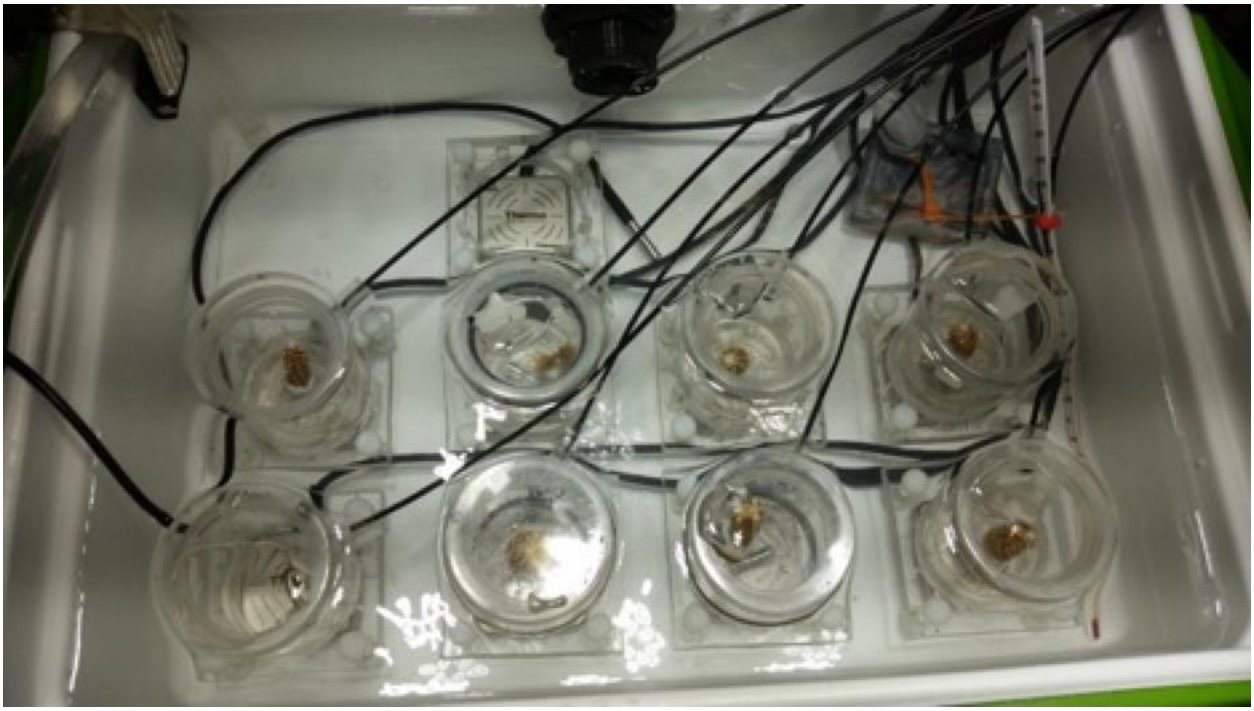

Figure 23. A photograph of the coral respirometry apparatus consisting of eight respiration chambers mounted on an acrylic base in an experimental tank. A HOBO logger attached to a dive weight and submerged in the tank (upper right of photograph) was calibrated to a NIST-calibrated thermometer (also pictured on right). Each chamber was fitted with a magnetic stir bar and a fiber optic O_2 sensor (black wires) connected to a Pre-Sens OXY-10 mini instrument (not shown).

25 min of darkness, the chambers were opened, flushed with tank water, and photochemical efficiency (F_V/F_M) was measured in triplicate in three distinct places on the nubbin using a pulse-amplitude modulated fluorometer (Junior-PAM, Heinz Walz GmbH). All chambers were resealed, and the tank was illuminated with an irradiance of 500 μmol photons m^{-2} s^{-2} via white LED lamps to saturate photosynthesis (Bedwell-Ivers et al. 2017). Incubation irradiances were verified using a Li-Cor 250A meter and scalar irradiance sensor. Net O_2 flux was measured for at least 10 minutes at each temperature. This process was repeated at five distinct temperatures during two experimental exposures.

Acute Exposure – Independent sets of nubbins, consisting of one nubbin from each genet selected at random, were transferred from the staging tank directly into temperature-stabilized chambers. Each nubbin was measured at a single temperature, then sacrificed. The first measurements were conducted at 25.4° C. The temperature was increased to 35.4° C for the second set of measurements, and successive measurements were made at decreasing temperatures. The same six genets were present at each measurement temperature in the acute exposure, with one exception: due to the previously mentioned mortality of a nubbin from genet F in the field, only five genets were measured at 27.9° C, resulting in 29 nubbins in the acute exposure.

Prolonged Exposure - As above, seven nubbins (genets B-J) were placed into chambers at 25.4° C. The O_2 metabolism of these individuals was measured repeatedly as temperature was incrementally ramped to five temperatures between 25.4° C and 35.7° C. Six of the seven genets were the same as those in the acute experiment. Nubbins from the cumulative experiment were exposed to each measurement temperature for at least 10 min, then ramped up by 2.5° C in 30 min. This design was chosen for several reasons. First, if different exposures produced the same physiological patterns, a cumulative exposure would substantially reduce the number of corals sacrificed. Second, the ramp rates were selected to capture physiological changes that may occur with increasing temperatures on par with a large tidal oscillation in a highly variable nearshore environment (as in Chapter 2). Third, F_V/F_M is constant in the daylight and lower at night, thus, to avoid day/night effect, all measurements were made between 0900 to 1700.

Temperature was monitored constantly with a NIST calibrated thermometer (Table 8), and salinity was measured at every temperature using a refractometer (Tables 9, 10). Metabolic

measurements commenced once the temperature had stabilized for several minutes and all measurements began with air-saturated seawater. Differences in O_2 solubility due to temperature and salinity were compensated for in all calculations during data processing.

Data Processing

Temperature was held within 0.1° C during each measurement (Figure 24, Table 8). The duration of each exposure period was recorded (Table 8), enabling the calculation of the thermal index Degrees Heating Minutes (DHM, ° C min) above the ambient temperature (25.4° C). In the acute exposure, coral nubbins were sacrificed immediately after measurements were completed, while cumulatively exposed nubbins were sacrificed at the end of the full exposure.

Triplicate measurements of photochemical efficiency were averaged for each nubbin at each measurement temperature, to give mean F_V/F_M for each genet in both exposure treatments. Metabolic rates of respiration (R) and gross photosynthesis (P_{GROSS}) were calculated from changes in dissolved O_2 concentration as in Aichelman et al. (2019). Raw oxygen evolution recorded by Pre-Sens software (version Oxy10v3_33fb) was corrected for temperature and salinity based on the correction calculations provided by Pre-Sens. The corrected, continuous [O_2] time series were plotted, and sections of each trace that corresponded to measurements in the light and dark were identified. These sections were fitted to a linear model to obtain slopes of $\Delta O_2/\Delta t$ (nmol O_2 mL^{-1} min^{-1}) in the dark (R) and in the light (P_{NET}). These metabolic rates in were corrected for the combined effects of instrument drift and microbial metabolism from the seawater, scaled to chamber volume (mL) and normalized to coral tissue surface area (cm^2, see below). Gross photosynthesis (P_{GROSS}) was calculated as $P_{NET} + |R|$.

Each metabolic rate was examined as a function of thermal stress, defined as DHM. Values of F_V/F_M, R, and P_{GROSS} vs. temperature were each fitted to a modified Schoolfield-Sharpe model, which assumes the activity of a single rate-controlling enzyme controls the apparent temperature dependence of the rate (Padfield et al. 2016):

$$\ln(b(T)) = E_a(1/kT_c - 1/kT) + \ln(b(T_c)) - \ln(1+e^{Eh(1/kTh - 1/kT)})$$

using the iterative curve fitting tool (CFTOOL) in MATLAB™ that also provided error estimates for each equation parameter. Symbols used for the models, and their definitions, are summarized in Table 9.

The lower limit of Symbiodiniaceae photosynthesis in culture has been reported to be 5° C (McBride et al. 2009); thus 5° C was chosen as the lower constraint for all models in order to achieve adequate fitting of thermal performance curves. Resulting model parameters were compared via t-tests to identify significant differences in curve features between acute and prolonged exposures. The temperature sensitivity (Q_{10}) was calculated over the exponentially increasing portion of the response curve from 25° C to 36° C for each metabolic rate with acute and cumulative exposures, as

$$Q_{10} = \left(\frac{R2}{R1}\right)^{\left(\frac{10}{T2-T1}\right)}.$$

Table 8. Thermal stress expressed as degrees heating minutes (DHM, ° C min) calculated above ambient (25.4° C), which encompasses exposure duration at each temperature in both acute and cumulative scenarios.

Metabolic Measurement Temperatures (˚C)		Time (minutes)		DHM > 25.4˚C	
acute	cumulative	acute	cumulative	acute	cumulative
25.4	25.5	41	46	7	1
27.9	28.0	21	65	77	97
30.5	30.7	75	26	234	324
32.9	33.1	120	39	388	559
35.4	35.7	85	63	488	1137

Table 9. Symbols, definitions and units used for model parameters. * indicates a constant.

Symbol	Definition	Units
$b(T)$	metabolic rate per unit surface area	nmol O_2 cm^{-2} min^{-1}
E_a	activation energy for the metabolic process	eV
E_h	temperature induced inactivation of enzyme kinetics > *Th*	eV
$b(T_c)$	metabolic rate at *Tc*	nmol O_2 cm^{-2} min^{-1}
T_c	reference temperature, 298.55*K* (25.5˚ C) *	*K*
T_h	temperature at which enzymatic inactivation begins	*K*
k	Boltzmann's constant (8.62 x 10e-5) *	eV K^{-1}
T	temperature	*K*

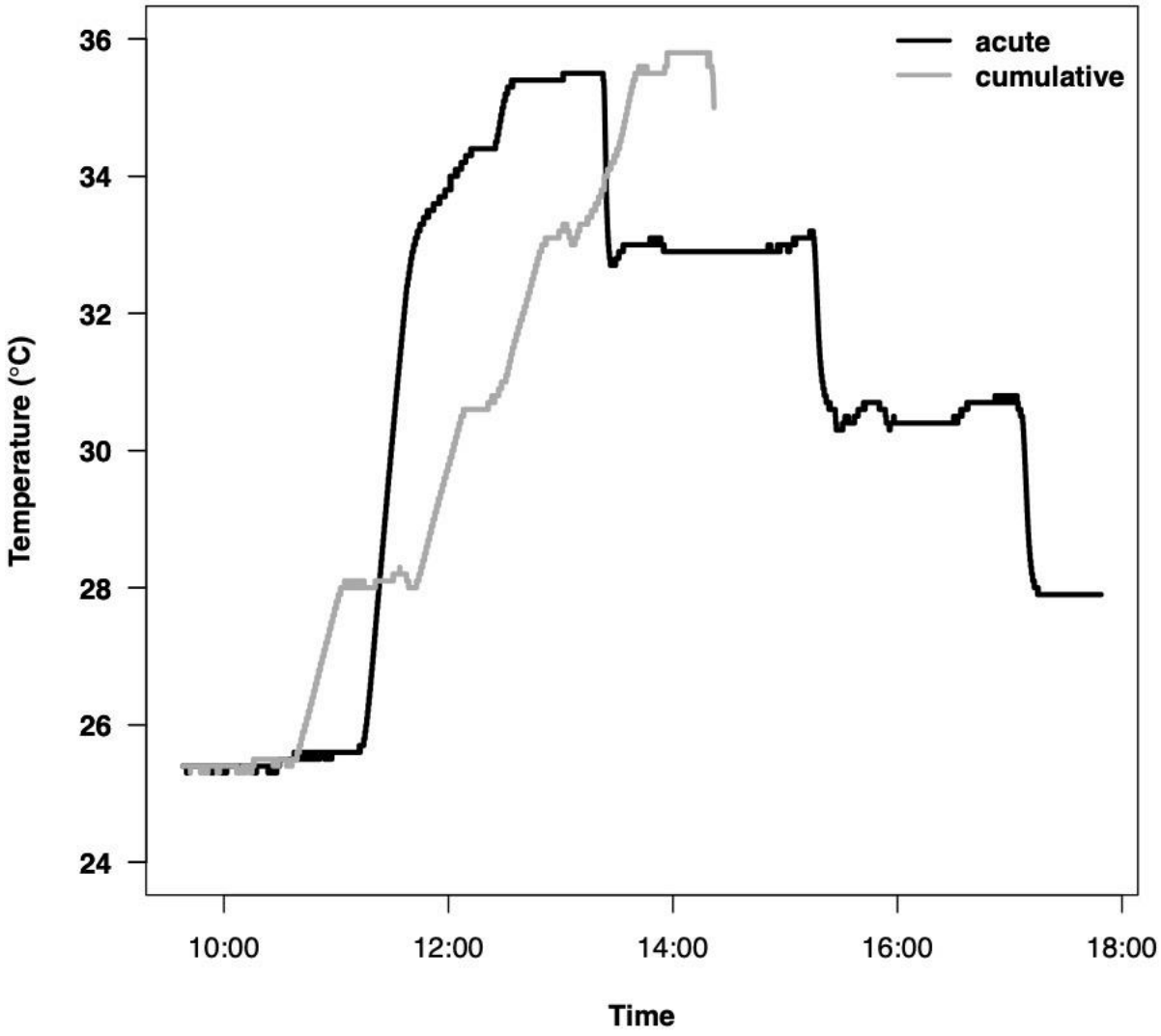

Figure 24. The temperature series of two thermal stress experiments, wherein coral holobiont respiration and net photosynthesis were measured at 5 discrete temperatures (flat breaks) for at least 20 minutes (10 minutes for dark respiration and 10 minutes for net photosynthesis).

Table 10. The exact measurement temperatures, salinities, and metabolic rates of coral nubbins during acute (a) and cumulative (b) exposure experiments. The coral host genet and rates of respiration (R), net photosynthesis (P_{NET}) and gross photosynthesis (P_{GROSS}) are identified.

a.

Acute Exposure

temperature (˚C)		Salinity	Host	Metabolic Rate (nmol O_2 cm^{-2} min^{-1})		
R	*P*	(PSS-78)	Genet	*R*	P_{NET}	P_{GROSS}
25.4	25.4	38	B	7.95	16.47	24.42
			C	6.38	20.17	26.55
			E	6.39	21.29	27.68
			F	5.12	16.24	21.36
			H	7.51	13.68	21.19
			J	5.38	22.20	27.58
27.8	27.9	39	B	11.56	16.78	28.34
			C	8.47	11.03	19.49
			E	8.57	9.09	17.66
			F	10.45	14.43	24.88
			H	9.76	11.19	20.95
30.6	30.6	39	B	17.07	19.73	36.80
			C	13.24	17.21	30.45
			E	10.69	15.48	26.17
			F	15.82	11.80	27.62
			H	10.48	14.51	24.99
			J	11.72	14.20	25.92
32.9	33.1	39	B	11.08	6.91	18.00
			C	11.66	12.31	23.96
			E	12.79	11.01	23.80
			F	10.78	-2.63	8.15
			H	14.32	10.37	24.68
			J	8.40	3.51	11.90
34.4	35.7	38	B	12.79	-6.10	6.70
			C	8.86	-1.21	7.65
			E	5.79	-0.94	4.85
			F	10.35	-7.11	3.24
			H	8.81	-0.46	8.35
			J	14.87	-0.13	14.75

Table 10b. continued

Cumulative Exposure						
temperature (˚C)		Salinity	Host	Metabolic Rate (nmol O_2 cm^{-2} min^{-1})		
R	*P*	(PSS-78)	Genet	*R*	P_{NET}	P_{GROSS}
25.4	25.5	38	C	7.51	12.74	20.25
			D	4.91	16.02	20.93
			E	8.67	21.94	30.61
			F	4.41	13.93	18.34
			H	7.15	15.29	22.44
			J	6.97	16.64	23.61
28.0	28.1	38	B	11.96	23.32	35.28
			C	7.96	16.92	24.88
			D	8.59	15.88	24.47
			E	10.90	22.92	33.82
			F	10.48	18.31	28.79
			H	10.61	15.63	26.24
			J	8.74	19.24	27.97
30.6	30.8	38	B	12.51	21.37	33.88
			C	12.08	14.85	26.93
			D	8.21	8.11	16.32
			E	15.40	19.52	34.92
			F	15.90	25.03	40.93
			H	12.32	19.22	31.53
			J	17.31	17.07	34.37
33.1	33.2	38	B	13.78	12.23	26.01
			C	10.98	11.16	22.14
			D	10.63	4.25	14.88
			E	25.83	17.98	43.82
			F	23.69	11.82	35.51
			H	12.50	9.95	22.45
			J	13.36	8.56	21.91
35.7	35.8	38	B	13.81	3.84	17.65
			C	11.42	2.79	14.21
			D	10.44	2.04	12.48
			E	20.63	2.32	22.95
			F	12.66	1.91	14.57
			H	15.38	1.17	16.55
			J	12.98	-0.50	12.48

RESULTS

Temperatures in the field and outdoor tank were identical and did not exceed 26° C (not shown). Thermal stress levels (DHM, ° C min) at each measurement temperature in both exposures were similar at measurement temperatures < 30° C. At temperatures > 30° C, nubbins were exposed to greater thermal stress in the cumulative exposure than in the acute exposure (Table 8, Figure 25).

Photochemical efficiency in both exposures conformed to the Schoolfield-Sharp model but did not match measurements of F_V/F_M at the reference temperature, $b(T_c)$ (Figure 26; Table 11a). The T_h of F_V/F_M was significantly lower (by 4.9° C) in the acute exposure (Table 11a-c, Figure 26). F_V/F_M decreased when temperatures exceeded 28° C, representing an accumulation of thermal stress > 75° C min in both treatments (Figures 25, 29). Mean F_V/F_M dropped from 0.58 to 0.46 in the cumulative exposure while F_V/F_M in the acute exposure dropped from 0.55 to 0.19 (Figure 26). In the acute exposure, F_V/F_M decreased linearly from 0 to 388° C min, then declined sharply at 488° C min (Figure 26). In contrast, the slope of F_V/F_M with cumulative exposure was less steep and never fell below 0.45, despite being exposed to > 1100° C min, more than twice the thermal stress of the acute exposure.

Exposure regime had a significant effect on the Schoolfield-Sharp model parameters of R and P_{GROSS} between the temperature exposure treatments (Table 11b, Figures 27, 28). Baseline values of R (i.e., $b(T_c)$) and temperature-induced enzyme activation, E_a, of respiration did not differ with exposure. E_h differed significantly with exposure; the cumulative exposure had a steeper decline in R after T_h than did the acute exposure. Holobiont respiration was not measured at temperatures greater than 35.7° C; thus, it is possible the critical thermal maximum was higher than the upper constraint of 40° C used in the model. However, T_h was 1.5° C lower

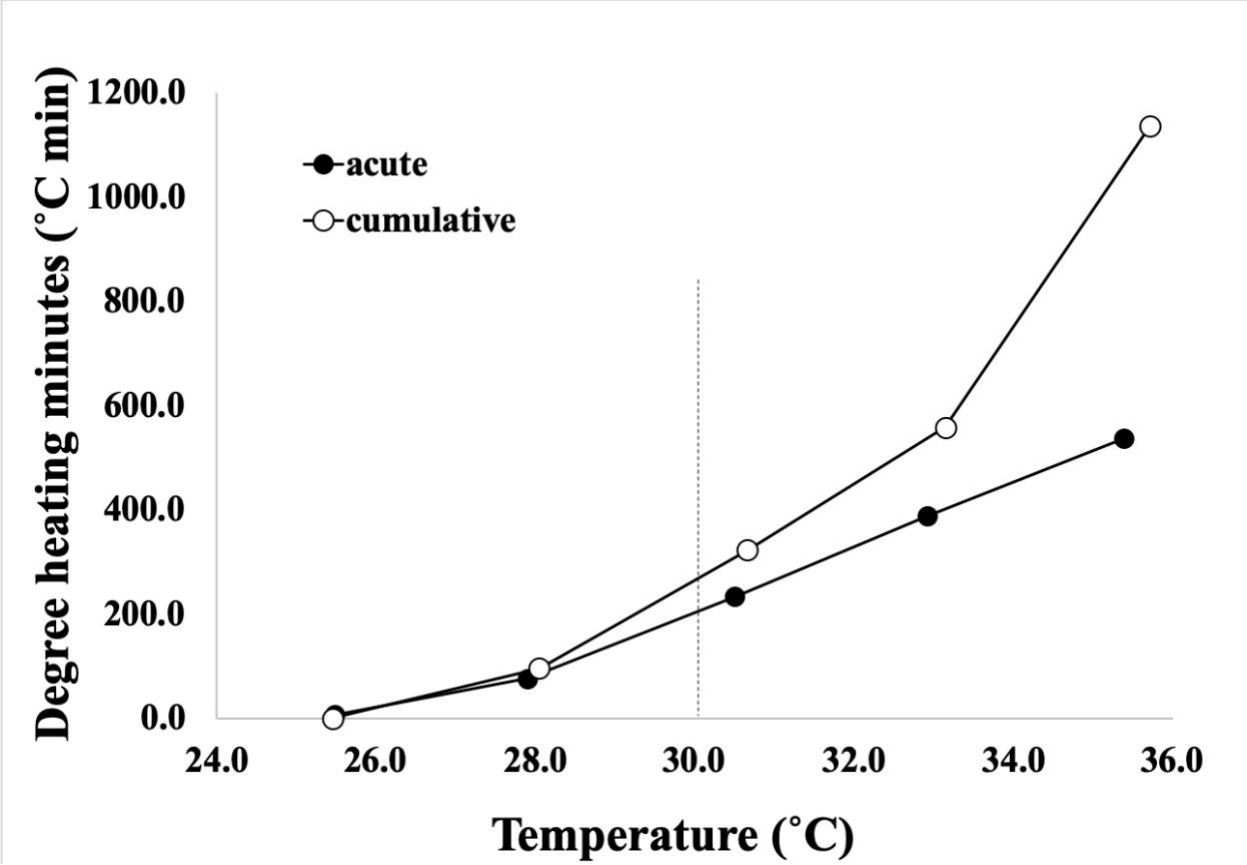

Figure 25. Plot of the degrees heating minutes (DHM, ° C min) of thermal stress above ambient, 25.4° C, for the acute and cumulative treatments. Dotted line shows the point at which thermal stress doses between treatments diverged.

Table 11. (a) Sum of squared errors (SSE), coefficient of determination (Adjusted R^2), and root mean square error (RMSE) for the Schoolfield-Sharpe models. (b) Mean parameters values ± SD for the effect of temperature on photochemical efficiency (F_V/F_M), respiration (R) and gross photosynthesis (P_{GROSS}) in acute and cumulative exposures. Temperatures are in ° C. (c) t-test results comparing the parameters from the acute and cumulative exposures, respectively. The t statistic (t), degrees of freedom (df), standard error of the difference, p-values (p), mean difference, and lower and upper confidence intervals (CI) are given.

a.

	Acute			Cumulative		
Performance	SSE	Adjusted R^2	RMSE	SSE	Adjusted R^2	RMSE
F_V/F_M	0.057	0.928	0.044	0.026	0.988	0.023
R	1.17	0.97	0.18	1.78	0.97	0.19
P_{GROSS}	2.60	0.97	0.26	1.75	0.98	0.20

b.

Model	F_V/F_M		R		P_{GROSS}	
Parameter	acute	cumulative	acute	cumulative	acute	cumulative
E_a	0.15 ± 0.02	0.16 ± 0.02	0.76 ± 0.07	0.74 ± 0.05	1.34 ± 0.19	1.15 ± 0.08
E_h	3.44 ± 1.30	1.57 ± 0.19	2.67 ± 0.60	4.30 ± 1.04	1.40 ± 0.30	1.93 ± 0.24
$b(T_c)$	1.42 ± 0.04	1.47 ± 0.03	3.15 ± 0.13	3.11 ± 0.08	4.84 ± 0.49	4.28 ± 0.17
T_h	36.6 ± 0.7	41.5 ± 0.2	36.1 ± 1.0	37.6 ± 0.6	28.6 ± 2.9	32.9 ± 1.1

c.

	Parameters	*t*	*df*	*Std. Err of Difference*	*p*	*Mean Difference*	*Lower CI*	*Upper CI*
F_V/F_M	E_a	1.17	11	0.009	0.267	-0.01	-0.03	0.01
	E_h	3.79	11	0.494	**0.003**	1.87	0.78	2.96
	$b(T_c)$	2.57	11	0.019	**0.026**	-0.05	-0.09	-0.01
	T_h	17.81	11	0.275	**< 0.0001**	-4.9	-5.5	-4.3
R	E_a	0.60	11	0.03	0.561	0.02	-0.05	0.09
	E_h	3.38	11	0.48	**0.006**	-1.63	-2.69	-0.57
	$b(T_c)$	0.68	11	0.06	0.510	0.04	-0.09	0.17
	T_h	3.34	11	0.4	**0.007**	-1.5	-2.5	-0.5
P_{GROSS}	E_a	2.42	11	0.08	**0.034**	0.19	0.02	0.36
	E_h	3.54	11	0.15	**0.005**	-0.53	-0.86	-0.20
	$b(T_c)$	2.85	11	0.20	**0.016**	0.56	0.13	0.99
	T_h	3.65	11	1.2	**0.004**	-4.3	-6.9	-1.7

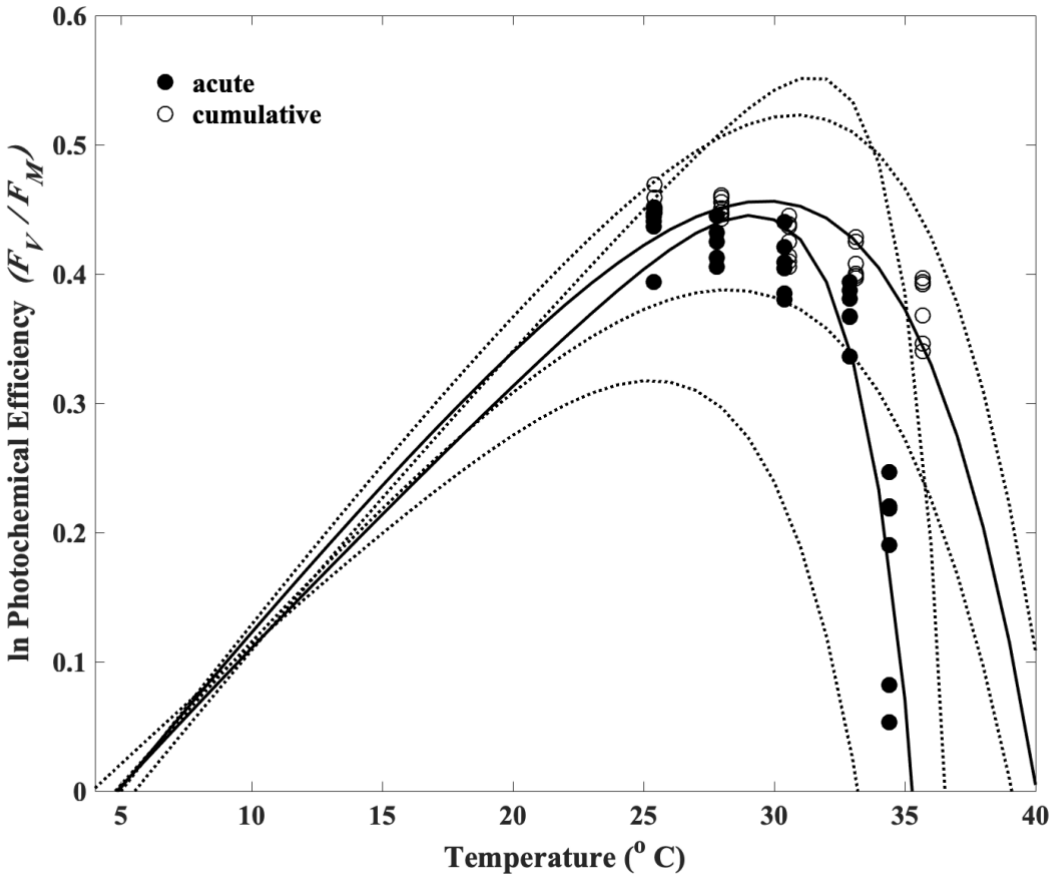

Figure 26. The effect of acute (solid points) and cumulative (open points) thermal stress on photochemical efficiency. The solid lines are the Schoolfield-Sharpe models of acute and cumulative exposures. Dotted lines are 95% confidence intervals.

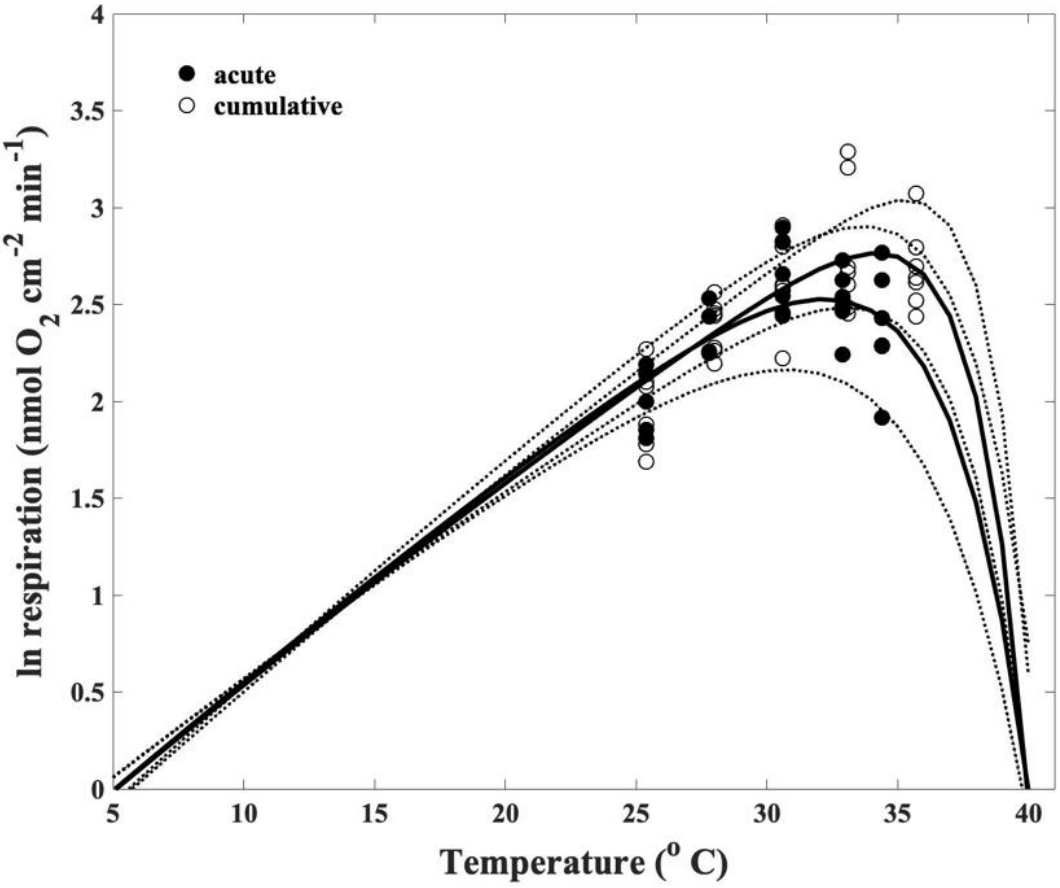

Figure 27. The effect of acute (solid points) and cumulative (open points) thermal stress on holobiont respiration. The solid lines are the Schoolfield-Sharpe models of acute and cumulative exposures. Dotted lines are 95% confidence intervals.

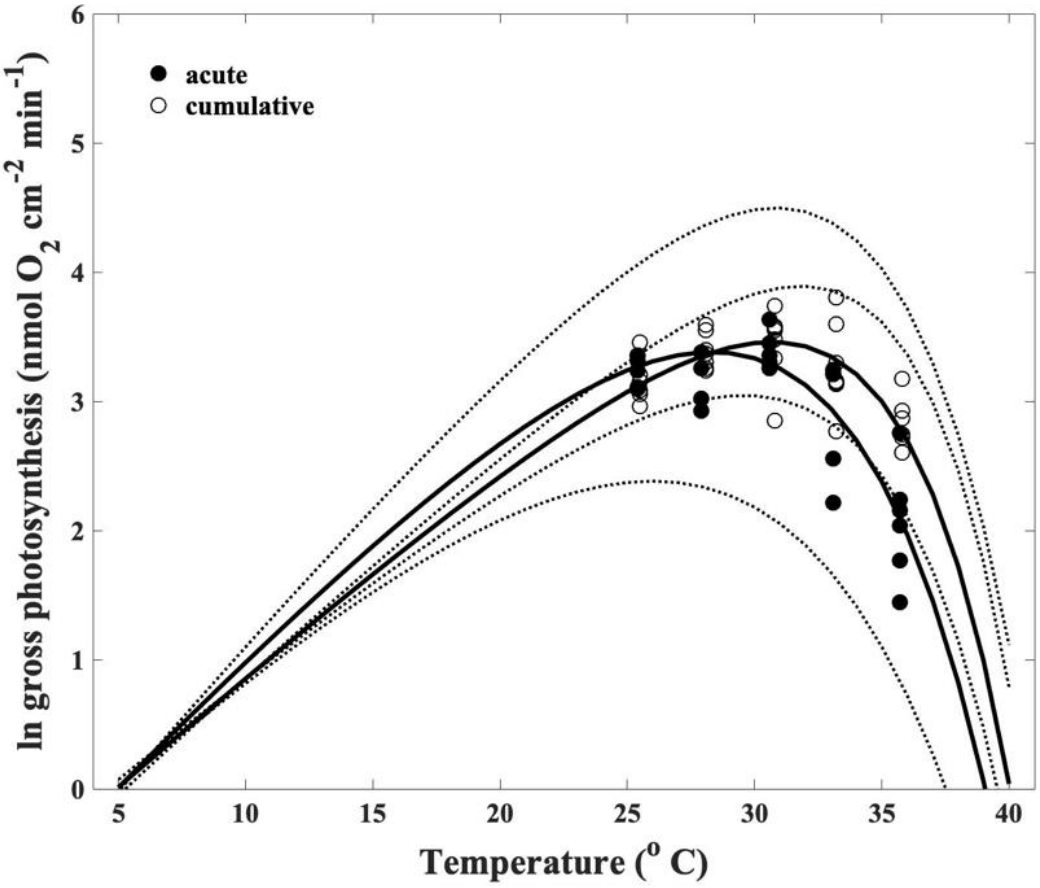

Figure 28. Effect of acute (solid points) and cumulative (open points) thermal stress on gross photosynthesis. The solid and dashed lines are the Schoolfield-Sharpe models of acute and cumulative exposures, respectively. Dotted lines are 95% confidence intervals.

in the acute exposure, indicating, as with F_V/F_M, that holobiont *R* was more sensitive to acute thermal stress than cumulative temperature exposure.

Every model parameter for P_{GROSS} differed with exposure. E_a and $b(T_c)$ were slightly, but significantly greater in the acute exposure. The mean differences in E_a and $b(T_c)$ were 0.19 and 0.56 higher in the acute exposure than in the cumulative exposure, respectively. T_h and E_h of P_{GROSS} were 4.3° C and 0.53 greater in the cumulative exposure, respectively (Table 11c). Of note, the acute exposure P_{GROSS} measurements displayed a high degree of variability, thus 95% confidence intervals overlapped (Figure 28). Rates of P_{GROSS} in both exposures and *R* in the acute exposure increased until thermal stress reached values greater than 324° C min (i.e., from 25° C to 31° C), then decreased with increasing DHM (Figures 30, 31). However, in the cumulative exposure treatment, *R* continued to increase at temperatures > 31° C and plateaued, despite being exposed to nearly twice the thermal stress of the acute treatment (Figure 30). P_{GROSS} increased with increasing thermal stress until the DHM dose exceeded 324° C min (Table 11, Figure 31).

R was three times more sensitive to increasing temperature than P_{GROSS} in the acute exposure and had 1.8 times higher sensitivity with cumulative stress (Table 12). P_{GROSS} was more 1.5 times more sensitive to the greater doses of thermal stress in the cumulative exposure, but *R* Q_{10} values were higher with acute exposure, indicating it was more sensitive to acute warming that cumulative.

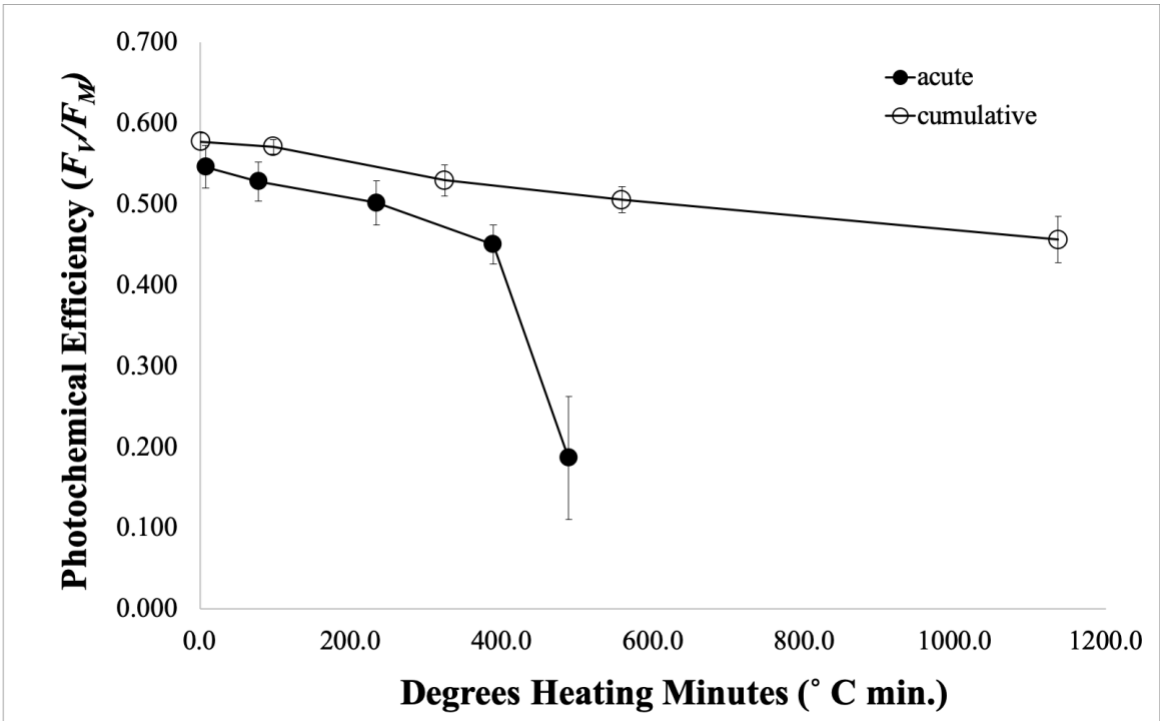

Figure 29. The relation of photochemical efficiency as a function of thermal stress, expressed as degrees heating minutes under both acute (solid circles) and cumulative (open circles) exposures. Error bars represent the 95% confidence intervals.

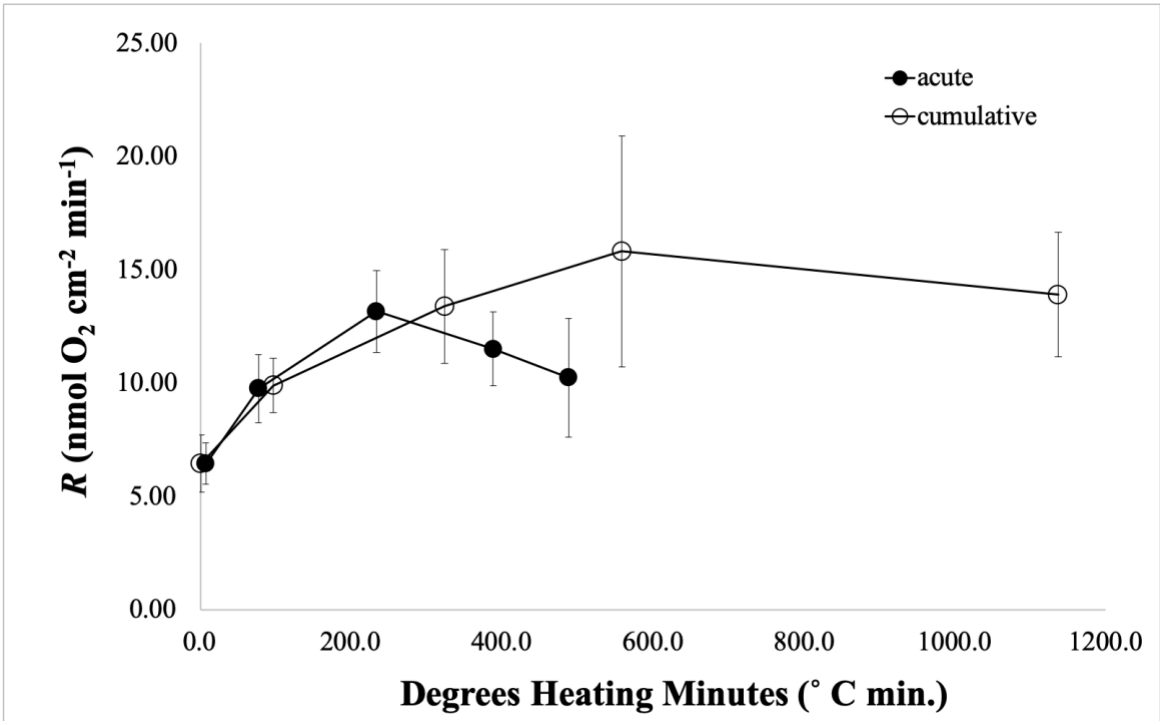

Figure 30. The relation of respiration as a function of thermal stress, expressed as degrees heating minutes under both acute (solid circles) and cumulative (open circles) exposures. Error bars represent the 95% confidence intervals.

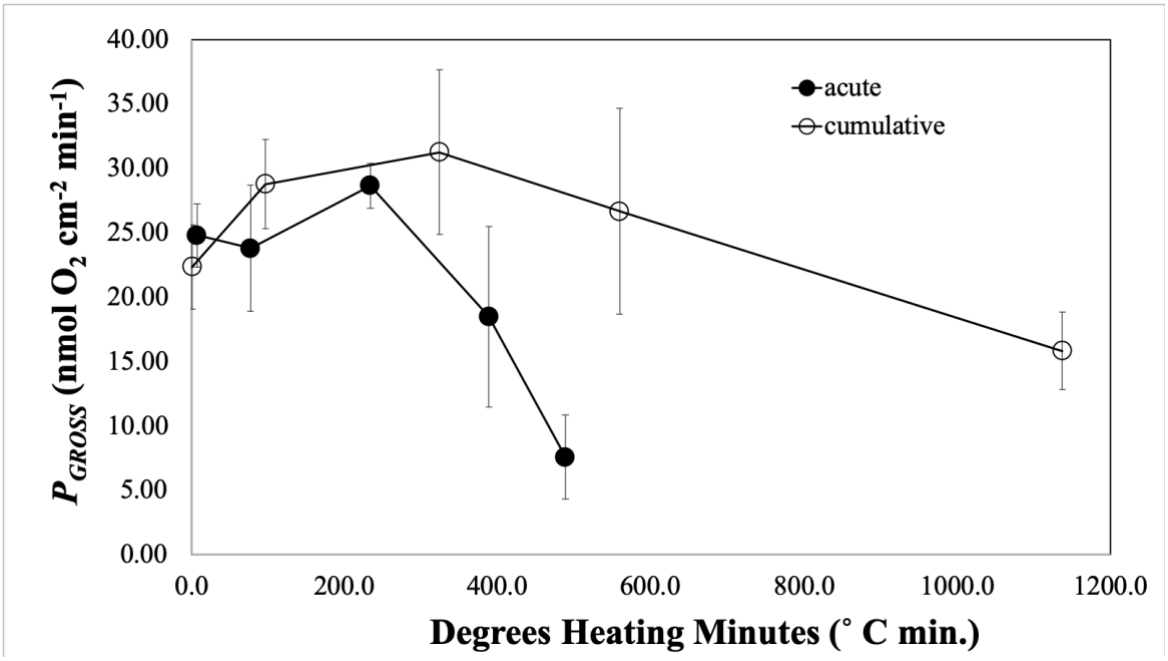

Figure 31. The relation of gross photosynthesis as a function of thermal stress, expressed as degrees heating minutes under both acute (solid circles) and cumulative (open circles) exposures. Error bars represent the 95% confidence intervals.

Table 12. The mean $Q_{10} \pm 1$ standard error of each metabolic rate with increasing temperature. Q_{10} of acute respiration and gross photosynthesis were calculated from 25° C to 31° C. Q_{10} was calculated from 25° C to 33° C for cumulative respiration.

	Q_{10}	
Metabolic Rate	Acute	Cumulative
Respiration	4.37 ± 0.97	3.57 ± 0.94
Gross Photosynthesis	1.38 ± 0.20	2.10 ± 0.47

DISCUSSION

Physiological symptoms of thermal stress were most apparent in the acute exposure, adhering to the prevailing thermal acclimation theory. All physiological measures had lower temperatures of inactivation, T_h, with acute exposure. In addition, E_h, the slopes of enzyme inactivation for R and P_{GROSS} were lower with acute exposure. Holobiont metabolism was not measured at temperatures greater than 36° C in this study, and the same upper constraints (40° C) were used for model fitting for both exposures; therefore, it is expected an increase in T_h would lead to a steeper E_h, as was observed in both R and P_{GROSS}. However, some enzymes and proteins critical to cellular function denature around 40° C; thus, a large shift in critical thermal maximum is unlikely (Angilletta 2009). Coral material available for this study was limited. Future work should be aimed at measuring greater numbers of nubbins perhaps at larger temperature intervals so the critical thermal maxima and minima can be determined to capture the full thermal performance breadth.

Holobiont respiration showed greater resiliency than photosynthesis at high doses of thermal stress (Figure 30), despite respiration rates being 3 times more sensitive to changes in temperature (Table 12). One possibility for the sharp decline P_{GROSS} compared to R at higher

doses of thermal stress might imply a limitation of carbon dioxide (CO_2), the substrate for symbiont photosynthesis. While pH wasn't measured during this experiment, CO_2 limitation under different exposures should be investigated. This observation would have gone unnoticed without equating the exposures to thermal stress dosage (DHM), underscoring the value of putting thermal stress experiments in a dose context for corals.

Changes in mitochondrial density and enzyme activity are common cellular compensatory mechanisms acting on the order of days to weeks (Bouchard and Guderley 2003, O'Brien 2011) in response to thermal stress in animals, with increases observed in cold water conditions (Pörtner and Knust 2007; Pörtner and Farrell 2008; Pörtner 2010), and reductions in warm water conditions (Kraffe et al. 2007). In contrast to the patterns found in fishes, wherein mitochondrial biogenesis is observed with cold acclimation, mitochondrial biogenesis appears to increase with warm temperature acclimation in corals (Hawkins and Warner 2017). Further, positive correlations have been observed between symbiont density and mitochondrial electron transport rates and enzyme activity in several coral species (Agostini et al. 2013, 2016) and the anemone *E. pallida* (Hawkins et al. 2016). Most scleractinians are obligately symbiotic, relying on the algal partners to meet their metabolic demands (Muscatine et al. 1981). Thus, it has been inferred that temperature increases may equate to increased carbon translocation, which, in turn, allows for mitochondrial biogenesis in response to thermal acclimation (Hawkins and Warner 2017). Carbon translocation was not measured in this study; however, the decline in gross photosynthesis at temperatures and thermal stress levels > 30° C and 300 ° C min, respectively negate the likelihood for carbon translocation above these levels of thermal stress. More likely, carbon translocation may increase under thermal stress to a point, but reductions in photosynthesis lead to a decline in the photosynthesis to respiration ratio, perhaps further

supporting the possibility of CO_2 limitation. Regardless of the cause, it appears the very symbiosis that has enabled coral persistence in oligotrophic seas makes corals extremely vulnerable to increasing temperatures, at least with respect to the short-term exposures used here.

F_V/F_M reduction in the cumulative exposure was much less severe than acutely exposed corals, despite higher doses of thermal stress (i.e., greater DHM at higher temperatures). The drastic reduction of F_V/F_M, and significantly reduced T_h of F_V/F_M with increased temperature are consistent with PSII damage in the alga with acute heat shock (Warner et al. 1999). This suggests that algal symbiont PSII was particularly sensitive to acute warming. The reduction in F_V/F_M in the cumulative exposure was significant but much less pronounced than that of the acute exposure, indicating that even at extremely high doses of thermal stress, the light harvesting complex of PSII was intact enough to continue harvesting photons. However, rapid declines in F_V/F_M with acute heat shock, such as those used in Chapter 2, may result in the inability to replace important PSII structural proteins, such as D1, quickly enough under such exposure regimes, leading to photosystem breakdown (Warner et al. 1999).

The experiments presented here clearly demonstrate that even with smaller doses of thermal stress, acute heat shock exposures elicited a markedly different physiological response than did more gradual exposures to temperature stress in the hermatypic coral *A. cervicornis*. This study further demonstrated that even the slightest change in exposure (i.e., from acute to more gradual on the order of minutes) enabled physiological adjustment by the holobiont. This response difference between acute vs. more gradual exposures is consistent with findings across the literature. Gradual warming invokes beneficial physiological responses, such as higher cellular thresholds of ROS and their associated enzymes (Lesser 1996, 2006; Lesser and Farrell 2004), the induction of different metabolic and immune pathways (Rebl et al. 2018), and

enhanced survival (Harada and Burton 2019). The increased thermal tolerance of metabolism with gradual exposure found here emphasizes that subtle differences in exposure can lead to vast physiological differences. Thermal stress is strongly dependent on exposure and dose across taxa; therefore, it is important to consider ecologically relevant thermal stress applications in the context of dose when designing experiments.

Thermal peaks of metabolic performance curves were positively shifted with cumulative warming, despite the relatively rapid rate in the cumulative exposure, further supporting that more gradual warming in a very short period of time enabled detectible physiological adjustment. In addition, the cumulative treatment thermal stress exposure in this study mimicked the variable nearshore environments of Ofu Island, which routinely experience 6° C temperature fluctuations daily, resulting in exposures between 0.36 to 1.14° C days above the local mean monthly maximum temperature on an austral summer day (Chapter 2). Corals in the cumulative treatment in this study received 0.79° C days of thermal stress above the ambient temperature (not the climatological mean monthly maximum, which would result in a lower thermal stress dose), making the thermal stress doses in this study ecologically relevant.

The differences in overall thermal performance identified between acute vs. gradual thermal stress in this study have important implications for the experimental design and interpretation of coral bleaching physiology. Heat shock exposures may be appropriate when used alongside more gradual exposures to identify pathways, genes and proteins related to thermal stress (Bay and Palumbi 2015), but the results from this study suggest they likely do not reflect the integrated physiological response of the holobiont to more realistic changes in temperature as simulated by the gradual treatment. Bleaching in nature is generally not the result of heat shock, thus it is possible results from studies using acute thermal stress may be

misleading. Acute exposure generated a vastly different physiological response than a more gradual exposure, despite the gradual exposure involving a rapid rate of warming, demonstrating a potential source of error in experimental design. The disconnect between the physiological response caused by a lack of ecological relevance may explain some of the difficulty coral researchers have in accurately predicting bleaching resistance and thermal tolerance. Therefore, to make thermal stress studies more comparable, it is recommended thermal stress exposures should be calculated as doses (e.g., in degrees heating times), supporting the importance of both magnitude and duration of stress on metabolism. When appropriate, doses should be ecologically relevant to relate the results to environmental conditions.

Thermal tolerance has been related to the coral genotype (Barshis et al. 2010; Lirman et al. 2014), symbiont genotypes (Baker 2004), and environmental influence (Kenkel et al. 2013). The use of nursery corals enabled reasonable control of those factors in this study. Acroporid corals commonly experience asexual fragmentation in the wild, creating dense monoclonal thickets of single coral host genotypes (Baums et al. 2010). Collection and genotyping of corals from the wild is both costly and can compromise threatened wild populations. Nursery-sourced corals allowed for selection of genets with *a priori* knowledge of their performance to capture as much performance variation within the population as possible. The use of nursery corals that were previously genotyped ensured distinct host colony identity, and enabled inclusion of as much variation in resiliencies as possible to accurately assess the thermal performance of the Broward County *A. cervicornis* population. Nursery corals were sourced from multiple Broward County sites but were held in a common nursery setting for six to ten years, thus removing any recent effects due to differences in the environment. For these reasons, the use of nursery corals could offer great benefit for future studies, particularly for coral species where clonality is a

concern (i.e., those that proliferate predominantly by asexual fragmentation, such as many branching species).

A. cervicornis has been found to harbor predominantly a single clonal strain of *Symbiodinium fitti*, Type A3 (Thornhill et al. 2006; Parkinson et al. 2018). Therefore, low variation in symbiont genotype and thus a uniform contribution by the algal symbionts to holobiont thermal performance was assumed for this study. The population from which these nubbins were collected appears to have high genetic diversity for the region (Drury et al. 2017). However, the population lies at the northern most edge of the species' range and a depression in connectivity between it and neighboring populations to the south may limit recruitment (Drury et al. 2017). As temperatures increase, northward migration may be possible, however unassisted sexual reproduction in this population is rarely observed in the wild (Goergen, *pers. comm.*). This population is in decline, thus northward migration is not likely without intervention, putting Broward County *A. cervicornis* at increased risk of extinction. Broward County is the seventeenth most populous county in the United States (U.S. Census 2017), and most thickets of *A. cervicornis* occur 100 m off of Fort Lauderdale Beach. Therefore, continued conservation efforts are warranted to effectively manage this population from local and global stressors.

This work suggests that while respiration appears to have an acclimatory potential, photosynthesis and thus the symbiosis on which the species depends, may lack the capacity to meet metabolic demands of the holobiont when challenged by high temperatures. Future studies will be aimed at the development of a model to estimate thermally-driven metabolic deficits to more accurately predict the timing of annual severe bleaching (van Hooidonk et al. 2016). There is also still a need to assess the acclimation potential of this species to the predicted thermal stress levels of the coming decades.

GOLDILOCKS AND THE THREE CORALS:

DOES PRIMING HAVE TO BE *JUST RIGHT* TO ALLAY CORAL BLEACHING?

INTRODUCTION

Corals may acclimatize to non-lethal thermal stress, a concept referred to as acquired thermal tolerance (Brown et al. 2002, 2014, Coles and Brown 2003, Middlebrook et al. 2008, Brown and Cossins 2011, Haslun et al. 2011, Bellantuono et al. 2012). There is evidence that a particular type of acquired thermal tolerance, coral stress memory, contributes to overall thermal tolerance of individual corals (e.g., Brown et al. 2002a, 2002b, 2014, Middlebrook et al. 2008). Stress memory is defined as the modified response to a stress event when preceded by a sublethal stress event, referred to as the priming event (Hilker et al. 2015). Much like athletic training, the priming stimulus involves exposure to a mild stressor that has an upfront physiological cost to the organism, but enables an improved response when confronted with a subsequent stressor (Karban 2008, Hilker et al. 2015). For stress memory to be successful, the priming stimulus should result in increased tolerance with subsequent stress (Hilker et al. 2015). The effects of priming are governed by the magnitude and duration of the exposure. In some cases, the priming response may be short-lived, with the organism returning to its naïve, unprimed state (Hilker et al. 2015; Figure 32).

Priming acts on the phenotype of individuals, resulting in elastic cellular and/hormonal changes while leaving the genetic information (i.e., the DNA sequence) unchanged. It can, however, lead to quasi-permanent epigenetic changes, such as DNA methylation and

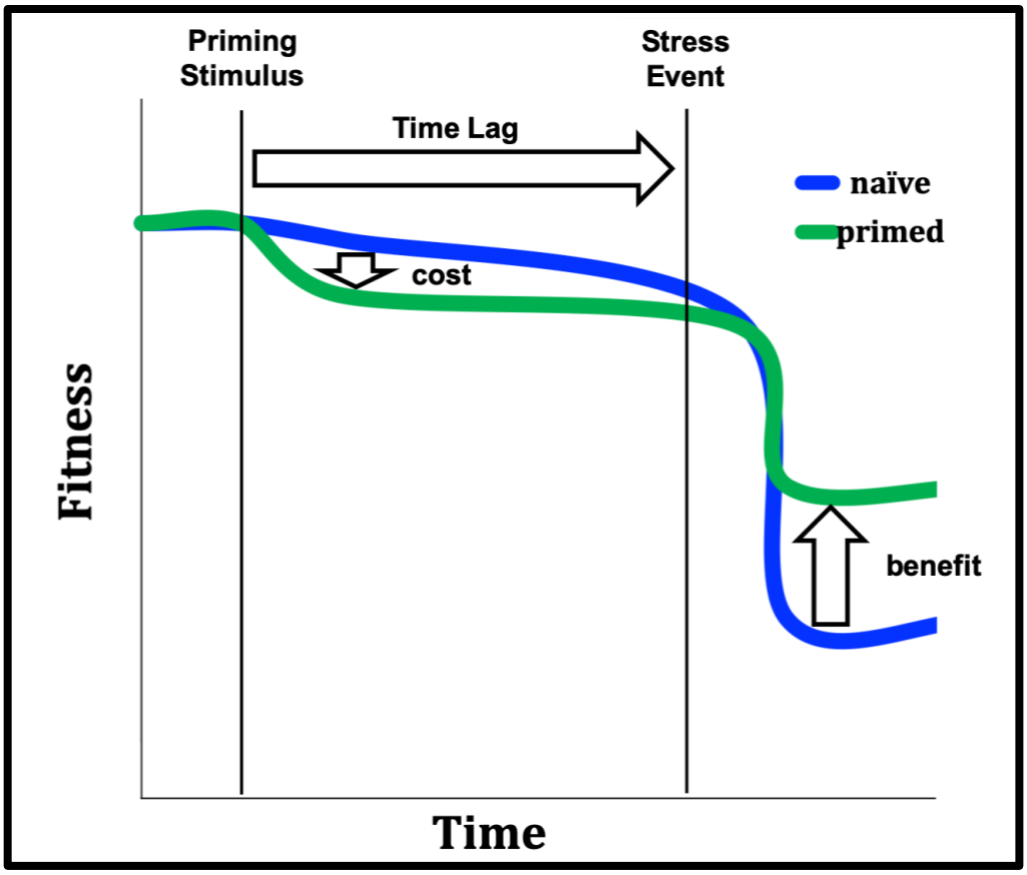

Figure 32. Diagrammatic representation of the stress memory model after Hilker et al. (2015). The blue line represents the response of a naïve organism to a stress event. The green line represents the response of a primed organism. The initial stimulus primes the organism, invoking a fitness cost; however, after some period of time, when confronted with a stress event, such as bleaching, the primed organism outperforms the naïve organism, ultimately conferring benefit.

histone modifications that occur in primed individuals and may be inherited by subsequent generations (Donelson et al. 2017, Agrawal et al. 1999, Molinier et al. 2006, Putnam and Gates 2015, Liew et al. 2018, Eirin-Lopez and Putnam 2019). The highly conserved nature of the stress memory phenomenon across disparate taxa (e.g., bacteria, yeast, plants, invertebrates, and vertebrates including humans) suggests stress memory is an important survival mechanism

(Feder 1999, Guan et al. 2012, Walter et al. 2013, Arts et al. 2016, Domínguez-Andrés et al. 2019).

There is evidence for coral stress memory in the literature (Brown et al. 2002a, 2014, Castillo and Helmuth 2005, Middlebrook et al. 2008, Haslun et al. 2011, Bellantuono et al. 2012a). The first study to suggest a stress memory capacity in corals found a differential bleaching response on only one side of irradiance-stressed colonies which persisted when the colonies were re-oriented (Brown et al. 2002, 2014). Remarkably, when the same corals were moved back to their original orientation, the stress tolerance was 'remembered' a decade later (Brown et al. 2014). Corals exposed to thermal stress in advance of a simulated bleaching event had more effective photoprotective mechanisms (Middlebrook et al. 2008), though metabolic tradeoffs have been found to exist for such pre-exposures (Rodrigues and Grottoli 2007, Grottoli et al. 2014, Gibbin et al. 2018). Indeed, as severity and frequency of thermal stress events continue to increase (Eakin et al. 2009), there is evidence for stress memory at the scale of entire reef ecosystems (Ainsworth et al. 2016, Hughes et al. 2019), though the influence and benefits of this memory are unclear (Baker et al. 2008, Bonesso et al. 2017).

To date, the majority of studies exploring thermal tolerance in corals have characterized phenotypic responses in the context of bleaching and linked phenotype to molecular changes (Thomas et al. 2018), biochemical/cellular composition (Hawkins and Warner 2017), and holobiont metabolism (Gibbin et al. 2018). Different modes of stress memory have been identified in a variety of corals. *Acropora hyacinthus* corals from warm, thermally variable habitats exhibited thermal tolerance-associated differences in baseline gene expression compared to conspecifics from cooler, more thermally stable microhabitats (Barshis et al. 2013). *Acropora millepora* exposed to sustained, but not pulsed, sub-lethal thermal stress had more effective

photoprotective mechanisms and greater symbiont retention compared to naïve corals (Middlebrook et al. 2008, Bellantuono et al. 2011). Increased chlorophyll retention was observed in *Acropora nana* following thermal challenge, after acclimation to both stable and variable temperature increases (Bay and Palumbi 2015). Increased gross photosynthesis, holobiont respiration and mitochondrial enzyme activity were observed in pre-conditioned *Exaiptasia pallida*, the latter of which were attributed to mitochondrial biogenesis/enlargement that ultimately delayed subsequent bleaching in primed anemones by several days (Hawkins and Warner 2017). In all cases, prior sub-lethal stress exposures led to enhanced thermal tolerance (i.e., reduced bleaching) when confronted with a simulated bleaching event.

Changes in gene expression, cellular function, and metabolism with acclimatization to repeated thermal stress provide evidence to suggest that stress memory plays a role in survival of corals. However, Chapter 2 revealed corals paid a price for resilience, and costs of priming remain largely unexplored. A comprehensive characterization of the physiological changes and costs (*sensu* Hilker et al. 2015) to both primed and unprimed corals is needed to better understand the potential benefits and tradeoffs associated with coral stress memory. To determine whether thermal stress memory reduced coral bleaching and to identify costs, phenotypic differences in bleaching were characterized in primed and unprimed *Acropora cervicornis* in the laboratory. Stress memory experiments can be confounded by the influence of the algal symbiont species (Abrego et al. 2008) and recent thermal history on thermal performance (e.g., Chapter 3, Castillo and Helmuth 2005, Thompson and van Woesik 2009, Donner 2011, Castillo et al. 2012). *A. cervicornis* was chosen for this study because it associates primarily with a single algal symbiont type (*Symbiodinium* spp. ITS2-type A3; Parkinson et al. 2018), thereby reducing stress memory influence caused by symbiont type association. In

addition, *A. cervicornis* corals used in this study were sourced from a nursery with a common thermal history to reduce thermal history effects.

This study sought to address three objectives: (1) whether priming had a cost to corals, (2) whether any observed cost persisted after a brief (eight-day) recovery period, and (3) whether thermal stress memory reduced coral bleaching, assessed here by changes in symbiont density, total chlorophyll, and chlorophyll per cell. Algal protein and photochemical efficiency were measured as additional physiological indicators. Experiments in Chapter 3 revealed corals exposed to gradually increasing stress displayed a higher capacity to acclimate, thus priming exposures in this study followed a more gradual approach. Standardized bleaching exposures were used to compare the degree of coral bleaching in *A. cervicornis* with and without priming.

MATERIALS AND METHODS

Field Sampling

A large number of distinct *Acropora cervicornis* coral genotypes (previously genotyped by Baums et al. 2010) were available in the coral nursery at Nova Southeastern University's (NSU) Halmos College of Natural Sciences and Oceanography. Corals were obtained from the NSU nursery in Broward County, FL (26° 07' N, 80° 05' W). The coral colonies used in this study originated in Broward County and had been in the nursery for more than six years. In late February 2017, 228 *A. cervicornis* coral fragments were created from nine coral host genotypes (i.e., genets) representing a range of coral resiliencies based on outplant growth and survival (Goergen and Gilliam 2018). Colony branches from each genet were cut

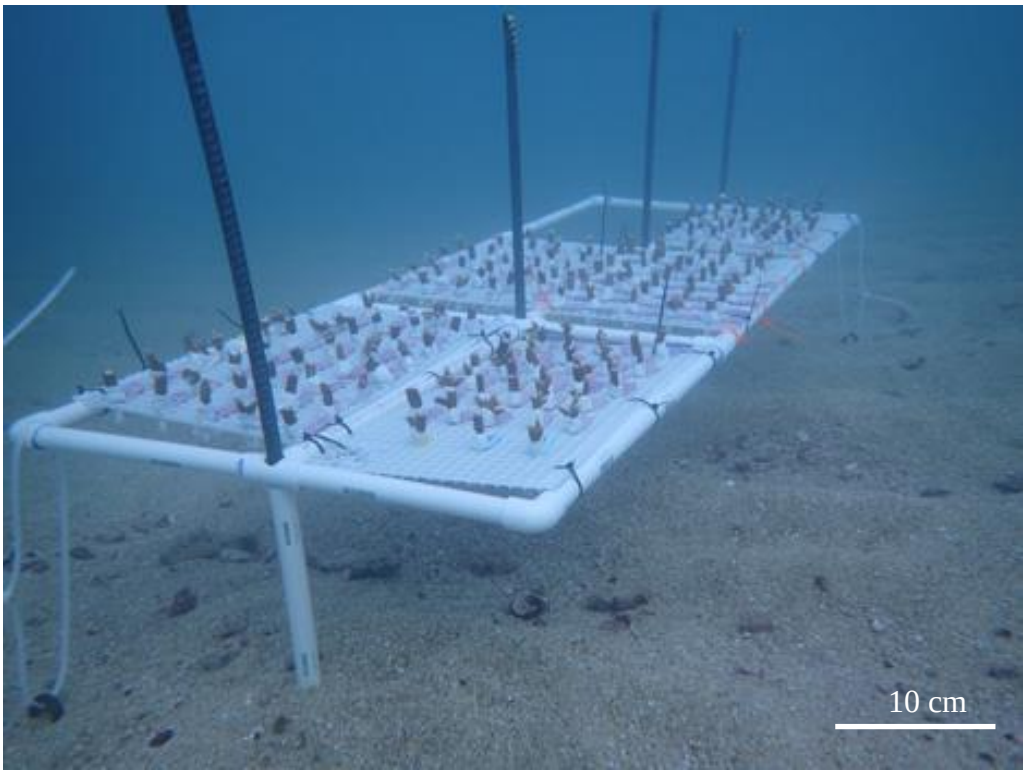

Figure 33. A photograph of experimental nubbins deployed at the coastal nursery in Broward County, FL on PVC arrays.

into 5 cm lengths (hereafter referred to as nubbins), epoxied to nylon bolts and labelled with tags to enable sample tracking for the duration of the experiment. The resulting coral nubbins were secured to grids on polyvinyl chloride (PVC) arrays anchored 0.5 m above the sand bottom with auger tie downs and rebar (Figure 33). *In situ* temperature was recorded by a HOBO temperature logger (Onset) every 30 s from the time of fragmenting until retrieval 35 and 63 days later. All nubbins appeared visibly healthy, were fully healed and had grown since the original cutting.

The nubbins were retrieved from the field and placed in a 1.5 m^3 outdoor tank plumbed with a recirculating seawater system and high multidirectional flow. The outdoor tank was covered with a clear tarp to exclude rainwater and a shade cloth to provide an irradiance (PAR) of ~550 µmol photons m^{-1} s^{-2} at local solar noon. Several water quality parameters were

monitored daily for the duration of the experiment: temperature was measured via additional loggers in all tanks and calibrated to daily measurements with a NIST-calibrated thermometer; salinity was measured using a refractometer (PSS-78, Lewis 1980); nitrate, ammonium, alkalinity (KH) and calcium were measured using a titration-based test kit (API). Turf algae and encrusting marine organisms were gently removed from non-tissue portions of each nubbin with a stainless-steel brush on a rotary tool at the time of collection from the field. Corals were rinsed with seawater, then returned to the tank.

The lab tank system was constructed from six independent recirculating tanks, as in Chapter 2 (Figure 4). Fresh seawater was supplied at a rate of 4 L h^{-1} into each head tank from a common reservoir, providing complete tank water turnover every 8 h. Each tank was supplied with 480 to 500 µmol photons m^{-2} s^{-1} of irradiance via white LED bulbs between 0700 and 1945 local time following local daylength. The temperature of each tank was controlled independently as in Chapter 3, with chilling achieved via heat exchange through coils in an ice bath. Temperature was recorded every 30 s in each tank with submersible temperature loggers. All probes and loggers were calibrated to the same NIST-calibrated thermometer to a precision of 0.1° C. Average *in situ* water temperatures in Southeast Florida in April are between 25° C and 26° C, so 25.5° C was selected as the ambient (i.e., control) temperature in all experiments (NOAA Coral Reef Watch 2017b).

Determination of a Standardized Bleaching Exposure

A preliminary experiment was performed to determine the thermal exposure required to significantly reduce symbiont density, simulating a severe bleaching event. In late March 2017, corals were retrieved from the field (n = 35) and held in the outdoor tank for ten days. Four

nubbins from each of nine genets (A – J, excluding H) were brought into the lab at 0800 h and one nubbin from each genet was placed into each of four treatment tanks. Due to mortality in the field, one tank had only eight genets.

Variable fluorescence (F_V/F_M) of each coral nubbin was measured in triplicate using a Walz Junior-PAM pulse amplitude modulation fluorometer. Corals were dark-adapted for at least 25 minutes before all measurements. Dark-adapted F_V/F_M was measured before heating began (0 h). Corals were illuminated and a bleaching exposure program was initiated once F_V/F_M measurements were completed.

Each treatment tank had a distinct maximum temperature: control (25.5° C), low (32° C), medium (33° C), and high (34° C). The water temperature in each heated tank was ramped up to the maximum at a constant rate over 3 h, held at the maximum for 3h, ramped down to ambient at the same rate over 3 h and held at ambient overnight for an additional 15 h. After the temperature ramp exposure, dark adapted F_V/F_M was measured again as above (23.5 h). Coral nubbins were individually wrapped in foil, and immediately stored at -20° C for 2.5 weeks. Coral nubbins were processed for symbiont density, algal protein, and chlorophyll concentration.

Priming Experiment

The priming experiment involved exposure to a sub-lethal thermal stress for one to two days, an eight-day recovery period in a common aquarium, and then exposed to standardized bleaching, as described above (Figure 34). Corals that benefit from a priming exposure should demonstrate increased resistance to bleaching when subsequently challenged by a temperature stress. All remaining nubbins were retrieved from the field and placed in the outdoor tank (n = 192) in late April 2017. After four days, they were transferred into one of six treatment tanks in

the lab for priming. Each treatment tank held four nubbins from each of eight genets (C – J), for a total of thirty-two nubbins per treatment (n = 4 corals/genet x 8 genets = 32 nubbins per treatment). Nubbin tag numbers in each treatment were recorded.

The control (C) nubbins were held at ambient temperature for the duration of the experiment (no thermal stress, negative bleaching control). Corals in the naïve treatment (N) were held at ambient during the priming period but subjected to the bleaching exposure, potentially eliciting the maximum bleaching response (positive bleaching control). The four additional treatments were primed with low and high durations and temperatures: 24 h at 28.0° C (LL), 24 h at 30.5° C (LH), 48 h at 28.0° C (HL), and 48 h at 30.5° C (HH). Heating and cooling in all treatments occurred at a rate of 1° C h^{-1}. Subsets of coral nubbins representing each of eight genets from each treatment (subset = 8 genets/treatment x 6 treatments = 48 corals) were sacrificed at three distinct timepoints for invasive sampling: after priming (day 2), after the recovery period (day 10), and at the conclusion of the bleaching exposure (day 11). Sacrificed corals were removed from the treatment, immediately wrapped in foil and placed at -20° C until processing (< 2 weeks).

Dark-adapted F_V/F_M was measured in triplicate from a subset of nubbins in N, LH and HH on day 1 and in all treatments on days 2, 3, 6, 10, and 11 of the experiment. Measurements were made between 1100 and 1330 each day. Different subsets were measured each day to minimize handling stress. Heating began in the high and low duration treatments at 1330 on days 1 and 2, respectively (Figure 34, 3a).

At the conclusion of the priming exposure (day 3), a subset of corals was sacrificed as above, and all remaining corals were transferred to the outdoor tank (Figure 34, 3b). Each day, nubbins were moved around the outdoor tank randomly to account for variation in irradiance or

flow in different areas of the tank. After 8 days of recovery (day 10), another subset of nubbins was sacrificed (Figure 34, 3d), and the remaining nubbins were brought into the lab for the bleaching exposure.

Control nubbins for the bleaching exposure were selected by randomly choosing nubbins kept at ambient during priming from either the C or N priming treatments. The remaining naïve and primed nubbins were randomly dispersed among the five heat tanks for the bleaching exposure (Figure 34, 3e).

Sample Processing

Coral tissues were airbrushed from the skeleton with seawater (100 psi), collected in 50 mL conical tubes, and kept on ice in the dark at all times during processing. Skeletons were dried and surface area was determined by the wax method (Stimson 1991). Tissue slurries were homogenized for 1 min with an electronic tissue homogenizer, and centrifuged at 5,000 x *g* for 5 min. The supernatant was discarded, and the algal pellet was resuspended in seawater to 25 mL final volume.

Symbiont Density

A small aliquot of the resuspended pellet was fixed in formaldehyde (1% v/v final concentration) and stored at 4° C for three weeks. Each sample was vortexed thoroughly and diluted with phosphate-buffered saline (PBS dilution factor = 5) for flow cytometry. Cell counts were performed on a MACS Quant Analyzer 10 flow cytometer using the PerCP Vio 700A and PE-A channels following the gating previously established in Chapter 2. *Symbiodiniaceae* cultures were used to confirm accurate gating and optimal sample dilution. The MACS Quant

Analyzer provided counts in cells mL^{-1}, which were multiplied by the dilution factor, fixative dilution, total sample volume, and normalized to surface area to give symbiont densities (cells cm^{-2}).

Algal Protein

Algal protein concentration was determined using the Bradford protein assay standardized against bovine serum albumen (Bradford 1976). An aliquot of resuspend pellet (1 mL) was bead beaten at 4000 rpm for 45 s in three, 15 s intervals with 0.5 mL of Zirconia/Silica beads (0.5 mm, Catalog# 11079105z, BioSpec Products, Inc.). Between intervals, samples were chilled on ice to prevent protein degradation. Microscopic examination was performed on four samples to verify complete cell rupture. Absorbance at 595 nm was measured on a FLUOstar Optima plate reader (BMG Labtech) to estimate protein concentration as determined by the standard curve. Algal protein was normalized to surface area ($\mu g\ cm^{-2}$) and symbiont cell number (ng prot $cell^{-1}$).

Chlorophyll Concentration

The remaining slurry was spun down at 5,000 x *g*, the supernatant was discarded, and the pellet was resuspended in a known volume of 90% acetone. The algal cells were sonicated in an ice bath, sealed, and extracted at -20° C for 24 h. Samples were centrifuged at 5000 x *g* for at least 1 min and the extract absorbance was measured. Absorbance spectra were corrected for the absorbance of 90% acetone and any residual turbidity by subtracting the difference in mean absorbance between 715 to 725 nm from absorbance at every wavelength from 400 to 725 nm.

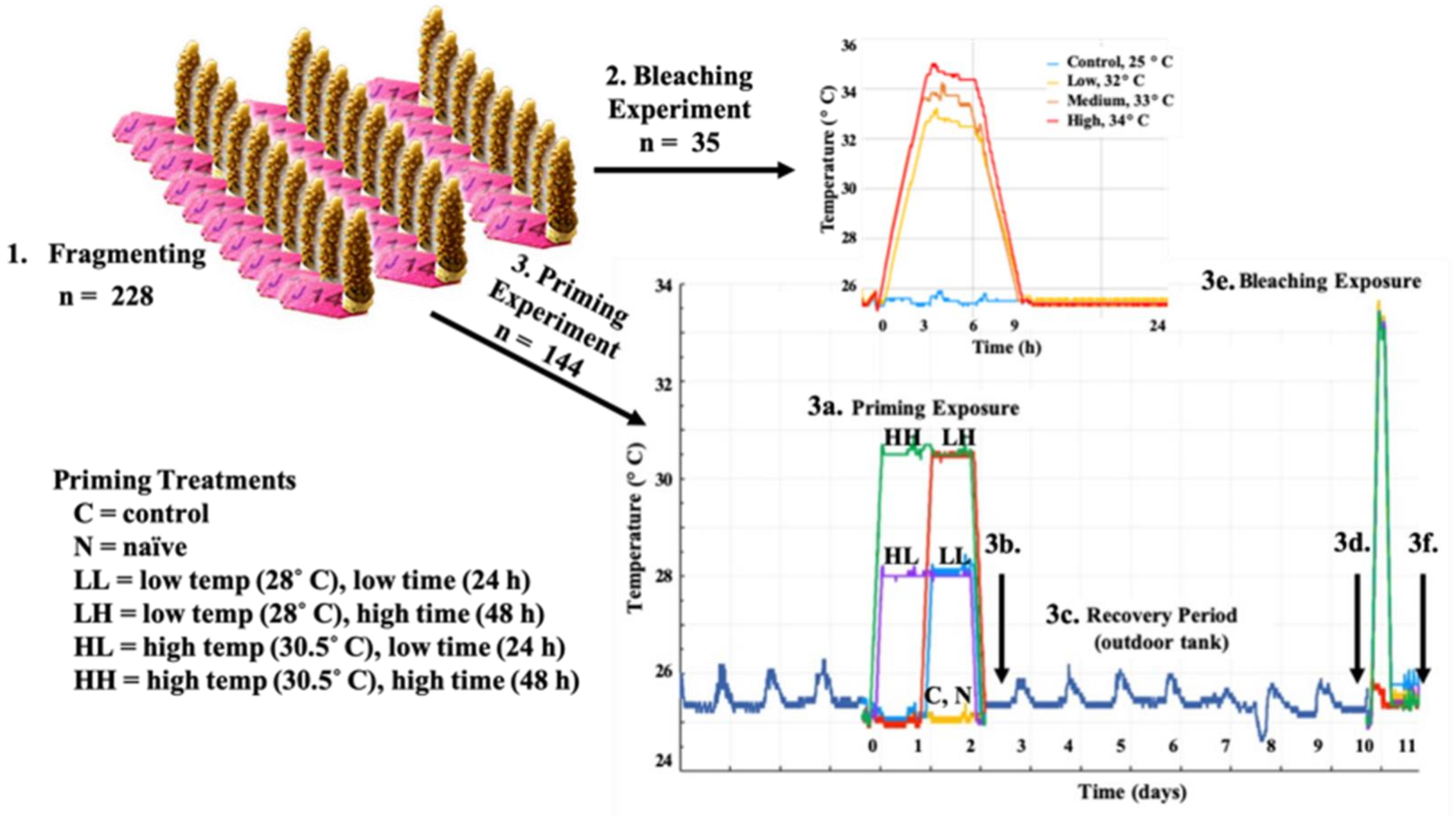

Figure 34. A cartoon of the series of experiments used in the study shows (1) Nubbins were fragmented in the field, then collected after 35 days of healing and used in a (2) Bleaching Experiment involving a standardized bleaching exposure with different thermal stress doses; Remaining nubbins were collected 63 days after fragmenting and used in the (3) Priming Experiment. Nubbins were subjected to one of six priming exposures over 2 days (3a, see legend). Control (C) and naïve (N) nubbins remained at 25° C during the priming period. Primed nubbins were exposed to low (28° C) or high (30.5° C) temperatures for low (24 h) or high (48 h) durations, resulting in four priming treatments. A subset of nubbins was sacrificed immediately after priming (3b), and remaining nubbins were transferred to an outdoor tank for an eight-day recovery period (3c). Another subset was sacrificed (3d). Remaining nubbins were subjected to the standardized bleaching exposure (3e), then sacrificed (3f).

Chlorophyll (Chl) *a* and c_2 concentrations were calculated using the spectrophotometric equations for Cnidarian dinoflagellates (Jeffrey and Haxo 1968). Chl *a* and c_2 values were normalized to acetone volume (mL) and surface area (cm^2), then summed to give total Chl ($\mu g\ cm^{-2}$). Total Chl was also normalized to cell number (pg Chl $cell^{-1}$).

Analyses

Thermal stress (i.e., degrees heating days, DHD) > 1° C above 26.8° C, the local mean monthly maximum temperature for April and May 2017, was calculated for each individual coral (NOAA Coral Reef Watch 2017b). Response variables greater than three standard deviations from the mean were identified as outliers and removed from remaining analyses. A correlation analysis was performed on all response variables and DHD to identify the strength of the linear relationships between all response variables and thermal stress. Response variables from each treatment in the bleaching exposure and priming experiments were tested for normality (normal quantile plots) and equal variances (Levene's test). One-way ANOVAs or Kruskal Wallis tests were conducted to identify significant differences ($\alpha = 0.05$) among treatments within each timepoint. The Dunnett's multiple comparisons test compares each treatment to the control (Dunnett 1955). Thus, to identify possible costs associated with priming and see whether they persisted after the recovery period, Dunnett's tests were conducted on significantly different response variables after priming (timepoint 1, Figure 34, 3b) and recovery (timepoint 2, Figure 34, 3d), respectively. The Dunn's multiple comparisons test compares all treatments following a non-parametric Kruskal Wallis test using rank sums (Dunn 1964). To determine whether priming conferred any benefit in the standardized bleaching exposure, Dunn's multiple comparisons tests were performed on significantly different response variables after the

bleaching exposure (timepoint 3, Figure 34, 3f). *P*-values were adjusted for familywise errors using Benjamini-Hochberg corrections. Median differences between treatments were calculated for response variables that were significantly different at all three timepoints. Median treatment differences in symbiont density (expressed as % loss) were calculated at each timepoint, to estimate the cost of priming immediately after the priming exposure (timepoint 1), after the eight-day recovery period (timepoint 2) and after the bleaching exposure (timepoint 3). Net losses in the bleaching exposure were calculated as the sum of the loss (difference relative to the control) and gain (difference relative to the naïve treatment). Degrees heating days (DHD) of the bleaching exposures from the standardized bleaching experiment and priming experiment were calculated. An unpaired t-test was conducted to compare thermal stress doses in the standardized bleaching exposures without and with priming.

RESULTS

All heat treatments in the preliminary standardized bleaching exposure resulted in significant reductions in symbiont density; thus, 32.5° C was used for the bleaching exposure in the priming experiment (Figure 35, Table 13). The same three samples of chlorophyll cell^{-1} and protein cell^{-1} in the priming experiment were identified as outliers, owing to low numbers of cells relative to total chlorophyll and algal protein, respectively, and thus removed from remaining analyses.

There were significant negative correlations between DHD and symbiont density, Chl, total protein and a positive correlation with F_V/F_M, indicating all response variables decreased with increasing thermal stress (Table 14). All performance metrics were significantly correlated with DHD except protein cell^{-1} (Table 14a, b). In addition, all response variables were

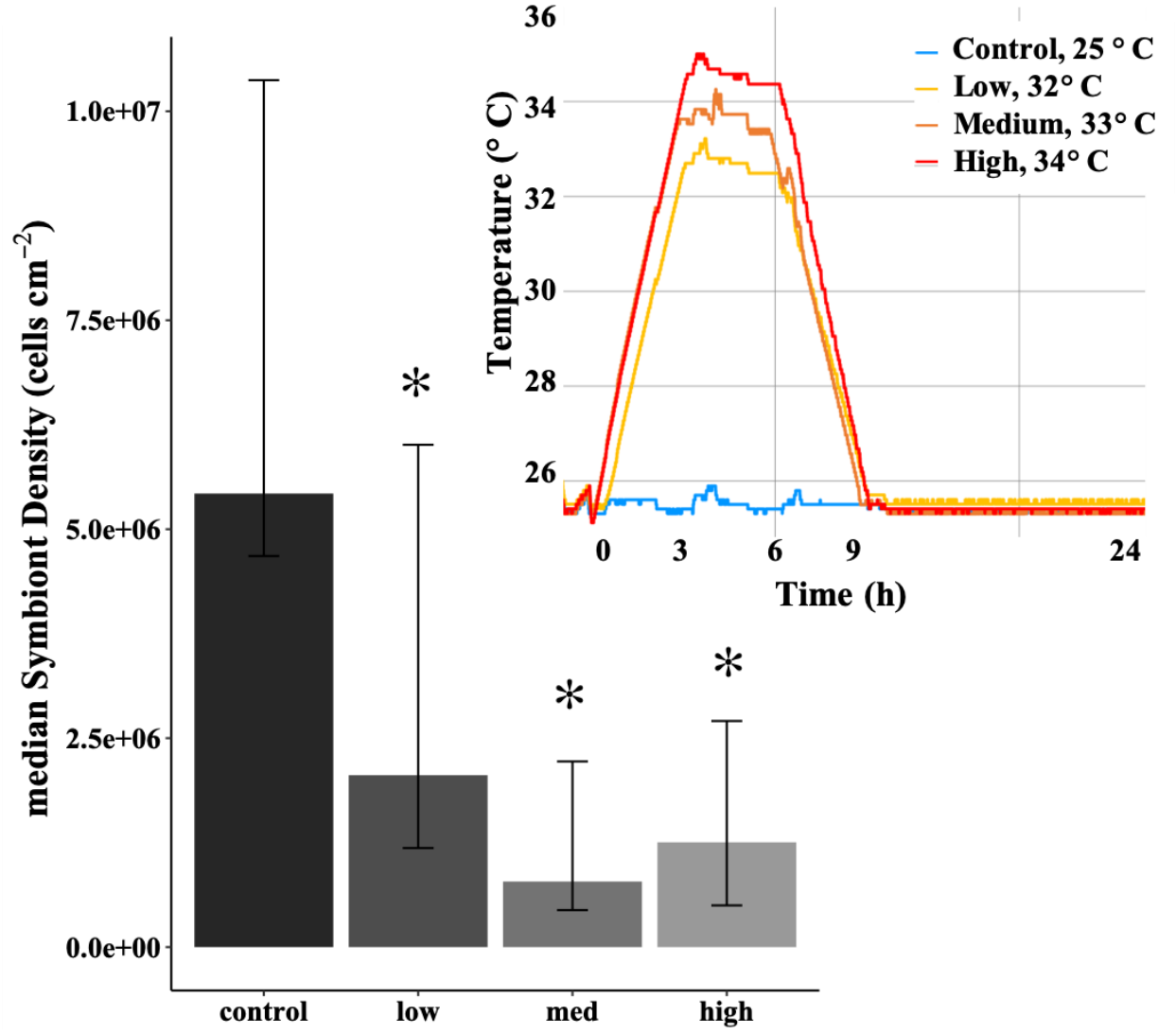

Figure 35. Median symbiont density in four treatments (control, low, medium and high thermal stress) in the standardized bleaching exposure experiment without priming. Error bars represent the range. Asterisks represent a significant difference from the control.

Table 13. (a) Kruskal Wallis test results from the standardized bleaching exposure experiment showed there was a significant effect of treatment on median symbiont density. The chi-squared statistic (χ^2), degrees of freedom (*df*) and *p*-value (*p*) are given. (b) A Dunnett's test of multiple comparisons between median symbiont densities in each heated treatment with the control. Estimated differences, lower and upper confidence intervals (CI) and *p*-values (*p*) are given.

a.

Source	χ^2	*df*	*p*
Treatment	23.801	3	**2.74E-05**

b.

Comparison	Difference	Lower CI	Upper CI	*p*
low - control	-3858066	-5534369	-2181762	**8.4E-06**
medium - control	-5314102	-6990405	-3637799	**9.9E-09**
high - control	-4907332	-6635225	-3179438	**3.7E-07**

Table 14. (a) The correlation coefficients (*r*) ± SD of each response variable with all other response variables and cumulative thermal stress, DHD. Correlations greater than 0.15 were significant at $p < 0.05$ and are bolded. (b) The *p*-value matrix corresponding to tests of the strength of correlation between variables. Significant correlations ($p < 0.05$) are bolded.

a.

Variable	Cells	Chl	Protein	ΔFv/Fm	Chl cell^{-1}	Protein cell^{-1}
Chl	**0.75 ± 0.07**					
Protein	**0.31 ± 0.14**	**0.47 ± 0.13**				
ΔFv/Fm	**-0.28 ± 0.13**	-0.03 ± 0.15	**0.31 ± 0.14**			
Chl cell^{-1}	**-0.16 ± 0.14**	**0.15 ± 0.15**	**-0.47 ± 1.05**	**-0.20 ± 0.14**		
Protein cell^{-1}	**-0.56 ± 0.10**	**-0.28 ± 0.13**	**0.45 ± 0.13**	**0.52 ± 0.12**	**-0.29 ± 0.13**	
DHD	**-0.24 ± 0.14**	**-0.18 ± 0.14**	**-0.31 ± 0.13**	**0.20 ± 0.15**	**0.35 ± 0.14**	-0.10 ± 0.15

b.

p-value	Cells	Chl	Protein	ΔFv/Fm	Chl cell^{-1}	Protein cell^{-1}
Chl	**<0.001**					
Protein	**<0.001**	**<0.001**				
ΔFv/Fm	**<0.001**	0.72	**<0.001**			
Chl cell^{-1}	**0.03**	**0.05**	**<0.001**	**0.01**		
Protein cell^{-1}	**<0.001**	**<0.001**	**<0.001**	**<0.001**	**<0.001**	
DHD	**<0.001**	**0.02**	**<0.001**	**0.01**	**<0.001**	0.19

significantly correlated with symbiont density, though not strongly ($0.15 > r > 0.75$). Specifically, total Chl ($r = 0.75$, Table 17) and protein ($r = 0.31$) were both positively correlated with symbiont density, while Chl cell^{-1}, protein cell^{-1}, and F_V/F_M were negatively correlated. All response variables were strongly correlated with symbiont density, and symbiont density showed the strongest correlation with DHD, indicating changes in symbiont density were the primary driver of the other response variables.

Response variables did not meet assumptions required for parametric analyses, thus, non-parametric Kruskal Wallis tests were used to identify significant differences among treatments at each timepoint. After priming (timepoint 1), significant differences in all response variables were identified except F_V/F_M (Table 15a, Figure 36). However, only symbiont density in the HH treatment and total Chl in the HL and HH treatments were significantly lower than the control (Table 15b, c; Figure 36). Algal protein in the naïve and LL treatments were significantly lower than the control (Table 15c, Figure 36). Priming appeared to reduce symbiont densities in proportion to the dose of thermal stress (Figure 36), indicating cell loss was dose dependent, as in Chapter 3. Though treatment differences after priming were not significant except for in the HH treatment, Chl cell^{-1} did not differ across treatments after priming.

After the eight-day recovery period, the symbiont density remained significantly lower in the HH treatment compared to the control (Table 16, b, Figure 37). Three nubbins in the HH treatment appeared visibly bleached by the end of the recovery period, causing high variance in HH treatment symbiont density, total Chl and F_V/F_M, despite the lack of a significant difference in median values of total Chl and F_V/F_M between the HH treatment and the control. This was not evident in algal protein, Chl cell^{-1} or prot cell^{-1}. No other response variables were significantly

Table 15. (a) Results from the Kruskal Wallis test of each response variables between treatments after the priming exposure (timepoint 1), with the chi-squared statistics (χ^2), degrees of freedom (*df*) and *p*-values (*p*). (b-f) Dunnett's multiple comparisons of each response variable testing for significant differences from the control treatment. The differences, lower and upper confidence intervals (CI) and *p*-values (*p*) are provided. Significant differences are bolded.

a.

Response Variable	χ^2	*df*	*p*
symbiont density	20.195	5	**0.001**
Chl	15.650	5	**0.008**
Protein	13.850	5	**0.017**
F_V/F_M	9.866	5	0.079
Chl cell^{-1}	13.195	5	**0.022**
protein cell^{-1}	18.052	5	**0.003**

b.

Symbiont density	Difference	Lower CI	Upper CI	*p*
Naïve - Control	-98202	-725019	528616	0.993
LL - Control	-119727	-746545	507090	0.983
LH - Control	-480900	-1107717	145918	0.183
HL - Control	-536109	-1162927	90709	0.116
HH - Control	-1364790	-1991608	-737973	**3.80E-06**

c.

Chl	Difference	Lower CI	Upper CI	*p*
Naïve - Control	0.05	-0.38	0.49	0.998
LL - Control	0.02	-0.41	0.46	1.000
LH - Control	-0.07	-0.51	0.36	0.990
HL - Control	-0.49	-0.93	-0.06	**0.021**
HH - Control	-0.56	-1.00	-0.13	**0.007**

d.

Protein	Difference	Lower CI	Upper CI	*p*
Naïve - Control	-0.14	-0.25	-0.02	**0.015**
LL - Control	-0.15	-0.26	-0.03	**0.008**
LH - Control	-0.11	-0.23	0.00	0.053
HL - Control	-0.07	-0.19	0.04	0.371
HH - Control	-0.06	-0.18	0.05	0.451

Table 15. continued

e.

Chl cell^{-1}	Difference	Lower CI	Upper CI	*p*
Naïve - Control	0.33	-0.72	1.38	0.879
LL - Control	0.30	-0.75	1.35	0.915
LH - Control	0.65	-0.40	1.71	0.359
HL - Control	-0.62	-1.68	0.43	0.404
HH - Control	0.87	-0.19	1.92	0.139

f.

Protein cell^{-1}	Difference	Lower CI	Upper CI	*p*
Naïve - Control	-0.04	-0.10	0.02	0.214
LL - Control	-0.04	-0.10	0.01	0.179
LH - Control	-0.02	-0.08	0.03	0.728
HL - Control	-0.01	-0.07	0.05	0.997
HH - Control	0.05	-0.01	0.11	0.105

Table 16. (a) Results from the Kruskal Wallis test of each response variables between treatments after the eight-day recovery period (timepoint 2) with the chi-squared statistics (χ^2), degrees of freedom (*df*) and *p*-values (*p*). (b) Dunnett's multiple comparisons of symbiont density testing for significant differences from the control treatment. Estimated differences, lower and upper confidence intervals (CI) and *p*-values (*p*) are provided. Significant differences are bolded.

a.

Response Variable	χ^2	*df*	*p*
symbiont density	12.048	5	**0.034**
Chl	7.522	5	0.185
protein	6.260	5	0.282
F_V/F_M	9.841	5	0.080
Chl cell^{-1}	10.725	5	0.057
Protein cell^{-1}	1.023	5	0.961

b.

Symbiont density	Difference	Lower CI	Upper CI	*p*
Naïve - Control	-239628	-1429218	949963	0.978
LL - Control	-437987	-1627578	751604	0.798
LH - Control	-2742	-1192333	1186848	1.000
HL - Control	-758888	-1948478	430703	0.334
HH - Control	-1869301	-3058891	-679710	**0.001**

Table 17. (a) Results from the Kruskal Wallis test of each response variables between treatments after the bleaching exposure (timepoint 3) in the priming experiment. The chi-squared statistics (χ^2), degrees of freedom (*df*) and *p*-values (*p*) are given. (b) Dunn's multiple comparisons of symbiont density with bleaching. *Z* statistics (*Z*) and adjusted *p*-values (adj. *p*) are given. Only comparisons to the control and naïve treatments are reported. Significant differences are bolded.

a.

Response Variable	χ^2	*df*	*p*
symbiont density	13.697	5	**0.018**
Chl	10.810	5	0.055
protein	7.240	5	0.203
F_V/F_M	9.269	5	0.099
Chl cell^{-1}	6.876	5	0.230
Protein cell^{-1}	10.893	5	0.054

b.

Symbiont density	Z	adj. *p*
Control - Naïve	2.911	**0.027**
Control - LL	2.393	0.063
Control - LH	2.536	0.056
Control - HL	1.822	0.206
Control - HH	3.304	**0.014**
Naïve - LL	-0.518	0.756
Naïve - LH	-0.375	0.758
Naïve - HL	-1.089	0.591
Naïve - HH	0.393	0.801

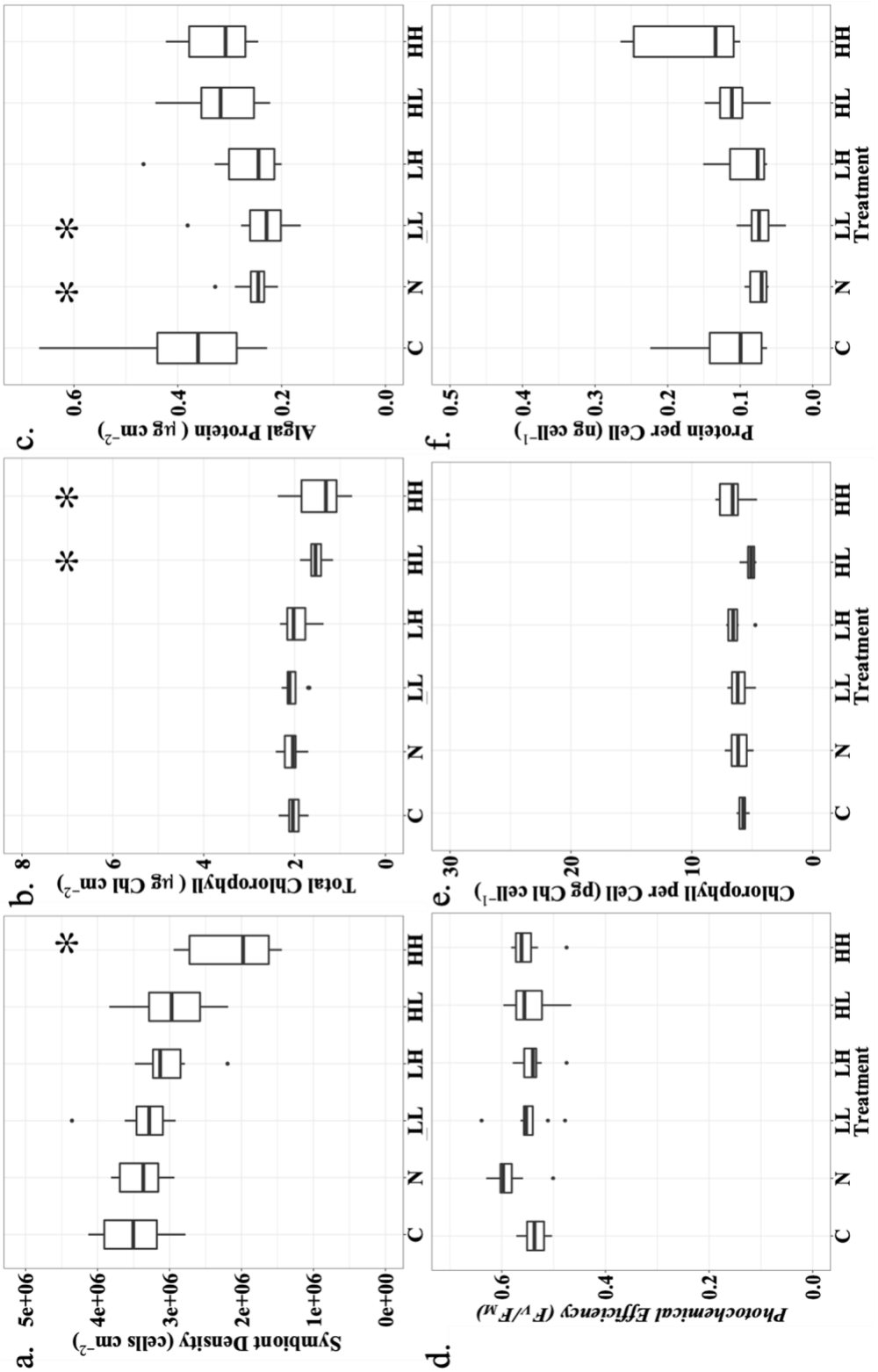

Figure 36. Symbiont density (a), total Chl (b), algal protein (c), photochemical efficiency (d), Chl cell^{-1} (e) and protein cell^{-1} (f) in six treatments subjected to a 48 h priming exposure in the priming experiment (see Figure 26, 3b). Control (C) and naïve (N) nubbins remained at 25° C. Primed nubbins were exposed to low (28° C) or high (30.5° C) temperatures for low (24 h) or high (48 h) durations, resulting in four priming treatments. Thick bars are median treatment values, boxes are the interquartile range, whiskers are the range and points are outliers. Asterisks represent treatments that were significantly different from the control

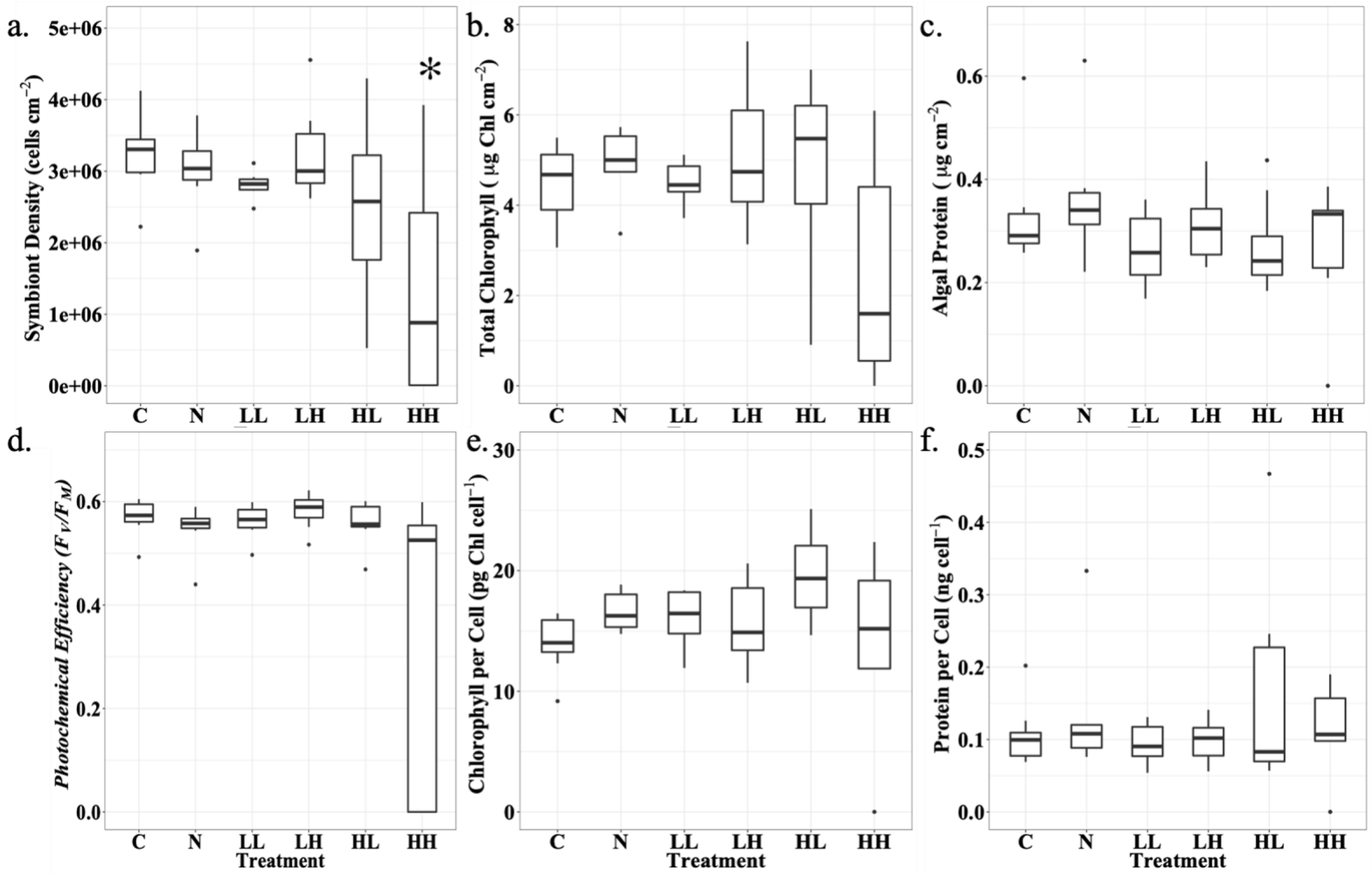

Figure 37. Symbiont density (a), total Chl (b), algal protein (c), photochemical efficiency (d), Chl cell^{-1} (e) and protein cell^{-1} (f) in six treatments 8 days after priming exposure in the priming experiment (see Figure 26, 3d). Control (C) and naïve (N) nubbins remained at 25° C. Primed nubbins were exposed to low (28° C) or high (30.5° C) temperatures for low (24 h) or high (48 h) durations, resulting in four priming treatments. Thick bars median treatment values, boxes are the interquartile range, whiskers are the range and points are outliers. Asterisks represent treatments that were significantly different from the control.

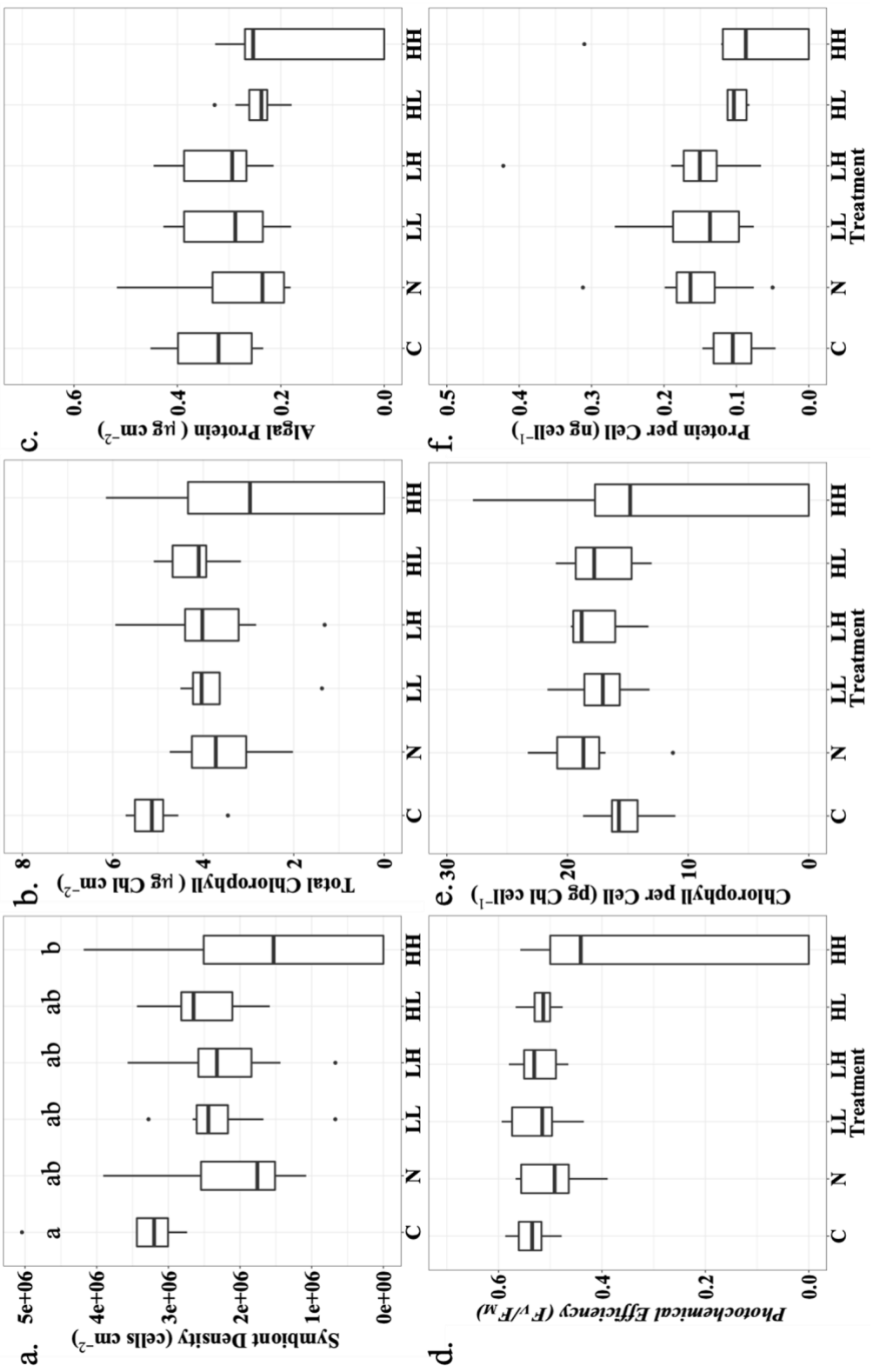

Figure 38. Symbiont density (a), total Chl (b), algal protein (c), photochemical efficiency (d), Chl cell^{-1} (e) and protein cell^{-1} (f) in six treatments after the bleaching exposure in the priming experiment (see Figure 26, 3d). Control (C) and naïve (N) nubbins remained at 25° C. Primed nubbins were exposed to low (28° C) or high (30.5° C) temperatures for low (24 h) or high (48 h) durations, resulting in four priming treatments. Thick bars are median treatment values, boxes are the interquartile range, whiskers are the range and points are outliers. Letters represent significant differences between treatments

different across treatments after recovery, suggesting nubbins in all but the HH treatment had recovered and no priming associated costs persisted after eight days.

Because the goal was to determine whether priming conferred any benefit to corals in a bleaching exposure, *post hoc* analyses were focused on the effect of treatment in the bleaching exposure (i.e., timepoint 3, Table 17, Figure 38). The standardized bleaching exposure (timepoint 3) significantly reduced symbiont density in the naïve and HH treatments relative to the control treatment (Table 17, b, Figure 38). However, no other response variables showed significant differences across treatments, including differences between either the control or naïve treatments compared to the LL, LH and HL primed treatments. Four HH treatment nubbins were completely bleached by the end of the priming experiment, leading to reductions in every response variable, though not significant.

Symbiont density was the only response variable with significant differences at all three timepoints (Figures 28-30), thus median treatment differences (% loss) are reported (Table 18). The bleaching exposure caused a 45 % reduction in symbiont density in the naïve treatment (i.e., the positive bleaching control). Symbiont density was reduced by 44 % in the HH treatment nubbins after priming and after 8 days, symbiont density remained significantly low, confirming the dose of thermal stress in the HH treatment was too hot. However, the other priming treatments did not show a significant reduction in cells with priming or recovery (Table 15, 16, 18, Figures 36, 37).

Table 18. Change (%) in median symbiont density from each treatment relative to the control were calculated to represent the immediate (After Priming) and sustained (After Recovery) costs of the priming exposure and the bleaching exposure (After Bleaching). Priming benefits were calculated as the difference in median symbiont density of each treatment relative to the naïve treatment (Benefit, %).

	After Priming	After Recovery	After Bleaching	
Treatment	Change (%)	Change (%)	Change (%)	Benefit (%)
N	-4	-8	-45	--
LL	-6	-15	-24	39
LH	-11	-9	-27	32
HL	-15	-22	-17	51
HH	-44	-73	-52	-13

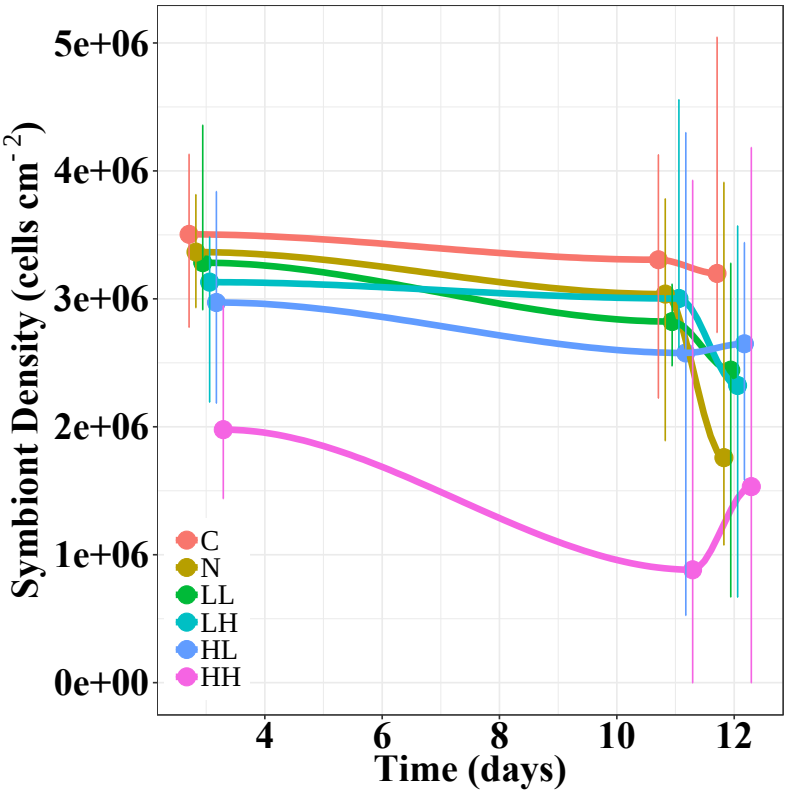

Figure 39. Symbiont density over the course of the priming experiment. Points are median symbiont densities in each treatment, error bars are the treatment range; the position of treatments have been spread out to reveal overlapping error bars.

Table 19. Unpaired t-test results comparing the mean thermal stress doses (DHD) in the standard bleaching exposures without and with previous priming.

Source	*d.f.*	Mean Diff.	Std. Error Diff.	*T*	*p*
DHD	6	-0.32 ± 0.28	0.12	2.80	**0.03**

DHD values in the standardized bleaching exposures without and with priming were compared. The primed corals were exposed to a bleaching exposure that was 0.32 DHD greater than corals from the preliminary standardized bleaching exposure (Table 19). Despite receiving greater bleaching stress, the primed corals bleached less (excluding the HH treatment, Figures 39, 40). Taken with the observed, but insignificant benefit (Figure 39), this suggests primed corals may have acquired some bleaching resistance (Figures 39, 40).

DISCUSSION

Following a model of stress memory (Hilker et al. 2015) this study invoked a series of priming exposures to explore possible benefits to corals in a subsequent bleaching exposure. Primed corals did not bleach significantly less than the naïve, unprimed corals in the priming experiment, nor were they significantly different from the control corals, likely due to the variance introduced by including multiple coral genets that represented a range of coral resiliency (Goergen and Gilliam 2018).

There was an exposure-driven pattern in the LL, LH and HL treatments, wherein the

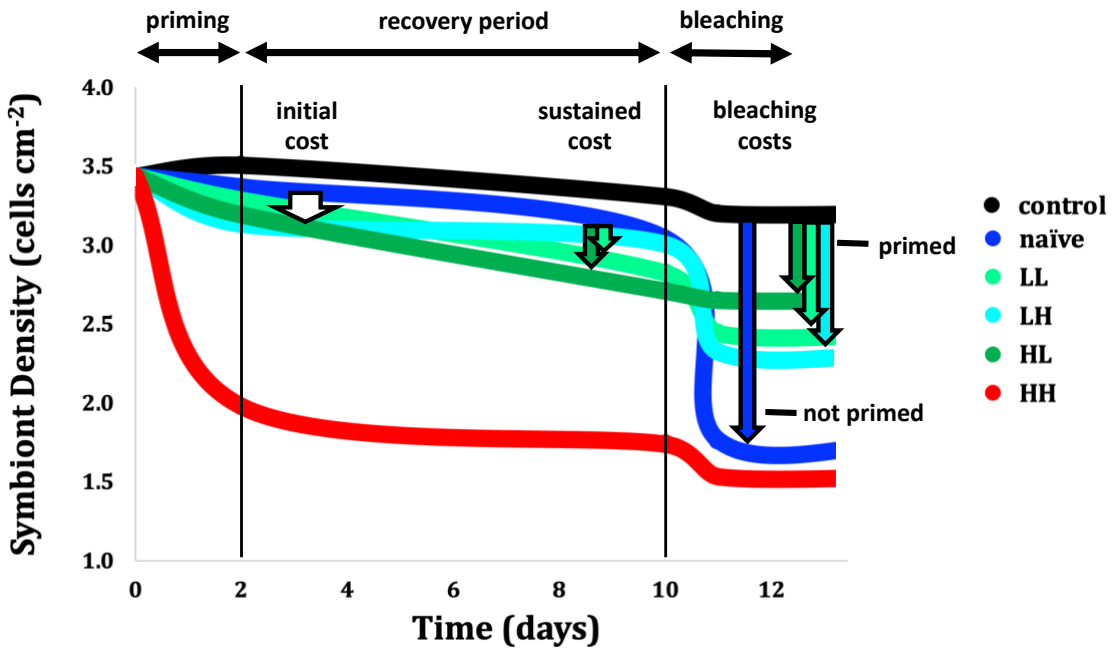

Figure 40. A cartoon of the difference in symbiont density over time, showing the initial costs for priming (white arrow), the sustained costs that were evident in some treatments, but not all (green arrows, sustained), and the reduction in symbiont densities with bleaching (bleaching costs).

greater the priming dose, the smaller the reduction in median symbiont density immediately after priming, though this trend did not follow after the eight-day recovery period, or in the bleaching exposure. Lower priming doses LL and LH lost more cells during bleaching, but fewer cells during priming, in relation to the controls. The greatest priming treatment, HH, lost a significant number of cells on par with the bleaching exposure of naïve corals, thus that treatment received too great a dose of thermal stress to enable recovery. Previous studies that have demonstrated evidence of reduced bleaching have either not detected it with pulsed thermal exposure (wherein corals were stressed and then allowed to recover for some time period; Middlebrook et al. 2008, Bellantuono et al. 2012), or were enacted over greater timescales (Hawkins and Warner, 2017).

Perhaps the priming exposures were too rapid, or the recovery period too long to detect any significant benefits in symbiont density.

Excluding the HH treatment, which was too hot, the primed corals in this study lost between 17 and 27 % cells, ~50% fewer cells on average after the recovery period than the corals from the standardized bleaching experiment without priming (62 to 86 % loss in symbiont density) , despite significantly greater thermal stress doses in the priming experiment. This supports multiple previous findings that repeated thermal stress influences bleaching outcomes and may reduce bleaching severity (Castillo and Helmuth 2005, Middlebrook et al. 2008, Thompson and van Woesik 2009, Donner 2011, Kenkel et al. 2012). Primed corals bleached less than unprimed corals in the priming experiment, suggesting a notable albeit insignificant benefit from priming. It is possible the putative stress memory elicited by the priming doses in this study lasted fewer than eight days, suggesting stress memory may act on daily (< 1 week) timescales (National Academy of Science, 2018, but see Brown et al. 2002a, 2014). It is important to note even primed corals bleached. While priming did not significantly reduce bleaching in the priming experiment, there were greater retention levels of symbionts despite a significantly greater dose of thermal stress in the standardized bleaching exposure.

The correlation of response variables with DHD and reduction of symbiont density with priming further support that, as in Chapters 2 and 3, coral bleaching is strongly dose dependent. Few studies put bleaching results in the context of dose, despite the obvious dose dependence of coral bleaching. In addition, the priming doses (2 to 9 DHD) used in this study were more gradual but greater than those experienced by backreef corals within a tidal cycle on a single day (0.36 to 1.8 DHD, Chapter 2). Hence, there is very likely some dependence on the rate of

heating as well that has gone largely untested. The dose and rate dependent nature of coral bleaching warrant further exploration to better understand what modulates natural bleaching.

The priming period reduced symbiont densities in proportion to the dose of thermal stress, thus, perhaps repeated thermal stress, and not priming *sensu stricto*, was responsible for reduced bleaching in the subsequent bleaching exposure. All treatments except the HH treatment appeared to recover fully after priming. However, bleaching recovery was not examined in this study; therefore, it is possible the reduction of symbiont densities from thermal stress doses during the priming period may have compromised metabolic balance and depleted lipid stores that would enable recovery after bleaching exposure (Grottoli et al. 2006, 2014). The priming mechanism alone may not confer bleaching resistance or any immediate acclimatory benefit in the exposed *A. cervicornis* individuals, and therefore may not be an appropriate technique to harden corals of the current generation. However, evidence has shown hardening in some coral species leave heritable epigenetic marks that confer benefits to subsequent generations (Putnam and Gates 2015, Liew et al. 2018) through post-translational modifications such as histone modifications and the methylation, phosphorylation, and ubiquitination of DNA, thus there may be some benefit in the long term (Eirin-Lopez and Putnam 2019). At present, large scale selective breeding efforts are underway that aim to capitalize on sexual crosses of resilient and/or resistant parents (e.g., SECORE International, van Oppen et al. 2015). Whether thermal hardening of parent colonies may benefit the success of such programs remains to be tested.

A broad range of resiliencies were selected *a priori* with the intent to capture the natural variability of bleaching resistance within the nursery population. This variation made it difficult to distinguish symbiont density losses that were significantly different from both the naïve and control treatments. In addition, perhaps bleaching is not the best phenotype to quantify stress

memory in corals. Bleaching is a coarse metric prone to error of estimation (due to sample processing) and representative of dysbiosis. Perhaps a metric that is indicative of symbiosis, such as the ratio of gross photosynthesis to holobiont respiration, would be more appropriate.

CONCLUSIONS

Corals are thermal specialists that live within a narrow margin of their thermal maxima, making them particularly sensitive to temperature. Yet, subtle differences in thermal performance and tolerance exist between members of the same species in different locations, populations, and individuals. The importance of corals to reef structure and function makes understanding what drives thermal acclimation and survival necessary in order to establish conservation protocols.

For the first objective, I sought to capture acclimatization signatures by comparing multiple bleaching resistance parameters in two massive coral species before and after a seven-month incubation period in three microhabitats with distinct levels of thermal variability. This study found no changes in symbiont community composition, thus removing any influence from the algal partner to bleaching resistance in this case. Colonies were sourced from a single, moderately variable site to control for the influential effect of origin and genotype previously found in one of the two study species (Barshis et al. 2018). Contrary to previous findings, wherein *Porites lobata* grew significantly faster in the most variable site compared to the lowest variability site, reduced growth rates and apparent poor health (Chapter 2, Figure 12, page 50) were found without evidence of acclimatization in the most thermally stressful site for both species examined (Chapter 2, Figures 11, 12, pp. 49-50). These results do not support the 'beneficial acclimation hypothesis' (Leroi et al. 1994). Rather, my results indicated thermal variability was deleterious to these species. It is possible the timescales required to see a notable increase in bleaching resistance for these species are longer than the incubation period; host cell turnover rates in faster growing branching species occur on daily to weekly timescales

(Gladfelter 1983), and *in hospite* algal cells are controlled by the host and arrested in S phase (Davy et al. 2012), thus occur on monthly scales, so growth rates presented in the study were shorter than cell doubling times. It is also possible thermal stress levels at all sites were too low to invoke acclimatization for corals at any site and the myriad other physical parameters between sites, such as flow, contributed to growth differences in *P. lobata*.

Bleaching resistance experiments, especially those involving heat shock (Palumbi et al. 2014), may not be the most appropriate means to assess thermal performance or tolerance. Bleaching resistance compares individuals or groups of individuals at a single point in time. The bleaching exposures used in bleaching resistant experiments were greater than the sum of cumulative thermal stress of any site in the previous 12 weeks, and greater than what was likely necessary to evoke bleaching. An ecologically relevant exposure (e.g., Barshis et al. 2018) along with finer-scale physiological measurements, such as those employed in Chapter 3, rather than solely crude bleaching metrics, provide the necessary detail to assess the physiology. For corals, thermal performance (i.e., measures of holobiont respiration and photosynthesis) are a better approach, because the metabolic budget is tied to all major partners in respiration and the algae in photosynthesis, so temperatures or thermal stress doses that elicit deficits in holobiont metabolism can be determined.

For my second objective, the role of exposure in mitigating thermal stress was investigated in the absence of acclimation. Thermal performance most certainly benefitted from gradual warming, as evidenced by the reduced sensitivity to temperature stress, especially at high doses, particularly for holobiont respiration (Chapter 3, Figures 27-30, pp. 89-93). However, gross photosynthesis was unable to keep pace at higher doses of thermal stress, indicating perhaps that the holobiont metabolic budget was hampered by carbon dioxide limitation of

photosynthesis at high doses of thermal stress (Chapter 3, Figure 31, pg. 94). There is a heavy reliance of most hermatypic scleractinians (Muscatine et al. 1981) on their algal partners to meet their metabolic demands. This implies that, despite the apparent benefit gradual warming can provide to animals, the holobiont is limited by the very symbiosis that enables its existence in oligotrophic environments (Stanley and van de Schootbrugge 2009). Thus, I contend that even rapid acclimation to warmer temperatures is unlikely to outpace the effects of rates of warming predicted in the coming decades on obligate holobiont symbioses (Torda et al. 2017).

The third objective was to determine whether corals could acquire bleaching resistance using a stress memory model (Hilker et al. 2015). There were no significant differences in bleaching resistance conferred by priming, thus stress memory of 8 days was not sufficient to reduce bleaching *sensu stricto* (Chapter 4, Figure 38, pg. 123). However, there was a measurable benefit to repeated thermal stress (Chapter 4, Figure 39, Table 18, pg. 125), wherein primed corals bleached less in a standardized bleaching experiment, giving the appearance of acquired thermal tolerance with repeated thermal stress (Middlebrook et al. 2008, Thompson and van Woesik 2009, Bellantuono et al. 2012b). First, it is important to acknowledge this reduced bleaching came at an upfront cost with priming (Hilker et al. 2015). Second, it is possible a significant benefit would have been seen with a shorter recovery time, however, this suggests the stress memory response is ephemeral. Regardless, the thermal stress doses applied in this study did not make corals significantly bleaching resistant. There is still utility in investigating the heritability of stress memory on corals, through epigenetic marks that confer thermal tolerance to offspring of subsequent generations (Putnam and Gates 2015, van Oppen et al. 2015, Eirin-Lopez and Putnam 2019).

Gradual warming and temperature variation are known to mitigate the effects of thermal stress in many organisms (Angilletta 2009). Indeed, the literature has a great deal of evidence for the benefits of thermal variability on corals by a variety of complex mechanisms (Brown et al. 2002b, Bellantuono et al. 2012a, b, Safaie et al. 2018, DeCarlo et al. 2019, Hughes et al. 2019, Middlebrook et al. 2008, Barshis et al. 2013, Bay and Palumbi 2015, Hawkins and Warner 2017, Oakley et al. 2017) and the current theory offers promise for coral survival in the coming decades.

However, the findings of this dissertation and other studies tell a different story. There may be deleterious tradeoffs for thermal tolerance (Baird and Marshall 2002, Grottoli et al. 2014, Camp et al. 2016, Gibbin et al. 2018). In some cases, variability appears to reduce thermal tolerance (Putnam and Edmunds 2011, Camp et al. 2016). Chapter 2 of this study found no benefit in a more variable habitat, but an apparent reduction in growth and health. Thermal variability, in this case, was deleterious. While gradual warming enabled physiological adjustment to a point (Chapter 3), adjustments were limited by the reliance on symbiosis that has allowed corals to persist for millions of years. Pre-exposure may reduce bleaching severity (Chapter 4), but it appears to be strongly dependent on dose and timing, and the benefits are short-lived. It seems unlikely most corals will encounter the required scenarios to acquire thermal tolerance in the wild through stress memory. In conclusion, thermal acclimation alone is insufficient to save corals in the Anthropocene.

REFERENCES

Abrego D, Ulstrup KE, Willis BL, van Oppen MJH (2008) Species-specific interactions between algal endosymbionts and coral hosts define their bleaching response to heat and light stress. P Roy Soc B-Biol Sci 275:2273–2282

Agrawal AA, Laforsch C, Tollrian R (1999) Transgenerational induction of defences in animals and plants. Nature 401:60–63

Agostini S, Fujimura H, Fujita K, Suzuki Y, Nakano Y (2013) Respiratory electron transport system activity in symbiotic corals and its link to calcification. Aquat Biol 18:125–139

Aichelman HE, Zimmerman RC, Barshis DJ (2019) Adaptive signatures in thermal performance of the temperate coral *Astrangia poculata* (Ellis & Solander, 1786). J Exp Biol 222:jeb189225

Ainsworth TD, Heron SF, Ortiz JC, Mumby PJ, Grech A, Ogawa D, Eakin CM, Leggat W (2016) Climate change disables coral bleaching protection on the Great Barrier Reef. Science 352:338–342

Ainsworth TD, Hoegh-Guldberg O, Heron SF, Skirving WJ, Leggat W (2008) Early cellular changes are indicators of pre-bleaching thermal stress in the coral host. J Exp Mar Biol Ecol 364:63–71

Angilletta MJ (2009) Thermal Adaptation: A Theoretical and Empirical Synthesis. Oxford University Press, Oxford

Anthony KRN, Connolly SR, Hoegh-Guldberg O (2007) Bleaching, energetics, and coral mortality risk: Effects of temperature, light, and sediment regime. Limnology and Oceanography 52:716–726

Arif C, Daniels C, Bayer T, Banguera-Hinestroza E, Barbrook A, Howe CJ, LaJeunesse TC, Voolstra CR (2014) Assessing *Symbiodinium* diversity in scleractinian corals via next-generation sequencing-based genotyping of the ITS2 rDNA region. Molecular Ecology 23:4418–4433

Arts RJW, Joosten LAB, Netea MG (2016) Immunometabolic circuits in trained immunity. Semin Immunol 28:425–430

Baird A, Marshall P (2002) Mortality, growth and reproduction in scleractinian corals following bleaching on the Great Barrier Reef. Marine Ecology Progress Series 237:133–141

Baker AC (2001) Ecosystems: Reef corals bleach to survive change. Nature 411:765–766

Baker AC (2003) Flexibility and specificity in coral-algal symbiosis: Diversity, ecology, and biogeography of *Symbiodinium*. Annu Rev Ecol Evol S 34:661–689

Baker AC (2004) Symbiont Diversity on Coral Reefs and Its Relationship to Bleaching Resistance and Resilience. In: Rosenberg E., Loya Y. (eds) Coral Health and Disease. Springer Berlin Heidelberg, Berlin, Heidelberg, pp. 177–194

Baker AC, Glynn PW, Riegl B (2008) Climate change and coral reef bleaching: An ecological assessment of long-term impacts, recovery trends and future outlook. Estuarine, Coastal and Shelf Science 80:435–471

Baker DM, Freeman CJ, Knowlton N, Thacker RW, Kim K, Fogel ML (2015) Productivity links morphology, symbiont specificity and bleaching in the evolution of Caribbean octocoral symbioses. ISME J 9:2620–9

Barshis DJ (2014) Genomic Potential for Coral Survival of Climate Change. In: Birkeland C. (eds) Coral Reefs in the Anthropocene. Springer, pp. 133–146

Barshis DJ, Birkeland C, Toonen RJ, Gates RD, Stillman JH (2018) High-frequency temperature variability mirrors fixed differences in thermal limits of the massive coral *Porites lobata*. J Exp Biology 221:jeb188581

Barshis DJ, Ladner JT, Oliver TA, Seneca FO, Traylor-Knowles N, Palumbi SR (2013) Genomic basis for coral resilience to climate change. Proc Natl Acad Sci USA 110:1387–92

Barshis DJ, Stillman JH, Gates RD, Toonen RJ, Smith LW, Birkeland C (2010) Protein expression and genetic structure of the coral Porites lobata in an environmentally extreme Samoan back reef: does host genotype limit phenotypic plasticity? Molecular ecology 19:1705–20

Baskett ML, Gaines SD, Nisbet RM (2009) Symbiont diversity may help coral reefs survive moderate climate change. Ecol Appl 19:3–17

Baums IB, Johnson ME, Devlin-Durante MK, Miller MW (2010) Host population genetic structure and zooxanthellae diversity of two reef-building coral species along the Florida Reef Tract and wider Caribbean. Coral Reefs 29:835–842

Bay RA, Palumbi SR (2015) Rapid Acclimation Ability Mediated by Transcriptome Changes in Reef-Building Corals. Genome Biol Evol 7:1602–12

Bedwell-Ivers HE, Koch MS, Peach KE, Joles L, Dutra E, Manfrino C (2017) The role of in hospite zooxanthellae photophysiology and reef chemistry on elevated pCO2 effects in two branching Caribbean corals: *Acropora cervicornis* and *Porites divaricata*. ICES J Mar Sci 74:1103–1112

Belkin IM (2009) Rapid warming of Large Marine Ecosystems. Progress in Oceanography 81:207–213

Bellantuono AJ, Granados-Cifuentes C, Miller DJ, Hoegh-Guldberg O, Rodriguez-Lanetty M (2012a) Coral Thermal Tolerance: Tuning Gene Expression to Resist Thermal Stress. PloS ONE 7:e50685

Bellantuono AJ, Hoegh-Guldberg O, Rodriguez-Lanetty M (2012b) Resistance to thermal stress in corals without changes in symbiont composition. P Roy Soc B-Biol Sci 279:1100–1107

Berkelmans R, van Oppen MJ (2006) The role of zooxanthellae in the thermal tolerance of corals: a "nugget of hope" for coral reefs in an era of climate change. Proc Biol Sci 273:2305–2312

Berkelmans R, Willis BL (1999) Seasonal and local spatial patterns in the upper thermal limits of corals on the inshore Central Great Barrier Reef. Coral Reefs 18:219–228

Berry DB, Gasch AP (2008) Stress-activated Genomic Expression Changes Serve a Preparative Role for Impending Stress in Yeast. Molecular Biology of the Cell 19:4580–4587

Berry DB, Guan Q, Hose J, Haroon S, Gebbia M, Heisler LE, Nislow C, Giaever G, Gasch AP (2011) Multiple Means to the Same End: The Genetic Basis of Acquired Stress Resistance in Yeast. PLOS Genetics 7:e1002353

Bonesso JL, Leggat W, Ainsworth TD (2017) Exposure to elevated sea-surface temperatures below the bleaching threshold impairs coral recovery and regeneration following injury. PeerJ 5:e3719

Bosch TCG, Miller DJ (2016a) The Holobiont Imperative: Perspectives from Early Emerging Animals. Springer-Verlag, Vienna

Bouchard P, Guderley H (2003) Time course of the response of mitochondria from oxidative muscle during thermal acclimation of rainbow trout, *Oncorhynchus mykiss*. J Exp Biol 206:3455–3465

Boulotte NM, Dalton SJ, Carroll AG, Harrison PL, Putnam HM, Peplow LM, van Oppen MJ (2016) Exploring the *Symbiodinium* rare biosphere provides evidence for symbiont switching in reef-building corals. ISME J 10:2693–2701

Bradford MM (1976) A rapid and sensitive method for the quantitation of microgram quantities of protein utilizing the principle of protein-dye binding. Anal Biochem 72:248–254

Brian JI, Davy SK, Wilkinson SP (2019) Elevated Symbiodiniaceae richness at Atauro Island (Timor-Leste): a highly biodiverse reef system. Coral Reefs 38:123-136

Brown BE (1997) Coral bleaching: causes and consequences. Coral Reefs 16:S129–S138

Brown BE, Cossins AR (2011) The Potential for Temperature Acclimatisation of Reef Corals in the Face of Climate Change. Z. Dubinsky and N. Stambler (eds) In: Coral Reefs: An Ecosystem in Transition. Springer Science. Pp. 421–433

Brown BE, Downs CA, Dunne RP, Gibb SW (2002a) Exploring the basis of thermotolerance in the reef coral *Goniastrea aspera*. Marine Ecology-Progress Series 242:119–129

Brown BE, Dunne RP, Edwards AJ, Sweet MJ, Phongsuwan N (2014) Decadal environmental 'memory' in a reef coral? Mar Biol 162:479–483

Brown BE, Dunne RP, Goodson MS, Douglas AE (2002b) Experience shapes the susceptibility of a reef coral to bleaching. Coral Reefs 21:119–126

Bruce TJ, Matthes MC, Napier JA, Pickett JA (2007) Stressful "memories" of plants: evidence for possible mechanisms. Plant Sci 173:603–608

Brunelle SA, Hazard ES, Sotka EE, Van Dolah FM (2007) Characterization of a dinoflagellate cryptochrome blue-light receptor with a possible role in circadian control of the cell cycle. J Phycol 43:509–518

Burriesci MS, Raab TK, Pringle JR (2012) Evidence that glucose is the major transferred metabolite in dinoflagellate-cnidarian symbiosis. J Exp Biol 215:3467–3477

Callahan BJ, McMurdie PJ, Rosen MJ, Han AW, Johnson AJA, Holmes SP (2016) DADA2: High-resolution sample inference from Illumina amplicon data. Nature Methods 13:581–583

Camp EF, Smith DJ, Evenhuis C, Enochs I, Manzello D, Woodcock S, Suggett DJ (2016) Acclimatization to high-variance habitats does not enhance physiological tolerance of two key Caribbean corals to future temperature and pH. Proc R Soc B 283:20160442

Carilli J, Donner SD, Hartmann AC (2012) Historical Temperature Variability Affects Coral Response to Heat Stress. PloS ONE 7:e34418

Carilli JE, Norris RD, Black B, Walsh SM, McField M (2010) Century-scale records of coral growth rates indicate that local stressors reduce coral thermal tolerance threshold. Global Change Biology 16:1247–1257

Carilli JE, Norris RD, Black BA, Walsh SA, McField M (2009) Local Stressors Reduce Coral Resilience to Bleaching. PloS ONE 4:e6324

Castillo KD, Helmuth BST (2005) Influence of thermal history on the response of *Montastraea annularis* to short-term temperature exposure. Mar Biol 148:261–270

Castillo KD, Ries JB, Weiss JM, Lima FP (2012) Decline of forereef corals in response to recent warming linked to history of thermal exposure. Nature Climate Change 2:756–760

Cesar H, Burke L, Pet-Soede L (2003) The Economics of Worldwide Coral Reef Degradation. Cesar Environmental Economics Consulting (CEEC), Arnhem

Cinner J (2014) Coral reef livelihoods. Current Opinion in Environmental Sustainability 7:65–71

Coles SL, Brown BE (2003) Coral bleaching - Capacity for acclimatization and adaptation. Advances in Marine Biology, Vol 46 46:183–223

Coles SL, Jokiel PL (1977) Effects of Temperature on Photosynthesis and Respiration in Hermatypic Corals. Mar Biol 43:209–216

Coles SL, Jokiel PL, Lewis CR (1976) Thermal Tolerance in Tropical versus Subtropical Pacific Reef Corals I. Pacific Science 30:159–166

Coles SL, Riegl BM (2013) Thermal tolerances of reef corals in the Gulf: a review of the potential for increasing coral survival and adaptation to climate change through assisted translocation. Mar Pollut Bull 72:323–332

Connell JH (1978) Diversity in tropical rain forests and coral reefs - high diversity of trees and corals is maintained only in a non-equilibrium state. Science 4335:1302–1310

Connell JH, Hughes TE, Wallace CC, Tanner JE, Harms KE, Kerr AM (2004) A long-term study of competition and diversity of corals. Ecol Monogr 74:179–210

Conrath U, Beckers GJ, Flors V, Garcia-Agustin P, Jakab G, Mauch F, Newman MA, Pieterse CM, Poinssot B, Pozo MJ (2006) Priming: getting ready for battle. Mol Plant Microbe Interact 19:1062–1071

Cook CB, Delia CF (1987) Are Natural-Populations of Zooxanthellae Ever Nutrient-Limited. Symbiosis 4:199–211

Costanza R, d'Arge R, deGroot R, Farber S, Grasso M, Hannon B, Limburg K, Naeem S, O'Neill RV, Paruelo J, Raskin RG, Sutton P, van denBelt M (1997) The value of the world's ecosystem services and natural capital. Nature 387:253–260

Craig P, Birkeland C, Belliveau S (2001) High temperatures tolerated by a diverse assemblage of shallow-water corals in American Samoa. Coral Reefs 20:185–189

Crossland CJ (1987) In situ release of mucus and DOC-lipid from the corals *Acropora variabilis* and *Stylophora pistillata* in different light regimes. Coral Reefs 6:35–42

Crossland CJ, Barnes DJ, Borowitzka MA (1980) Diurnal lipid and mucus production in the staghorn coral *Acropora acuminata*. Mar Biol 60:81–90

Cunning R, Silverstein RN, Baker AC (2015) Investigating the causes and consequences of symbiont shuffling in a multi-partner reef coral symbiosis under environmental change. Proc R Soc B 282:20141725

Darriba D, Taboada GL, Doallo R, Posada D (2012) jModelTest 2: more models, new heuristics and parallel computing. Nature Methods 9:772

Davies PS (1989) Short-term growth measurements of corals using an accurate buoyant weighing technique. Mar Biol 101:389–395

Davy SK, Allemand D, Weis VM (2012) Cell Biology of Cnidarian-Dinoflagellate Symbiosis. Microbiol Mol Biol R 76:229–261

Davy SK, Cook CB (2001) The relationship between nutritional status and carbon flux in the zooxanthellate sea anemone *Aiptasia pallida*. Mar Biol 139:999–1005

Davy SK, Withers KJT, Hinde R (2006) Effects of host nutritional status and seasonality on the nitrogen status of zooxanthellae in the temperate coral *Plesiastrea versipora* (Lamarck). J Exp Mar Biol Ecol 335:256–265

DeCarlo TM, Harrison HB, Gajdzik L, Alaguarda D, Rodolfo-Metalpa R, D'Olivo J, Liu G, Patalwala D, McCulloch MT (2019) Acclimatization of massive reef-building corals to consecutive heatwaves. Proc R Soc B: Biol Sci 286:20190235

DeVantier HG, Huang D, Johan O, Licuanan A, Obura DO, Sheppard C, Syahrir M, Turak E (2014) *Goniastrea retiformis*. The IUCN Red List of Threatened Species 2014. http://dx.doi.org/10.2305/IUCN.UK.2014-1.RLTS.T133634A54295467.en

Ding Y, Avramova Z, Fromm M (2011) Two distinct roles of *Arabidopsis* Homolog Trithorax-1(*ATX1*) at promoters and within transcribed regions of *ATX1*-regulated genes. Plant Cell 23:350–363

Ding Y, Liu N, Virlouvet L, Riethoven J-J, Fromm M, Avramova Z (2013) Four distinct types of dehydration stress memory genes in *Arabidopsis thaliana*. BMC Plant Biol 13:1–11

Domínguez-Andrés J, Joosten LA, Netea MG (2019) Induction of innate immune memory: the role of cellular metabolism. Curr Opin Immunol 56:10–16

Donelson, JM, Salinas S, Munday PL, Shama LNS (2017) Transgenerational plasticity and climate change experiments: Where do we go from here? GCB 24:13–34

Donner SD (2011) An evaluation of the effect of recent temperature variability on the prediction of coral bleaching events. Ecol Appl 21:1718–1730

Douglas AE (2003) Coral bleaching - how and why? Mar Poll Bull 46:385–392

Dove S, Ortiz JC, Enriquez S, Fine M, Fisher P, Iglesias-Prieto R, Thornhill D, Hoegh-Guldberg O (2006) Response of holosymbiont pigments from the scleractinian coral *Montipora monasteriata* to short-term heat stress. Limnol Ocean 51:1149–1158

Downs CA, Fauth JE, Halas JC, Dustan P, Bemiss J, Woodley CM (2002) Oxidative stress and seasonal coral bleaching. Free Rad Biol Med 33:533–543

Downs CA, McDougall KE, Woodley CM, Fauth JE, Richmond RH, Kushmaro A, Gibb SW, Loya Y, Ostrander GK, Kramarsky-Winter E (2013) Heat-stress and light-stress induce different cellular pathologies in the symbiotic dinoflagellate during coral bleaching. PloS one 8:e77173

Drury C, Schopmeyer S, Goergen E, Bartels E, Nedimyer K, Johnson M, Maxwell K, Galvan V, Manfrino C, Lirman D (2017) Genomic patterns in *Acropora cervicornis* show extensive population structure and variable genetic diversity. Ecol Evol 7:6188–6200

Dubinsky Z, Stambler N, Benzion M, Mccloskey LR, Muscatine L, Falkowski PG (1990) The Effect of External Nutrient Resources on the Optical-Properties and Photosynthetic Efficiency of *Stylophora pistillata*. Proc R Soc Ser B-Bio 239:231

Dunn OJ (1964) Multiple Comparisons Using Rank Sums. Technomet 6:241–252

Dunn SR, Thomason JC, Le Tissier MDA, Bythell JC (2004) Heat stress induces different forms of cell death in sea anemones and their endosymbiotic algae depending on temperature and duration. Cell Death and Differentiation 11:1213–1222

Dunnett CW (1955) A Multiple Comparison Procedure for Comparing Several Treatments with a Control. J Amer Stat Assoc 50:1096–1121

Eakin CM, Sweatman HPA, Brainard RE (2019) The 2014-2017 global-scale coral bleaching event: insights and impacts. Coral Reefs https://doi.org/10.1007/s00338-019-01844-2

Eakin CM, Lough JM, Heron SF (2009) Climate Variability and Change: Monitoring Data and Evidence for Increased Coral Bleaching Stress. In: van Oppen M.J.H., Lough J.M. (eds) Coral Bleaching: Patterns, Processes, Causes and Consequences. Springer Berlin Heidelberg. pp 41–67

Eakin CM, Liu G, Gomez A, De La Cour J, Heron SF, Skirving WJ, Geiger E, Marsh B, Tirak K, Strong A (2018) Unprecedented three years of global coral bleaching 2014-2017 [in "State of the Climate in 2017"]. Bull Amer Meteor Soc 99:S74–S75

Eakin CM, Skirving WJ, Heron SF, Liu G, Hughes T, Donner S, Geiger E, De La Cour J, Gomez A, Marsh B, Devotta D (2019) The 2014 Global Coral Bleaching Event and Global Coral Bleaching in the Anthropocene. ASLO 2019 Aquatic Sciences Meeting 69

Edmondson CH (1928) The Ecology of a Hawaiian Coral Reef. Bernice P Bish Mus B 45:3–64

Edmunds PJ (2014) Is acclimation beneficial to Scleractinian corals, *Porites* spp.? Mar Biol 161:1531–1542

Eirin-Lopez JM, Putnam HM (2019) Marine Environmental Epigenetics. Ann Rev Mar Sci 11:335–368

Emerson R, Arnold W (1932) The photochemical reaction in photosynthesis. J Gen Physiol 16:191–205

Falkowski PG, Knoll AH (2007) Evolution of Primary Producers in the Sea. Elsevier.

Falkowski PG, Raven JA (2013) Aquatic Photosynthesis: Second Edition. Princeton University Press.

Fay SA, Weber MX, Lipps JH (2009) The distribution of *Symbiodinium* diversity within individual host foraminifera. Coral Reefs 28:717–726

Feder ME (1999) Organismal, Ecological, and Evolutionary Aspects of Heat-Shock Proteins and the Stress Response: Established Conclusions and Unresolved Issues. Amer Zool 39:857–864

Ferrario F, Beck MW, Storlazzi CD, Micheli F, Shepard CC, Airoldi L (2014) The effectiveness of coral reefs for coastal hazard risk reduction and adaptation. Nat Comm 5:3794

Fisher R, O'Leary RA, Low-Choy S, Mengersen K, Knowlton N, Brainard RE, Caley MJ (2015) Species richness on coral reefs and the pursuit of convergent global estimates. Curr Biol 25:500–5

Fitt W, Brown B, Warner M, Dunne R (2001) Coral bleaching: interpretation of thermal tolerance limits and thermal thresholds in tropical corals. Coral Reefs 20:51–65

Fitt WK, McFarland FK, Warner ME, Chilcoat GC (2000) Seasonal patterns of tissue biomass and densities of symbiotic dinoflagellates in reef corals and relation to coral bleaching. Limnol Ocean 45:677–685

Fitt WK, Warner ME (1995) Bleaching Patterns of Four Species of Caribbean Reef Corals. Biol Bull 189:298–307

Fournier A (2013) The story of symbiosis with zooxanthellae, or how they enable their host to thrive in a nutrient poor environment. BioSci Rev 1–8

Franklin EC, Stat M, Pochon X, Putnam HM, Gates RD (2012) GeoSymbio: a hybrid, cloud-based web application of global geospatial bioinformatics and ecoinformatics for *Symbiodinium*-host symbioses. Mol Ecol Resour 12:369–373

Frieler K, Meinshausen M, Golly A, Mengel M, Lebek K, Donner SD, Hoegh-Guldberg O (2012) Limiting global warming to 2 °C is unlikely to save most coral reefs. Nat Clim Change 3:165–170

Gardiner JS (1903) The fauna and geography of the Maldive and Laccadive Archipelagoes, being the account of the work carried on and of collections made by an expedition during the years 1899 and 1900 (2 volumes). Cambridge University Press, Cambridge, UK

Gates RD, Baghdasarian G, Muscatine L (1992) Temperature stress causes host cell detachment in symbiotic cnidarians: Implications for coral bleaching. Biol Bull 182:324–332

Gibbin EM, Krueger T, Putnam HM, Barott KL, Bodin J, Gates RD, Meibom A (2018) Short-Term Thermal Acclimation Modifies the Metabolic Condition of the Coral Holobiont. Front Mar Sci 5:10

Gladfelter EH (1983) Spatial and Temporal Patterns of Mitosis in the Cells of the Axial Polyp of the Reef Coral *Acropora cervicornis*. Biol Bull 165:811–815

Glynn PW (1984) Widespread coral mortality and the 1982–83 El Niño warming event. Env Conserv 11:133–146

Glynn PW (1993) Coral reef bleaching: ecological perspectives. Coral Reefs 12:1–17

Glynn PW (1996) Coral reef bleaching: facts, hypotheses and implications. GCB 2:495–509

Glynn PW, D'Croz L (1990) Experimental evidence for high temperature stress as the cause of El Niño-coincident coral mortality. Coral Reefs 8:181–191

Goergen EA, Gilliam DS (2018) Outplanting technique, host genotype, and site affect the initial success of outplanted *Acropora cervicornis*. PeerJ 6:e4433

Goreau TF (1959) The Physiology of Skeleton Formation in Corals. I. A Method for Measuring the Rate of Calcium Deposition by Corals under Different Conditions. Biol Bull 116:59–75

Grottoli AG, Rodrigues LJ, Parady JE (2006) Heterotrophic plasticity and resilience in bleached corals. Nature 440:1186–1189

Grottoli AG, Warner ME, Levas SJ, Aschaffenburg MD, Schoepf V, McGinley M, Baumann J, Matsui Y (2014) The cumulative impact of annual coral bleaching can turn some coral species winners into losers. GCB 20:3823–3833

Guan Q, Haroon S, Bravo DG, Will JL, Gasch AP (2012) Cellular memory of acquired stress resistance in *Saccharomyces cerevisiae*. Genetics 192:495–505

Guest JR, Baird AH, Maynard JA, Muttaqin E, Edwards AJ, Campbell SJ, Yewdall K, Affendi YA, Chou LM (2012) Contrasting patterns of coral bleaching susceptibility in 2010 suggest an adaptive response to thermal stress. PLoS one 7:e33353

Guindon S, Gascuel O (2003) A simple, fast, and accurate algorithm to estimate large phylogenies by maximum likelihood. Syst Biol 52:696–704

Harada AE, Burton RS (2019) Ecologically Relevant Temperature Ramping Rates Enhance the Protective Heat Shock Response in an Intertidal Ectotherm. Physiol Biochem Zool 92:152–162

Harland AD, Davies PS, Fixter LM (1992) Lipid content of some Caribbean corals in relation to depth and light. Mar Biol 113:357–361

Haslun JA, Strychar KB, Buck G, Sammarco PW (2011) Coral Bleaching Susceptibility Is Decreased Following Short-Term (1–3 Year) Prior Temperature Exposure and Evolutionary History. J Mar Biol 2011:1–13

Hawkins TD, Hagemeyer JCG, Hoadley KD, Marsh AG, Warner ME (2016) Partitioning of Respiration in an Animal-Algal Symbiosis: Implications for Different Aerobic Capacity between *Symbiodinium* spp. Front Physiol 7:128

Hawkins TD, Warner ME (2017) Warm preconditioning protects against acute heat-induced respiratory dysfunction and delays bleaching in a symbiotic sea anemone. J Exp Biol 220:969–983

Hengge R (2009) Principles of c-di-GMP signaling in bacteria. Nat Rev Micro 7:263–273

Hennige SJ, Suggett DJ, Warner ME, McDougall KE, Smith DJ (2009) Photobiology of *Symbiodinium* revisited: bio-physical and bio-optical signatures. Coral Reefs 28:179–195

Hernandez-Delgado EA (2015) The emerging threats of climate change on tropical coastal ecosystem services, public health, local economies and livelihood sustainability of small islands: Cumulative impacts and synergies. Mar Pollut Bull 101:5–28

Heron SF, Maynard JA, van Hooidonk R, Eakin CM (2016) Warming Trends and Bleaching Stress of the World's Coral Reefs 1985–2012. Sci Rep 6:38402

Hilker M, Schwachtje J, Baier M, Balazadeh S, Baurle I, Geiselhardt S, Hincha DK, Kunze R, Mueller-Roeber B, Rillig MC, Rolff J, Romeis T, Schmulling T, Steppuhn A, van Dongen J, Whitcomb SJ, Wurst S, Zuther E, Kopka J (2015) Priming and memory of stress responses in organisms lacking a nervous system. Biol Rev Camb Philos Soc 91(4):1118-1133

Hillyer KE, Tumanov S, Villas-Boas S, Davy SK (2016) Metabolite profiling of symbiont and host during thermal stress and bleaching in a model cnidarian-dinoflagellate symbiosis. J Exp Biol 219:516–27

Hoegh-Guldberg O (1999) Climate change, coral bleaching and the future of the world's coral reefs. Mar Fresh Res 50:839–866

Hoegh-Guldberg O (2006) Thermal biology of coral reefs: will coral reefs survive global warming? Comp Biochem Physiol -Mol Integr Physiol 143:S131–S131

Hoegh-Guldberg O, Mumby PJ, Hooten AJ, Steneck RS, Greenfield P, Gomez E, Harvell CD, Sale PF, Edwards AJ, Caldeira K, Knowlton N, Eakin CM, Iglesias-Prieto R, Muthiga N, Bradbury RH, Dubi A, Hatziolos ME (2007) Coral reefs under rapid climate change and ocean acidification. Science 318:1737–1742

Hoegh-Guldberg O, Smith GJ (1989) The Effect of Sudden Changes in Temperature, Light and Salinity on the Population Density and Export of Zooxanthellae from the Reef Corals *Stylophora pistillata* (Esper) and *Seriatopora hystrix* (Dana). J Exp Mar Biol Ecol 129:279–303

Hoogenboom MO, Campbell DA, Beraud E, Dezeeuw K, Ferrier-Pages C (2012) Effects of light, food availability and temperature stress on the function of photosystem II and photosystem I of coral symbionts. PloS one 7:e30167

van Hooidonk R, Maynard J, Tamelander J, Gove J, Ahmadia G, Raymundo L, Williams G, Heron SF, Planes S (2016) Local-scale projections of coral reef futures and implications of the Paris Agreement. Sci Rep 6:39666

Howells EJ, Beltran VH, Larsen NW, Bay LK, Willis BL, van Oppen MJH (2011) Coral thermal tolerance shaped by local adaptation of photosymbionts. Nat Clim Change 2:116–120

Huey RB, Berrigan D (1996) Testing evolutionary hypotheses of acclimation. Johnston IA, Bennettm AF (eds) In: Animals and Temperature: Phenotypic and Evolutionary Adaptation. Cambridge University Press, Great Britain. pp. 205–237

Hughes S, Yau A, Max L, Petrovic N, Davenport F, Marshall M, McClanahan TR, Allison EH, Cinner JE (2012) A framework to assess national level vulnerability from the perspective of food security: The case of coral reef fisheries. Env Sci Pol 23:95–108

Hughes TP (1993) Disturbance Effects of Coral Reef Dynamics. Coral Reefs 12:115–115

Hughes TP (1994a) Catastrophes, Phase-Shifts, and Large-Scale Degradation of a Caribbean Coral Reef. Science 265:1547–1551

Hughes TP (1994b) Coral Reef Catastrophe - Reply. Science 266:1932–1933

Hughes TP, Baird AH, Bellwood DR, Connolly SR, Folke C, Grosberg R, Hoegh-Guldberg O, Jackson JBC, Kleypas J, Lough JM, Marshall P, Nystrom M, Palumbi SR, Pandolfi JM, Rosen B, Roughgarden J (2003) Climate Change, Human Impacts, and the Resilience of Coral Reefs. Science 301:929–933

Hughes TP, Connell JH (1999) Multiple stressors on coral reefs: A long-term perspective. Limnol Ocean 44:932–940

Hughes TP, Kerry JT, Álvarez-Noriega M, Álvarez-Romero JG, Anderson KD, Baird AH, Babcock RC, Beger M, Bellwood DR, Berkelmans R, Bridge TC, Butler IR, Byrne M, Cantin NE, Comeau S, Connolly SR, Cumming GS, Dalton SJ, Diaz-Pulido G, Eakin CM, Figueira WF, Gilmour JP, Harrison HB, Heron SF, Hoey AS, Hobbs J-PA, Hoogenboom MO, Kennedy EV, Kuo C, Lough JM, Lowe RJ, Liu G, McCulloch MT, Malcolm HA, McWilliam MJ, Pandolfi JM, Pears RJ, Pratchett MS, Schoepf V, Simpson T, Skirving WJ, Sommer B, Torda G, Wachenfeld DR, Willis BL, Wilson SK (2017) Global warming and recurrent mass bleaching of corals. Nature 543:373

Hughes TP, Kerry JT, Connolly SR, Baird AH, Eakin CM, Heron SF, Hoey AS, Hoogenboom MO, Jacobson M, Liu G, Pratchett MS, Skirving WJ, Torda G (2019) Ecological memory modifies the cumulative impact of recurrent climate extremes. Nat Clim Chan 9:40

Hume B, D'Angelo C, Burt J, Baker AC, Riegl B, Wiedenmann J (2013) Corals from the Persian/Arabian Gulf as models for thermotolerant reef-builders: Prevalence of clade C3 *Symbiodinium*, host fluorescence and ex situ temperature tolerance. Mar Pollut Bull 72:313–322

Hume BCC, D'Angelo C, Smith EG, Stevens JR, Burt J, Wiedenmann J (2015) *Symbiodinium thermophilum* sp. nov., a thermotolerant symbiotic alga prevalent in corals of the world's hottest sea, the Persian/Arabian Gulf. Sci Rep 5:8562

Iglesias-Prieto R, Trench RK (1994) Acclimation and Adaptation to Irradiance in Symbiotic Dinoflagellates: Responses of the Photosynthetic Unit to Changes in Photon Flux-Density. MEPS 113:163–175

Jackson AE, Miller DJ, Yellowlees D (1989) Phosphorus-Metabolism in the Coral Zooxanthellae Symbiosis - Characterization and Possible Roles of 2 Acid-Phosphatases in the Algal Symbiont *Symbiodinium* Sp. Proc R Soc Ser B-Bio 238:193–202

Jackson AE, Yellowlees D (1990) Phosphate-Uptake by Zooxanthellae Isolated from Corals. P Roy Soc B-Biol Sci 242:201–204

Jeffrey SW, Haxo FT (1968) Photosynthetic Pigments of Symbiotic Dinoflagellates (Zooxanthellae) from Corals and Clams. Biol Bull 135:149–165

Jones AM, Berkelmans R (2010) Potential Costs of Acclimatization to a Warmer Climate: Growth of a Reef Coral with Heat Tolerant vs. Sensitive Symbiont Types. PLoS One 5:e10437

Jones AM, Berkelmans R, van Oppen MJH, Mieog JC, Sinclair W (2008) A community change in the algal endosymbionts of a scleractinian coral following a natural bleaching event: field evidence of acclimatization. Proc Biol Sci 275:1359–1365

Jones RJ, Yellowlees D (1997) Regulation and control of intracellular algae (zooxanthellae) in hard corals. Phil Trans Roy Soc Biol Sci 352:457–468

Kaplan F, Kopka J, Sung DY, Zhao W, Popp M, Porat R, Guy CL (2007) Transcript and metabolite profiling during cold acclimation of *Arabidopsis* reveals an intricate relationship of cold-regulated gene expression with modifications in metabolite content. The Plant Journal 50:967–981

Karban R (2008) Plant behaviour and communication. Ecol Lett 11:727–739

Kelley R, Ideker T (2009) Genome-Wide Fitness and Expression Profiling Implicate Mga2 in Adaptation to Hydrogen Peroxide. PLoS Genet 5:e1000488

Kenkel CD, Goodbody-Gringley G, Bartels E, Davies SW, Percy AL, Matz MV (2012) Evidence of local thermal adaptation in a Caribbean coral. Integr Comp Biol 52:E92–E92

Kenkel CD, Matz MV (2016) Gene expression plasticity as a mechanism of coral adaptation to a variable environment. Nat Ecol Evol 1:0014

Kenkel CD, Meyer E, Matz MV (2013) Gene expression under chronic heat stress in populations of the mustard hill coral (*Porites astreoides*) from different thermal environments. Mol Ecol 22:4322–4334

Kent G (1997) Fisheries, food security, and the poor. Food Pol 22:393–404

Knowlton N, Brainard RE, Fisher R, Moews M, Plaisance L, Caley MJ (2010) Coral Reef Biodiversity. In: Life in the World's Oceans: Diversity, Distribution, and Abundance. McIntyre, AD (ed.), 65–77. Wiley-Blackwell

Knowlton N, Rohwer F (2003) Multispecies Microbial Mutualisms on Coral Reefs: The Host as a Habitat. Amer Nat 162:S51–S62

Koop K, Booth D, Broadbent A, Brodie J, Bucher D, Capone D, Coll J, Dennison W, Erdmann M, Harrison P, Hoegh-Guldberg O, Hutchings P, Jones GB, Larkum AWD, O'Neil J, Steven A, Tentori E, Ward S, Williamson J, Yellowlees D (2001) ENCORE: The effect of nutrient enrichment on coral reefs. Synthesis of results and conclusions. Mar Pollut Bull 42:91–120

Kraffe E, Marty Y, Guderley H (2007) Changes in mitochondrial oxidative capacities during thermal acclimation of rainbow trout *Oncorhynchus mykiss*: roles of membrane proteins, phospholipids and their fatty acid compositions. J Exp Biol 210:149–165

Kunihiro S, Reimer JD (2018) Phylogenetic analyses of *Symbiodinium* isolated from Waminoa and their anthozoan hosts in the Ryukyu Archipelago, southern Japan. Symbio 76:253–264

LaJeunesse TC, Loh WKW, Woesik R van, Hoegh-Guldberg O, Schmidt GW, Fitt WK (2003) Low symbiont diversity in southern Great Barrier Reef corals, relative to those of the Caribbean. Limnol Ocean 48:2046–2054

LaJeunesse TC, Parkinson JE, Gabrielson PW, Jeong HJ, Reimer JD, Voolstra CR, Santos SR (2018a) Systematic Revision of Symbiodiniaceae Highlights the Antiquity and Diversity of Coral Endosymbionts. Curr Biol 2816:2570–2580

LaJeunesse TC, Smith RT, Finney J, Oxenford H (2009) Outbreak and persistence of opportunistic symbiotic dinoflagellates during the 2005 Caribbean mass coral 'bleaching' event. P Roy Soc B: Biol Sci 276:4139–4148

LaJeunesse TC, Thornhill DJ, Cox EF, Stanton FG, Fitt WK, Schmidt GW (2004) High diversity and host specificity observed among symbiotic dinoflagellates in reef coral communities from Hawaii. Coral Reefs 23:596–603

LaJeunesse TC, Wham DC, Pettay DT, Parkinson JE, Keshavmurthy S, Chen CA (2014) Ecologically differentiated stress-tolerant endosymbionts in the dinoflagellate genus *Symbiodinium* (Dinophyceae) Clade D are different species. Phycologia 53:305–319

Lathuilière B, Marchal D (2009) Extinction, survival and recovery of corals from the Triassic to Middle Jurassic time. Terra Nova 21:57–66

Leletkin VA (2000) The Energy Budget of Coral Polyps. Russ J Mar Biol 26:231–240

Leroi AM, Bennett AF, Lenski RE (1994) Temperature acclimation and competitive fitness: an experimental test of the beneficial acclimation assumption. PNAS 91:1917–1921

Lesser M (1996) Elevated temperatures and ultraviolet radiation cause oxidative stress and inhibit photosynthesis in symbiotic dinoflagellates. Limnol Ocean 41:271–283

Lesser MP (2006) Oxidative stress in marine environments: biochemistry and physiological ecology. Annu Rev Physiol 68:253–278

Lesser MP, Farrell JH (2004) Exposure to solar radiation increases damage to both host tissues and algal symbionts of corals during thermal stress. Coral Reefs 23:367–377

Lesser MP, Stat M, Gates RD (2013) The endosymbiotic dinoflagellates (*Symbiodinium* sp.) of corals are parasites and mutualists. Coral Reefs 32:603–611

Lesser MP, Weis VM, Patterson MR, Jokiel PL (1994) Effects of Morphology and Water Motion on Carbon Delivery and Productivity in the Reef Coral, *Pocillopora damicornis* (Linnaeus) - Diffusion-Barriers, Inorganic Carbon Limitation, and Biochemical Plasticity. J Exp Mar Biol Ecol 178:153–179

Lewis E (1980) The practical salinity scale 1978 and its antecedents. IEEE J Ocean Eng 5:3–8

Liew YJ, Howells EJ, Wang X, Michell CT, Burt JA, Idaghdour Y, Aranda M (2018) Intergenerational epigenetic inheritance in reef-building corals. bioRxiv https://doi.org/10.1101/269076

Lima FP, Wethey DS (2012) Three decades of high-resolution coastal sea surface temperatures reveal more than warming. Nat Comm 3:704

Lirman D, Schopmeyer S, Galvan V, Drury C, Baker AC, Baums IB (2014) Growth Dynamics of the Threatened Caribbean Staghorn Coral *Acropora cervicornis*: Influence of Host Genotype, Symbiont Identity, Colony Size, and Environmental Setting. PLoS One 9: e107253

Matz MV, Treml EA, Aglyamova GV, Bay LK (2018) Potential and limits for rapid genetic adaptation to warming in a Great Barrier Reef coral. PLoS Genet 14: e1007220

Maynard JA, Anthony KRN, Marshall PA, Masiri I (2008) Major bleaching events can lead to increased thermal tolerance in corals. Mar Biol 155:173–182

McBride BB, Muller-Parker G, Jakobsen HH (2009) Low thermal limit of growth rate of *Symbiodinium californium* (Dinophyta) in culture may restrict the symbiont to southern populations of its host anemones (*Anthopleura* spp.; Anthozoa, Cnidaria)1. J Phycol 45:855–863

McClanahan T, Allison EH, Cinner JE (2015) Managing fisheries for human and food security. Fish Fisher16:78–103

McDougall KE, Gibb SW, Boyd KG, Brown BE (2006) “Chlorophyll-like” compounds as novel biomarkers of stress in corals. MEPS 325:137–144

Middlebrook R, Hoegh-Guldberg O, Leggat W (2008) The effect of thermal history on the susceptibility of reef-building corals to thermal stress. J Exp Biol 211:1050–1056

Mieog JC, van Oppen MJH, Cantin NE, Stam WT, Olsen JL (2007) Real-time PCR reveals a high incidence of *Symbiodinium* clade D at low levels in four scleractinian corals across the Great Barrier Reef: implications for symbiont shuffling. Coral Reefs 26:449–457

Mittler R, Finka A, Goloubinoff P (2012) How do plants feel the heat? Trends Biochem Sci 37:118–25

Moberg F, Folke C (1999) Ecological goods and services of coral reef ecosystems. Ecol Econ 29:215–233

Molinier J, Ries G, Zipfel C, Hohn B (2006) Transgenerational memory of stress in plants. Nature 442:1046–1049

Morikawa MK, Palumbi SR (2019) Using naturally occurring climate resilient corals to construct bleaching-resistant nurseries. PNAS 116:10586–10591

Muscatine L, Cernichiari E (1969) Assimilation of Photosynthetic Products of Zooxanthellae by a Reef Coral. Biol Bull 137:506–523

Muscatine L, Falkowski PG, Porter JW, Dubinsky Z (1984) Fate of Photosynthetic fixed carbon in light-adapted and shade-adapted colonies of the symbiotic coral *Stylophora pistillata*. P Roy Soc B-Biol Sci 222:181–202

Muscatine L, Hand C (1958) Direct evidence for the transfer of materials from symbiont algae to the tissues of a coelenterate. PNAS 44:1259–1263

Muscatine L, McCloskey LR, Marian RE (1981) Estimating the daily contribution of carbon from zooxanthellae to coral animal respiration. Limnol Ocean 26:601–611

Muscatine L, Porter JW (1977) Reef Corals: Mutualistic Symbioses Adapted to Nutrient-Poor Environments. BioSci 27:454–460

Mydlarz LD, McGinty ES, Harvell D (2010) What are the physiological and immunological responses of coral to climate warming and disease? J Exp Biol 213:934–945

National Academies of Sciences, Engineering, and Medicine (2019) A Research Review of Interventions to Increase the Persistence and Resilience of Coral Reefs. Washington, DC: The National Academies Press. https://doi.org/10.17226/25279

NOAA Coral Reef Watch (2017a) NOAA Coral Reef Watch Version 3.0 Daily Global 5-km Satellite Virtual Station Time Series Data for Ofu Island, Jan. 1, 2016-Jan. 30, 2016. Silver Spring, Maryland, USA: NOAA Coral Reef Watch. Data set accessed 2017-04-11 at https://coralreefwatch.noaa.gov/satellite/vs/americansamoa.php#Ofu

NOAA Coral Reef Watch (2017b) NOAA Coral Reef Watch Version 3.0 Daily Global 5-km Satellite Virtual Station Time Series Data for Southeast Florida, Mar. 12, 2013-Mar. 11, 2014. College Park, Maryland, USA: NOAA Coral Reef Watch

Nyström T (2002) Aging in bacteria. Curr Opin Microbiol 5:596–601

Oakley CA, Durand E, Wilkinson SP, Peng L, Weis VM, Grossman AR, Davy SK (2017) Thermal Shock Induces Host Proteostasis Disruption and Endoplasmic Reticulum Stress in the Model Symbiotic Cnidarian *Aiptasia*. J Proteome Res 16:2121–2134

O'Brien KM (2011) Mitochondrial biogenesis in cold-bodied fishes. J Exp Biol 214:275–285

Odum HT, Odum EP (1955) Trophic Structure and Productivity of a Windward Coral Reef Community on Eniwetok Atoll. Ecol Monogr 25:291–320

Oliver TA, Palumbi SR (2009) Distributions of stress-resistant coral symbionts match environmental patterns at local but not regional scales. MEPS 378:93–103

Oliver TA, Palumbi SR (2011) Do fluctuating temperature environments elevate coral thermal tolerance? Coral Reefs 30:429–440

van Oppen MJH, Oliver JK, Putnam HM, Gates RD (2015) Building coral reef resilience through assisted evolution. PNAS 112:2307–2313

Orr AP, Moorhouse FW (1933) Scientific Report of the Great Barrier Reef Expedition 2, No. 4(a), 87

Padfield D, Lowe C, Buckling A, French-Constant R, Jennings S, Shelley F, Ólafsson JS, Yvon-Durocher G (2017) Metabolic compensation constrains the temperature dependence of gross primary production. Ecol Lett 20:1250–1260

Padfield D, Yvon-Durocher G, Buckling A, Jennings S, Yvon-Durocher G (2016) Rapid evolution of metabolic traits explains thermal adaptation in phytoplankton. Ecol Lett 19:133–142

Palumbi SR, Barshis DJ, Traylor-Knowles N, Bay RA (2014) Mechanisms of Reef Coral Resistance to Future Climate Change. Science 344(6186):895–898

Parkinson JE, Banaszak AT, Altman NS, LaJeunesse TC, Baums IB (2015) Intraspecific diversity among partners drives functional variation in coral symbioses. Sci Rep 5:15667

Parkinson JE, Bartels E, Devlin-Durante MK, Lustic C, Nedimyer K, Schopmeyer S, Lirman D, LaJeunesse TC, Baums IB (2018) Extensive transcriptional variation poses a challenge to thermal stress biomarker development for endangered corals. Mol Ecol 27:1103–1119

Pastor V, Luna E, Mauch-Mani B, Ton J, Flors V (2013) Primed plants do not forget. Env Exp Bot 94:46–56

Pearse VB, Muscatine L (1971) Role of symbiotic algae zooxanthellae in coral calcification. Biol Bull 141:350–363

Petersen C, Round JL (2014) Defining dysbiosis and its influence on host immunity and disease. Cell Microbiol 16:1024–1033

Peterson ME, Daniel RM, Danson MJ, Eisenthal R (2007) The dependence of enzyme activity on temperature: determination and validation of parameters. Biochem J 402:331–337

Pochon X, Putnam HM, Burki F, Gates RD (2012) Identifying and Characterizing Alternative Molecular Markers for the Symbiotic and Free-Living Dinoflagellate Genus *Symbiodinium*. PLoS One 7:e29816

Polato NR, Voolstra CR, Schnetzer J, DeSalvo MK, Randall CJ, Szmant AM, Medina M, Baums IB (2010) Location-specific responses to thermal stress in larvae of the reef-building coral *Montastraea faveolata*. PloS one 5:e11221

Porter JW, Muscatine L, Dubinsky Z, Falkowski PG (1984) Primary production and photoadaptation in light-adapted and shade-adapted colonies of the symbiotic coral, *Stylophora pistillata*. P Roy Soc B-Biol Sci 222:161

Pörtner H-O (2010) Oxygen- and capacity-limitation of thermal tolerance: a matrix for integrating climate-related stressor effects in marine ecosystems. J Exp Biol 213:881–893

Pörtner HO, Farrell AP (2008) Physiology and Climate Change. Science 322:690–692

Pörtner HO, Knust R (2007) Climate change affects marine fishes through the oxygen limitation of thermal tolerance. Science 315:95–97

Putnam HM, Edmunds PJ (2011) The physiological response of reef corals to diel fluctuations in seawater temperature. J Exp Mar Biol Ecol 396:216–223

Putnam HM, Gates RD (2015) Preconditioning in the reef-building coral *Pocillopora damicornis* and the potential for trans-generational acclimatization in coral larvae under future climate change conditions. J Exp Biol 218:2365–2372

Putnam HM, Stat M, Pochon X, Gates RD (2012) Endosymbiotic flexibility associates with environmental sensitivity in scleractinian corals. Proc Biol Sci 279:4352–4361

Reaka-Kudla ML, Feingold JS, Glynn W (1996) Experimental studies of rapid bioerosion of coral reefs in the Galapagos Islands. Coral Reefs 15:101–107

Rebl A, Verleih M, Nipkow M, Altmann S, Bochert R, Goldammer T (2018) Gradual and Acute Temperature Rise Induces Crossing Endocrine, Metabolic, and Immunological Pathways in Maraena Whitefish (*Coregonus maraena*). Front Genet 9:241

Reed KC, Muller EM, van Woesik R (2010) Coral immunology and resistance to disease. Dis Aquat Org 90:85–92

Reich HG, Robertson DL, Goodbody-Gringley G (2017) Do the shuffle: Changes in *Symbiodinium* consortia throughout juvenile coral development. PLoS One 12:e0171768

Rodolfo-Metalpa R, Hoogenboom MO, Rottier C, Ramos-Espla A, Baker AC, Fine M, Ferrier-Pages C (2014) Thermally tolerant corals have limited capacity to acclimatize to future warming. GCB 20:3036–3049

Rodrigues LJ, Grottoli AG (2007) Energy reserves and metabolism as indicators of coral recovery from bleaching. Limnol Ocean 52:1874–1882

Rohwer F, Seguritan V, Azam F, Knowlton N (2002) Diversity and distribution of coral-associated bacteria. MEPS 243:1–10

Runde S, Molière N, Heinz A, Maisonneuve E, Janczikowski A, Elsholz AKW, Gerth U, Hecker M, Turgay K (2014) The role of thiol oxidative stress response in heat-induced protein aggregate formation during thermotolerance in *Bacillus subtilis*. Mol Microbiol 91:1036–1052

Safaie A, Silbiger NJ, McClanahan TR, Pawlak G, Barshis DJ, Hench JL, Rogers JS, Williams GJ, Davis KA (2018) High frequency temperature variability reduces the risk of coral bleaching. Nat Commun 9:1671

Scheufen T, Krämer WE, Iglesias-Prieto R, Enríquez S (2017) Seasonal variation modulates coral sensibility to heat-stress and explains annual changes in coral productivity. Sci Rep 7:4937

Schnitzler CE, Hollingsworth LL, Krupp DA, Weis VM (2011) Elevated temperature impairs onset of symbiosis and reduces survivorship in larvae of the Hawaiian coral, *Fungia scutaria*. Mar Biol 159:633–642

Smith LD, Hughes TP (1999) An experimental assessment of survival, re-attachment and fecundity of coral fragments. J Exp Mar Biol Ecol 235:147–164

Smith LW, Barshis DJ, Birkeland C (2007) Phenotypic plasticity for skeletal growth, density and calcification of *Porites lobata* in response to habitat type. Coral Reefs 26:559–567

Smith LW, Wirshing HH, Baker AC, Birkeland C (2008) Environmental versus Genetic Influences on Growth Rates of the Corals *Pocillopora eydouxi* and *Porites lobata* (Anthozoa: Scleractinia). Pacific Science 62:57–69

Sorek M, Levy O (2012) Influence of the quantity and quality of light on photosynthetic periodicity in coral endosymbiotic algae. PLoS One 7:e43264

Stanley GD, van de Schootbrugge B (2009) The Evolution of the Coral–Algal Symbiosis. van Oppen M.J.H., Lough J.M. (eds) In: Coral Bleaching: Patterns, Processes, Causes and Consequences. Springer Berlin, Heidelberg, pp 7–19

Stanley GD, Shepherd HME, Robinson AJ (2018) Paleoecological Response of Corals to the End-Triassic Mass Extinction: An Integrational Analysis. J Earth Sci 29:879–885

Stanley GD, Swart PK (1995) Evolution of the Coral-Zooxanthenllae Symbiosis During the Triassic: A Geochemical Approach. Paleobiol 21:179–199

Stat M, Carter D, Hoegh-Guldberg O (2006) The evolutionary history of *Symbiodinium* and scleractinian hosts—Symbiosis, diversity, and the effect of climate change. Perspect Plant Ecol Evol System 8:23–43

Stat M, Gates RD (2011) Clade D *Symbiodinium* in Scleractinian Corals: A "Nugget" of Hope, a Selfish Opportunist, an Ominous Sign, or All of the Above? Mar Biol 2011:1–9

Steen GR, Muscatine L (1987) Low-Temperature Shock Evokes Rapid Exocytosis of Symbiotic Algae by a Sea Anemone. Biol Bull 172:246–263

Stimson J (1991) The temporal pattern and rate of release of zooxanthellae from the reef coral *Pocillopora damicornis* under nitrogen-enrichment and control conditions. J Exp Mar Biol Ecol 153:63–74

Tagkopoulos I, Liu Y-C, Tavazoie S (2008) Predictive Behavior Within Microbial Genetic Networks. Science 320:1313–1317

Tchernov D, Gorbunov MY, de Vargas C, Narayan Yadav S, Milligan AJ, Haggblom M, Falkowski PG (2004) Membrane lipids of symbiotic algae are diagnostic of sensitivity to thermal bleaching in corals. PNAS 101:13531–13535

Thomas L, Rose NH, Bay RA, López EH, Morikawa MK, Ruiz-Jones L, Palumbi SR (2018) Mechanisms of Thermal Tolerance in Reef-Building Corals across a Fine-Grained Environmental Mosaic: Lessons from Ofu, American Samoa. Front Mar Sci 4:434

Thompson DM, van Woesik R (2009) Corals escape bleaching in regions that recently and historically experienced frequent thermal stress. Proc Biol Sci 276:2893–2901

Thornhill DJ, LaJeunesse TC, Kemp DW, Fitt WK, Schmidt GW (2006) Multi-year, seasonal genotypic surveys of coral-algal symbioses reveal prevalent stability or post-bleaching reversion. Mar Biol 148:711–722

Tomascik T (1997) The Ecology of the Indonesian Seas. Oxford University Press, pp. 776

Torda G, Donelson JM, Aranda M, Barshis DJ, Bay L, Berumen ML, Bourne DG, Cantin N, Foret S, Matz M, Miller DJ, Moya A, Putnam HM, Ravasi T, Oppen MJH van, Thurber RV, Vidal-Dupiol J, Voolstra CR, Watson S-A, Whitelaw E, Willis BL, Munday PL (2017) Rapid adaptive responses to climate change in corals. Nat Clim Change 7:627–636

Varshney R, Graner A, Sorrells M (2005) Genomics-assisted breeding for crop improvement. Trends Plant Sci 10:621–630

Vaughan TW (1914) Reef corals of the Bahamas and Southern Florida. Carnegie Institution, Washington, pp. 222–226

Walter J, Jentsch A, Beierkuhnlein C, Kreyling J (2013) Ecological stress memory and cross stress tolerance in plants in the face of climate extremes. Env Exp Botany 94:3–8

Wang LH, Liu YH, Ju YM, Hsiao YY, Fang LS, Chen CS (2008) Cell cycle propagation is driven by light-dark stimulation in a cultured symbiotic dinoflagellate isolated from corals. Coral Reefs 27:823–835

Warner ME, Berry-Lowe S (2006) Differential xanthophyll cycling and photochemical activity in symbiotic dinoflagellates in multiple locations of three species of Caribbean coral. J Exp Mar Biol Ecol 339:86–95

Warner ME, Fitt WK, Schmidt GW (1996) The effects of elevated temperature on the photosynthetic efficiency of zooxanthellae in hospite from four different species of reef coral: A novel approach. Plant Cell Env 19:291–299

Warner ME, Fitt WK, Schmidt GW (1999) Damage to Photosystem II in symbiotic dinoflagellates: A determinant of coral bleaching. PNAS 96:8007–8012

Weier J (2001) Mapping the Decline of Coral Reefs. Earth Observatory, March 12, 2001. www.earthobservatory.nasa.gov/Study/Coral/

Weis VM (2008) Cellular mechanisms of Cnidarian bleaching: stress causes the collapse of symbiosis. J Exp Biol 211:3059–66

Wilkerson FP, Kobayashi D, Muscatine L (1988) Mitotic index and size of symbiotic algae in Caribbean Reef corals. Coral Reefs 7:29–36

Wilkinson (2008) Status of the coral reefs of the world: 2008. Global Coral Reef Monitoring Network and Reef and Rainforest Research Centre, Townsville, pp. 296

Winters G, Beer S, Zvi BB, Brickner I, Loya Y (2009) Spatial and temporal photoacclimation of *Stylophora pistillata*: zooxanthella size, pigmentation, location and clade. MEPS 384:107–119

Yorifuji M, Takeshima H, Mabuchi K, Watanabe T, Nishida M (2015) Comparison of *Symbiodinium* dinoflagellate flora in sea slug populations of the *Pteraeolidia ianthina* complex. MEPS 521:91–104

Zevian SC, Yanowitz JL (2014) Methodological Considerations for Heat Shock of the Nematode *Caenorhabditis elegans*. Nat Methods 68:450–457

Zhang H, Campbell DA, Sturm NR, Rosenblad MA, Dungan CF, Lin S (2013) Signal recognition particle RNA in dinoflagellates and the Perkinsid *Perkinsus marinus*. Protist 164:748–761

VITA

Harmony Alise Martell née Hancock
Department of Biological Sciences
Old Dominion University, Norfolk, VA 23529

EDUCATION

Old Dominion University	Ecological Sciences	
Nova Southeastern University	Marine Biology, Coastal Zone Management	MS, 2012
College of Saint Elizabeth	Biology	BS, 2003

PROFESSIONAL EXPERIENCE

Ocean Leaders Postdoctoral Fellow, *University of British Columbia, BC, CAN*	2019
Research Intern, *Sandia National Laboratory, Bioenergy & Defense Technologies, NM*	2014
Program Assistant, *Nurture Nature Center, PA*	2013
Conservation Coordinator, *International Game Fish Association, FL*	2012
Field Biologist/Scientist I, *Coastal & Marine Ecology Consultants, Inc., FL*	2011
Research Assistant, *USGS Seagrass Laboratory & National Coral Reef Institute, FL*	2008
Science Teacher, *Bridgewater-Raritan Regional High School, NJ*	2004

SELECTED GRANTS RECEIVED

Martell, HA. 2019. ASLO 2019 Aquatic Sciences Meeting Student Travel Award. $870.
Martell, HA. 2018. NOAA CRC Reef Futures 2018 Symposium Scholarship Award. $2000.
Hancock, HA. 2018. Marshall Endowed Scholarship Award. $4962.
Hancock, HA. 2017. Training Corals to Resist Bleaching Crowdfunding Campaign. $7175.
Hancock, HA. 2016. NSF Coral Bleaching Workshop Travel Award. $868.
Hancock, HA. 2016. ODU SEES Graduate Research Award. $500.
Hancock, HA. 2015. ODU Biology Graduate Student Organization Travel Award. $550.
Hancock, HA. 2015. Bagley Endowed Scholarship Award. $7563.
Hancock, HA. 2010. EPA Star Fellowship. Developing a Non-Invasive Technique to Quantify Coral Health. $74,000.
Hancock, HA. 1999. Elizabethan Scholarship for Academic Excellence. $39,995.

SELECTED PUBLICATIONS

Murton J, Nagarajan A, Nguyen AY, Liberton M, **Hancock HA**, Pakrasi HB, Timlin JA. (2017) Population level coordination of pigment response in individual cyanobacterial cells under altered nitrogen levels. *Photosynthesis Research*. doi:10.1007/s11120-017-0422-7